UNIVERSITY OF CALIFORNIA, SAN DEIGO

Two MAP kinases regulate novel aspects of the endoplasmic reticulum stress response

A dissertation submitted in partial satisfaction of the requirements for the degree of Doctor of Philosophy

in

Biology

by

Alicia Anne Bicknell

Committee in charge:

Professor Maho Niwa, Chair
Professor Don W. Cleveland
Professor Arshad Desai
Professor Randolph Y. Hampton
Professor Lorraine Pillus
Professor James G. Umen

2009

The Dissertation of Alicia Anne Bicknell is approved, and is acceptable in quality and form for publication on microfilm and electronically:

Chair

University of California, San Diego

2009

Table of Contents

List of Abbreviations

ADP	-	Adenosine diphosphate
ALP	-	Alkaline phosphatase
ATP	-	Adenosine triphosphate
BME	-	β-Mercaptoethanol
cER	-	Cortical endoplasmic reticulum
CFW	-	Clacoflour white
CIVS	-	Cylindrical intravacuolar structure
CP	-	Caspofungin
CWI	-	Cell wall integrity
DIC	-	Differential Interference Contrast
DMSO	-	Dimethylsulfoxide
DNA	-	Deoxyribonucleic acid
DOC	-	Deoxycorticosterone
DTT	-	Dithiothreitol
EDTA	-	Ethylenediaminetetraacetic acid
ER	-	Endoplasmic reticulum
ERAD	-	Endoplasmic reticulum associated degradation
ERC	-	Extrachromosomal rDNA circles
ERSE	-	Endoplasmic reticulum stress element
ERSU	-	Endoplasmic reticulum surveillance
GFP	-	Green fluorescence protein
GRE	-	Glucocorticoid responsive element
HRP	-	Horseradish peroxidase
Ig	-	Immuniglobulin
LatB	-	Latrunculin B
MAPK	-	Mitogen activated protein kinase
MEF	-	Mouse embryonic fibroblast
MEK	-	MAPK/ERK kinase
MEKK	-	MAPK/ERK kinase kinase
MHC	-	Major Histocompatibility Complex
mRNA	-	Messenger ribonucleic acid
OD	-	Optical density
PAS	-	Pre-autophagosomal structure
PBS	-	Phosphate buffered saline
PCR	-	Polymerase chain reaction
PMSF	-	Phenylmethansulphonylflouride
RNA	-	Ribonuceic acid
RNase	-	Ribondonuclease
rRNA	-	ribosomal ribonucleic acid
RT-PCR	-	Reverse transcription polymerase chain reaction

SD	-	Standard deviation
SDS	-	Sodium dodecyl sulfate
SEM	-	Standard error of the mean
Tm	-	Tunicamycin
UPR	-	Unfolded protein response
UPRE	-	Unfolded protein response element
UTR	-	Untranslated region
WT	-	Wild type

List of Figures

Chapter 2

Chapter 3

List of Tables

Acknowledgements

I would like to thank my thesis advisor, Maho Niwa, for her years of invaluable support, guidance, dedication, and optimism. Other members of the Niwa lab, especially Anna Babour, Aditi Chawla, Jenny DuRose, and Arvin Tam, have profoundly enriched my Ph.D. experience through their incredible scientific abilities, their generous willingness to share those abilities, and the personal support that they have always given me. I was also lucky to work with two very talented masters students, Jeffrey Sperling and Joel Tourtellotte, who not only contributed intellectually to my work, but also helped make lab fun. The Niwa lab has had many amazing undergraduate students, but Carolyn Nohejl and David Phang deserve special note for their intelligence, curiosity, and attitude, which inspired me. I am very grateful for all five of my thesis committee members, Don Cleveland, Arshad Desai, Randy Hampton, Lorraine Pillus, and Jim Umen, who have provided invaluable intellectual insights to my work, and who have always been sincerely dedicated to helping my scientific development, and helping me achieve my goals.

I could not have completed this work without the unwavering support of my family and friends, especially my parents Michael and Anne Ware, and my husband Jesse. My son Eliot deserves acknowledgement for just being him.

Chapter 1 is modified from material that has been accepted for publication in *Handbook of Cell Signaling, 2nd Edition*, 2009, Elsevier, Ralph A. Bradshaw and Edward A. Dennis (Eds.). Alicia A. Bicknell and Maho Niwa. I was the primary author of this chapter under the direction of Maho Niwa.

Chapter 2 is modified from material that was published in *The Journal of Cell Biology*, 2007, Vol. 177, No. 6, 1017-1027. Alicia A. Bicknell, Anna Babour, Christine M. Federovitch, and Maho Niwa. I was the primary investigator and author of this paper under the supervision of Maho Niwa. Anna Babour conducted experiments depicted in Figures 3.7B-D and Figures 3.8B-D and Christine M. Federovitch conducted experiments depicted in Figure 3.9D.

Chapter 3 is modified from material that has been submitted for publication. Anna Babour, Alicia A. Bicknell, Joel Tourtelotte, and Maho Niwa. I was the secondary investigator and secondary author of this paper. The specific experiments that I conducted are depicted in Figures 3.1D, 3.4A, 3.5A, 3.7A-C, 3.8B-D, and 3.8F-G. Joel Tourtelotte conducted experiments depicted in Figures 4.2A, 4.2B, 4.5B, and 4.5G; Anna Babour conducted the remaining experiments and Maho Niwa supervised the work.

Chapter 4 is modified from material that has been submitted for publication. Alicia A. Bicknell and Maho Niwa. I was the primary investigator and author of this paper under the supervision of Maho Niwa.

Vita

Objective

To obtain a post-doctoral position studying post-transcriptional gene regulation in neurons

Education

• Ph.D.	Biology	University of California San Diego	2002-2009
• B.A.	Biochemistry	Rice University	1997-2001

Research Experience

Doctoral Studies, Division of Biological Sciences, UCSD (2002-2009)

I conducted research on two aspects of the unfolded protein response (UPR) pathway, which is a signal transduction pathway that detects and resolves the accumulation of unfolded proteins within the endoplasmic reticulum. Firstly, I studied a pathway that links the cell cycle to ER function. Secondly, I investigated the mechanism and purpose of MAP Kinase activation during UPR signaling. Dissertation Advisor: Maho Niwa.

Undergraduate Honors Research, Biochemistry Dept, Rice University (1999-2001)

I used a biochemical approach to analyze binding partners of the homeodomain protein, Ultrabithorax (Ubx), and determine how protein-protein interactions affect Ubx's function as a transcription factor. Undergraduate Thesis Advisor: Kathleen S. Matthews.

Honors and Awards

• National Science Foundation Graduate Research Fellowship	2004-2007
• Association for Women in Science, San Diego Chapter Award for Outreach or Community Service	2006
• Cell, Molecular, and Genetics NIH Training Grant	2002-2004
• Rice University John E. Parish Fellowship	2000-2001
• Rice University Scholars Program	1999-2000

Teaching Experience

• Teaching Assistant	Molecular Biology, UCSD	Winter 2006
• Teaching Assistant	Molecular Biology, UCSD	Winter 2005
• Teaching Assistant	Recombinant DNA Techniques, UCSD	Spring 2004
• Teaching Assistant	Experimental Biosciences, Rice University	Fall 1996

Leadership and Service Experience

- Graduate Student Member: Women in Science and Engineering Committee, UCSD 2003-2007
- Co-chair: San Diego Chapter Association for Women in Science Outreach Committee (Committee Volunteer: 2003-2007) 2004-2006
- Graduate Student Representative: Committee on Affirmative Action and Diversity, UCSD 2004-2005

Publications

Bicknell A.A., Niwa M. (2009) Hog1 MAP kinase plays a central role in a late-phase endoplasmic reticulum stress response pathway (*submitted*).

Babour A., **Bicknell A.A.**, Tourtellotte, J., Niwa M. (2009) ER surveillance (ERSU) pathway monitors functional fitness of the endoplasmic reticulum (ER) during the cell cycle (*submitted*).

Bicknell A.A., Niwa M. (2008) Regulating endoplasmic reticulum function through the unfolded protein response. In R. Bradshaw and E. Dennis (Eds.) *The Handbook of Cell Signaling* (in press).

Brunsing R., Omari S.A., Weber F., **Bicknell A**, Friend L., Rickert R., Niwa M. (2008) B- and T-cell development both involve activity of the unfolded protein response pathway, *J Biol Chem* **283:** 17954-17961

Bicknell A.A., Babour A., Federovitch C.M., Niwa M. (2007) A novel role in cytokinesis reveals a housekeeping function for the unfolded protein response. *J Cell Biol* **177:** 1017-1027

Bondos S.E., Catanese D.J., Jr., Tan X.X., **Bicknell A.**, Li L., Matthews K.S. (2004) Hox transcription factor ultrabithorax 1b physically and genetically interacts with disconnected interacting protein 1, a double-stranded RNA-binding protein. *J Biol Chem* **279:** 26433-26444.

Bondos S.E., **Bicknell A**. (2003) Detection and prevention of protein aggregation before, during, and after purification. *Anal Biochem* **316:** 223-231

Presentations

Bicknell, A.A., Babour, A., and Niwa, M. ER-induced cell cycle delay. UCSD Division of Biological Sciences Annual Retreat, September 2006.

Bicknell, A.A., Babour, A., and Niwa, M.. ER-induced cell cycle delay in yeast (Poster Presentation). Society For Experimental Biology Cell Cycle Meeting, July 2006.

Bicknell, A.A., Babour, A., and Niwa, M. ER-induced cell cycle delay in yeast (Poster Presentation). Cold Spring Harbor Meeting on The Cell Cycle, May 2006.

Bicknell, A.A., Babour, A., and Niwa, M. Induction of the unfolded protein response impacts cytokinesis in budding yeast. Membrane and Organelle Biology Meeting, UCSD, March 2006.

Abstract of the Dissertation

Two MAP kinases regulate novel aspects of the endoplasmic reticulum stress response

by

Alicia Anne Bicknell

Doctor of Philosophy in Biology

University of California, San Diego, 2009

Professor Maho Niwa, Chair

Secreted proteins, plasma membrane proteins, and proteins that reside within the secretory pathway must be folded in the endoplasmic reticulum (ER), which provides an environment that allows the proper folding and assembly of these nascent proteins. In response to environmental and developmental signals, the cellular requirement for the ER's protein folding function can fluctuate. When the protein folding demand exceeds the ER's capacity, this results in the accumulation of unfolded proteins in the ER, a toxic condition known as ER stress. Currently, the only pathway known to respond to ER stress is the unfolded protein response (UPR) pathway, which rapidly activates genes that help expand the ER's folding capacity.

A genetic screen in yeast suggests that two mitogen-activated protein kinases (MAPKs), Slt2 and Hog1, might also become activated along with the UPR to help cells cope with ER stress. MAPKs function throughout eukaryotic cell biology to initiate cellular changes in response to environmental stimuli. In this dissertation, I show that Slt2 and Hog1 are activated by ER stress, I investigate the mechanism of activation for each kinase, and I define several downstream functions of the MAPKs during ER stress.

First, I show that ER stress in budding yeast induces a cytokinesis delay that correlates with alterations in the septin complex, an important regulator of cytokinesis. This cytokinesis delay is accompanied by a delay in ER inheritance. Both may serve to prevent the propagation of ER stress. The cytokinesis delay, septin alterations, and ER inheritance delay all depend upon the MAPK *SLT2*.

Second, I show that Hog1 becomes activated during late-stage ER stress, through a mechanism with UPR-dependent and UPR-independent components. Upon activation, Hog1 translocates from the cytoplasm to the nucleus, and then later returns to the cytoplasm. In the nucleus, Hog1 activates the transcription of at least one gene, *HSP12*. Hog1 also regulates the induction of autophagy during ER stress and appears to perform this function from the cytoplasm.

Overall, I show that the cellular response to ER stress is much broader than the UPR, involving the activation of additional signaling modules, and affecting a wide range of cellular processes.

Chapter 1: Introduction

1.1 INTRODUCTION

Secreted proteins and proteins that reside on the cell surface or within the secretory pathway begin their maturation process in the endoplasmic reticulum (ER). These proteins are synthesized in the cytosol, then targeted and translocated into the ER as nascent peptides (1). Upon entry into the ER lumen, nascent proteins associate with ER chaperones and protein modification enzymes to fold into their native functional structures. Because misfolded proteins may be toxic to the cell, only properly folded proteins are allowed to exit the ER to arrive at their final cellular or extracellular destinations. Incompletely folded proteins are retained in the ER for further processing and permanently misfolded proteins are marked within the ER for proteasome-mediated degradation (2-5). Thus, the ER serves as a master regulator for the complex and error-prone process of protein maturation, quality control, and trafficking. Furthermore, the ER must match its capacity for protein processing with the cell's dynamic need for protein synthesis, dictated by developmental and environmental cues.

The ER regulates its own protein processing capacity through an inter-organelle signaling pathway termed the unfolded protein response (UPR). The UPR is activated in the ER lumen when molecular sensors detect an accumulation of unfolded proteins that exceeds the ER's folding capacity, a condition known as ER stress. These sensors initiate a series of signaling events that reduce the influx of unfolded proteins into the ER and increase the ER's ability to properly process proteins and degrade those proteins that are

permanently misfolded (6). UPR regulation also extends beyond the ER, increasing the efficiency of post-ER protein processing steps to broadly enhance the cell's secretory capacity (2, 7). Under certain conditions, such as prolonged ER stress, or ER stress that cannot be reversed, the UPR pathway also has the ability to induce apoptotic cell death (8).

1.2 MOLECULAR SENSORS

In the mammalian ER, there are at least three molecular sensors that initiate UPR activation: IRE1, PERK, and ATF6. Each of these sensors is a transmembrane protein with a luminal domain that detects ER stress and a cytosolic domain that activates a downstream UPR signal. In *S. cerevisiae*, there is no homologue of PERK or ATF6; Ire1p is the only known UPR component at the ER membrane.

IRE1 is a bifunctional kinase/endoribonuclease ER-transmembrane protein that has two isoforms in mammalian cells, IRE1α and IRE1β. When its N-terminal luminal domain detects ER stress, IRE1 dimerizes or oligomerizes within the ER membrane (9, 10). Subsequently, its cytosolic kinase domain undergoes trans-autophosphorylation, thus causing the activation of its cytosolic endoribonuclease domain. IRE1's nuclease then cleaves a single UPR-specific intron from the mRNA encoding Hac1p in yeast, or XBP-1 in mammalian cells (11-14). In yeast, once this UPR-specific intron is removed from *HAC1*, the two exons are joined by tRNA ligase to produce the spliced form of the transcript (15). The *HAC1* mRNA splicing mechanism resembles that of tRNA splicing, such that a 2' phosphate remains at the splice junction after ligation (16). This phosphate

is subsequently removed by a 2' phospotransferase (Tpt1p) (17). In mammalian cells, Xbp-*1* exons are also joined following cleavage by IRE1, but the ligase that joins these exons has not yet been identified. Mouse embryonic fibroblats (MEFs) lacking *Tpt1* show no *Xbp-1* splicing phenotype (18), suggesting that tRNA ligase is not involved in mammalian UPR splicing. In addition to utilizing a unique mechanism, UPR-specific mRNA splicing is also unique in that it occurs in the cytoplasm (19) independently of the spliceosome.

This *HAC1*/*Xbp-1* splicing event is a key regulatory step in the UPR signal transduction pathway. Once spliced, *Xbp-1* and *HAC1* are translated to become transcription factors that bind to promoters of target genes and activate a broad UPR-specific transcriptional program that helps cells cope with ER stress (2, 7). XBP-1 binds at least three promoter elements with differing affinities; it binds strongly to the unfolded protein response element (UPRE) and more weakly to ER stress elements I and II (ERSE and ERSE-II) (20). Hac1p binds and activates the yeast UPRE-1, UPRE-2, and UPRE-3 (21, 22). However, only the spliced form of Hac1 or XBP-1 can serve this function. In yeast, the UPR intron is inhibitory to translation of *HAC1* (19, 23), so the unspliced protein has never been detected in the cell. In mammalian cells, splicing of *Xbp-1* mRNA results in a translational frame shift causing the production of a second form of the XBP-1 protein, with a unique C-terminus. This spliced form of XBP-1 is a far more potent transcriptional activator than the unspliced form (24). In addition, the *Xbp-1* and *HAC1* genes contain an ERSE and UPRE, respectively within their own promoters, allowing the

encoded proteins to potentiate the UPR signal by inducing their own transcription (25). Furthermore, in yeast, the splicing of *HAC1* leads to an increase in the level of Gcn4p protein by an unknown mechanism. Gcn4p is a transcription factor that activates, along with Hac1p, all three yeast UPRE's (22).

In mammalian cells, IRE1 has the additional function of recruiting the protein TRAF2 to the ER membrane (26). TRAF2, in turn, recruits, and activates ASK1 (27). ASK1 is a MAPK/ERK kinase kinase (MEKK) that ultimately activates the MAP kinase (MAPK), JNK (28). JNK is a well-known stress response protein that has the power to regulate multiple transcription factors (29). However, the precise function of JNK activation during ER stress is not yet clear.

PERK, the second ER sensor in mammalian cells, is a type-I ER-transmembrane kinase that also senses protein folding demands in the ER through its N-terminal domain (30, 31). Once activated by ER stress, PERK oligomerizes and autophosphorylates, thus activating its cytosolic kinase domain. PERK then phosphorylates the α subunit of eukaryotic translation initiation factor 2 (eIF2α), which rapidly shuts down translation in the cell (32-34). Translation attenuation during the UPR reduces the influx of newly synthesized proteins into the ER, thus alleviating ER stress. In addition, when translation efficiency drops, cyclin D1 levels rapidly diminish due to an intrinsically high turnover rate (35). This leads to a G1 phase cell cycle arrest, which is thought to expand the window of time for the cell to decide between adapting to the stress or undergoing apoptosis (36).

Although eIF2α phosphorylation signals a global decline in translation, it actually increases the translation of the transcription factor, ATF4 (37), which goes on to transcribe a second set of UPR-responsive genes (38). In addition to eIF2α, activated PERK phosphorylates the transcription factor Nrf2, thus allowing it to enter the nucleus (39) where it presumably regulates UPR-dependent gene expression. Currently, PERK is only known to phosphorylate eIF2α and Nrf2. However, multiple forms of phosphorylated PERK accumulate under certain UPR-inducing conditions (40), suggesting that this kinase may have additional undiscovered substrates. Future work will characterize these different forms of PERK and identify their unique cellular targets, if such targets exist.

ATF6, the third UPR molecular sensor, exists as two isoforms, ATF6α and ATF6β. It is a type-I ER transmembrane transcription factor that is required for the activation of many UPR target genes (41, 42). When its luminal domain senses ER stress, ATF6 moves into the Golgi, where it is accessible to Site 1 Protease (S1P) and Site 2 Protease (S2P). These proteases sequentially cleave ATF6, liberating the soluble N terminal domain into the cytosol (43). Upon release, this domain moves into the nucleus where it binds to ERSE and ERSE-II promoter elements to regulate a third branch of the UPR-specific transcriptional program (44, 45).

1.3 HOW MOLECULAR SENSORS DETECT ER STRESS

Although their downstream signals vary, IRE1, PERK, and ATF6 share the ability to self-activate upon sensing unfolded proteins in the ER. Precisely how these sensors

detect unfolded proteins is currently an area of active research, which focuses primarily on understanding the sensors' ER luminal domains. Despite little sequence homology among their luminal domains, IRE1, PERK, and ATF6 share some features of their unfolded protein-sensing mechanisms.

Shortly after the discovery of Ire1, it was proposed that a negative regulator might release Ire1's luminal domain during ER stress, thus causing its activation (46). Subsequently, it was discovered that the luminal domains of all three molecular sensors bind to the ER resident chaperone BiP in unstressed cells. Upon exposure to ER stress, they release BiP with kinetics that correlate well with their own activation (47). Therefore, an initial model suggested that BiP was the proximal sensor of ER stress, with its binding and release comprising the UPR activation switch for all three sensors. While this model was attractive, several recent findings suggest that the mechanism of unfolded protein sensing may not rely solely upon a simple model of BiP binding and release. *IRE1* deletion studies found that *ire1* mutants that cannot bind BiP are not constitutively active (48). Furthermore, a recent study monitored the kinetics of each sensor's activation during different types of ER stress. This study suggested that BiP release is not the rate limiting step for UPR sensor activation (40). Therefore, although it seems evident that BiP binding has a role to play in regulating the UPR pathway, we still do not fully understand the nature of this role, and whether this role is the same or different for each of the molecular sensors.

Recently, the crystal structure of the yeast Ire1p core luminal domain was solved, providing another clue about Ire1's activation mechanism (49). The crystal structure

shows that two monomers of Ire1p, when joined together, create a deep groove that is reminiscent of the peptide-binding pocket of the Major Histocompatibility Complex (MHC). Since the MHC binds a wide variety of peptides, this structural feature strongly suggests that Ire1's luminal domain directly binds misfolded proteins. This study also showed that residues lining the MHC-like groove are required for unfolded protein detection. However, a direct peptide-binding function for the groove has not yet been verified. If Ire1 does bind misfolded peptides, future work will need to address how this binding interplays with Ire1's binding of BiP to regulate activity.

Crystal structures for PERK and ATF6 have not been solved. Like IRE1, PERK and ATF6 release BiP from their luminal domains during UPR activation (47). However, BiP release may play a more prominent role in the activation of these sensors, as deletion of the BiP binding site in their luminal domains is sufficient for constitutive activation (50, 51). In addition, it is possible that PERK directly binds unfolded peptides, as secondary structure predictions indicate that PERK's luminal domain folds similarly to IRE1 (49).

In addition to BiP release and possible peptide binding, post-translational modifications within the luminal domains of UPR sensors may also play a role in their activation. In response to ER stress, ATF6 becomes hypo-glycosylated and its disulfide bonds reduced. Reducing ATF6's intermolecular disulfide bonds converts it from an oligomer to a monomer, a conversion that is necessary but not sufficient for its transport to the Golgi and efficient cleavage by S1P (52). Hypo-glycosylation of ATF6 also contributes to its Golgi transport and activation, although the precise reasons for this are

not yet clear (53). A potential role for luminal modifications of PERK and IRE1 has not been thoroughly examined. However, mutating four conserved cysteines in PERK's luminal domain (54) or one conserved glycosylation site in IRE1's luminal domain (55) had no impact on the ability of either sensor to detect unfolded proteins.

Although we do not yet have a complete understanding of how the three UPR sensors detect unfolded proteins, emerging evidence indicates that slight differences in this sensing mechanism allow each sensor to respond with different sensitivities to specific types of ER stress. The use of pharmacological agents such as DTT or the ER calcium importin inhibitor thapsigargin has been instrumental in revealing these sensitivity differences. For example, breaking disulfide bonds in the ER rapidly activates ATF6 and slowly activates PERK-mediated eIF2α phosphorylation, whereas depleting calcium in the ER quickly phosphorylates eIF2α and slowly activates ATF6 (40). Various physiological conditions of ER stress impose unique types of protein-folding load on the ER, and each activated sensor elicits a different, but overlapping, transcriptional program. Therefore, the distinct ER-sensing mechanisms may be adapted to differentially activate each sensor according to the specific type of stress present in the ER lumen, thus allowing a fine-tuning of the mammalian UPR pathway.

1.4 DOWN-REGULATING THE UPR

The three sensors of the UPR pathway induce a wide array of overlapping, but non-identical, physiological changes. Some of these changes promote adaptation to ER stress and survival, while others lead to apoptosis. Down-regulation of each branch of

the pathway is therefore critical in achieving the appropriate cell fate following ER stress. Although we still have a limited understanding of how the cells shuts off the UPR, it is clear that each branch is down-regulated by several mechanisms, each of which is a potential point for modulation of the pathway.

As autophosphorylation of Ire1 is critical for its activation, attenuation of Ire1 is likely to involve phosphatase activity. Two phosphatases, Ptc2p (56) and Dcr2p (57), have been implicated in the dephosphorylation and down-regulation of yeast Ire1p, but an IRE1 phosphatase in mammalian cells has not yet been found. However, mammalian cells do have an interesting mechanism of down-regulating the XBP-1. During the induction phase of the UPR, XBP-1 up-regulates its own transcription. The combined kinetics of IRE1 activation and *Xbp-1* transcription, coupled with the distinct degradation rates of the spliced and unspliced proteins, leads to an immediate accumulation of spliced XBP-1 protein, followed by a gradual increase in the unspliced protein. During the late stages of UPR induction, unspliced XBP-1 dimerizes with the spliced form, causing it to be removed from the nucleus and degraded by the proteasome (58), thus shutting down XBP-1-mediated transcription and turning off the pathway.

Reminiscent of XBP-1 down-regulation by its own unspliced isoform, ATF6α-mediated transcription may be down-regulated by the activation of ATF6β. Both isoforms of ATF6 are activated by ER stress, but ATF6α has a much shorter half-life than ATF6β (59). *In vitro*, the two proteins can compete for binding to the ERSE, but ATF6α is a much stronger transcription factor than ATF6β. These data suggest a model in which the ERSE is primarily bound by ATF6α during UPR induction, and target gene

transcription is therefore strongly activated. During later UPR stages, because ATF6β is more stable than ATF6α, it begins to outcompete ATF6α for ERSE binding. Since ATF6β is a weak transcription factor, this binding reduces the transcription of ERSE-containing genes (60). The ATF6 branch of the UPR pathway is also down-regulated upstream of transcription, at the level of ATF6 proteolytic cleavage. NUCB1 is a Golgi-localized protein that gets induced by ATF6 during UPR activation. Upon increased expression in the Golgi, NUCB1 interferes with the S1P-ATF6 interaction, thus causing reduced ATF6 cleavage and nuclear translocation, and shutting off the ATF6 pathway by a negative feedback mechanism (61).

Like ATF6, PERK can be inhibited both at the level of its own activation, and at the downstream event that it regulates, in this case eIF2α phosphorylation. To directly inhibit PERK activity, ATF6 activates the transcription of *P58*^{IPK}. P58^{IPK} is a DnaJ family protein that binds and inhibits PERK's kinase domain, causing the downregulation of eIF2α phosphorylation, and the reversal of translational inhibition (62, 63). In addition, ATF4 activates the transcription of *GADD34*, a subunit of PP1c phosphatase, which directly dephosphorylates eIF2α during the later stages of ER stress, thus allowing cells to resume normal translation rates (64-66). PERK inactivation and recovery of protein synthesis are crucial to the adaptive function of the other two branches of the UPR pathway, as these branches rely upon an increased transcription and translation of protein-folding enzymes, as well as the translation of spliced XBP-1. In the absence of functional GADD34, when protein synthesis rates do not recover, spliced *Xbp-1* does not accumulate and XBP-1 target genes are not expressed.

1.5 CELLULAR EFFECTS OF UPR INDUCTION

Broadly, the UPR is defined as a pathway that senses ER stress, and elicits cellular changes in response to this stress. Most of these cellular changes are adaptive, allowing the cell to cope with the toxic conditions imposed by ER stress. As part of this adaptive response, the UPR increases the cell's protein folding and secretory capacity, adjusts the protein-folding load in the ER, and degrades potentially toxic misfolded proteins. When adaptation is not possible or not desired, the UPR can also induce apoptosis. These adaptive and apoptotic responses are discussed in detail below.

Increase in Secretory Capacity

To help cells cope with an insufficiency in secretory protein processing, the UPR utilizes all three of its transcription factors (XBP1/Hac1p, ATF4, ATF6) to expand the cellular machinery that produces mature secretory proteins. Specifically, UPR target genes increase the ER's physical volume, as well as its protein-folding activity, and also act to enhance post-ER protein processing functions.

In both yeast and mammals, ectopic expression of the spliced, active form of *HAC1*/*Xbp-1* transcription factor has been shown to expand the volume of the rough ER (7, 67, 68). In yeast, it is clear that the UPR pathway transcriptionally activates many phospholipid and inositol metabolism genes (2). Although it is presumed that these genes are responsible for the lipid biogenesis that the ER's physical expansion requires, the exact mechanism for generating extra ER membrane is not yet known. In mammals, expression of spliced *Xbp-1* increases the production of phosphatidyl choline, the primary

phospholipid component of ER membranes (68, 69). This lipid production is accompanied by the XBP-1 mediated production of choline cytidylyltransferase, a rate limiting enzyme of the phosphatidyl choline biosynthetic pathway (69, 70) Presumably, activation of this enzyme is at least partially responsible for the dramatic expansion of the ER that is induced during the UPR.

In addition to expanding the ER's physical volume, the UPR also increases the production of enzymes that reside in the ER and facilitate the process of protein folding. Chaperones, co-chaperones, disulfide bond catalyzing enzymes, and glycosylation enzymes are all transcriptional targets of UPR activation in yeast and mammalian systems (2, 7, 71). Chaperone proteins fall into two main classes: heat shock family chaperones and chaperone lectins (carbohydrate-binding proteins). Heat shock family proteins, which include BiP (Grp78) and Grp94, recognize hydrophobic regions of unfolded proteins and assist these proteins in achieving their appropriate conformation through a process that utilizes repeated rounds of ATP hydrolysis and ADP exchange. Co-chaperones, such as ERdj4, assist in ATP hydrolysis, and are required for proper chaperone function (72, 73). The second class of chaperones, the chaperone lectins, includes the ER membrane protein, calnexin, and the luminal protein, calreticulin. These proteins bind to carbohydrate moieties of unfolded glycoproteins to promote their proper folding and exit from the ER (74).

Secretory protein maturation also requires the formation of specific intramolecular disulfide bonds. Disulfide bonds are formed within the ER by a series of reactions that ultimately uses molecular oxygen to oxidize free thiol groups on cysteine

residues. These reactions are catalyzed by the ER resident oxidoreductases, ERO1 and PDI (Protein Disulfide Isomerase), both of which are strongly induced by the UPR pathway (75-78).

Finally, the UPR is responsible for inducing a large number of ER resident glycosylation enzymes. Glycosylation within the ER promotes proper protein folding in two key ways. First, glycosylation moieties are often an intrinsic component of a protein's native conformation, as they can help stabilize the structure of a protein, or increase its solubility. Second, glycans are used to tag unfolded proteins, so that they can be recognized by lectin chaperones to promote proper folding. If they remain unfolded for too long, glycan-tagged proteins are recognized and processed by the cell's protein degradation machinery (74).

Although the signal to stimulate UPR activity is initiated specifically within the lumen of the ER, the cell takes a very broad approach in responding to this signal. In addition to increasing the ER's protein-folding capacity, the UPR appears to enhance the processing and trafficking of secretory proteins after they exit the ER. Genes involved in ER to Golgi transport, Golgi function, Golgi to ER transport, and exocytosis are all activated by UPR transcription factors in response to ER stress (2, 70, 79).

Adjustment of Protein-Folding Load

After exiting the nucleus, mRNAs associate with ribosomal subunits in the cytosol to form an initiation complex and begin translation. During translation, those nascent proteins that are destined for the secretory pathway reveal a signal sequence that

emerges from the ribosome and is recognized by the signal recognition particle (SRP). The SRP associates with the SRP receptor on the ER membrane to deliver the peptide and its associated ribosome to the translocon. Here, translocation of the secretory protein proceeds co-translationally into the ER lumen (1).

To cope with high levels of ER stress, the UPR adjusts the influx of nascent proteins into the ER. Thus, any step in the process of protein production and translocation is a potential point of regulation by the UPR. To date, studies have shown that mRNA stability, translation, and translocation are altered during ER stress. Modulating these points of protein production can stop the arrival of nascent proteins to the ER, where the protein-folding machinery is already overwhelmed. In addition, this modulation might free ribosomes and transolocons to engage in the production of chaperones and other proteins critical for re-establishment of ER homeostasis.

mRNA stability

A genome-wide study, examining steady state mRNA levels and transcriptional changes in mammalian cells (80), revealed that more than 800 transcripts become destabilized in response to ER stress. The purpose and mechanism for this destabilization are not yet clear, but one clue may come from a study in *Drosophila* (81). Here, it has been shown that IRE1 mediates the degradation of a specific subset of mRNAs, in a manner that is independent of XBP-1. Specifically, IRE1 promotes the internal cleavage of certain transcripts, generating RNA fragments that are subject to degradation by housekeeping machinery. It is not yet known how IRE1 signals this event, but one intriguing possibility is that IRE1's ribonuclease domain directly catalyzes the

endonucleolytic cleavage of the transcripts in question. In this case, IRE1 might simply act as a nonspecific nuclease, and regulation of mRNA stability might occur via IRE1 activation and mRNA recruitment to the ER membrane, where IRE1 resides.

Genome-wide analysis shows that IRE1-mediated mRNA degradation specifically targets transcripts that encode plasma membrane and other secreted proteins, but spares transcripts that directly promote protein folding within the ER (80), suggesting that the purpose of degradation is to reduce the load of unfolded protein substrates in the ER. How the cell achieves this specificity is not yet clear. Interestingly, the ER-targeting signal sequence is necessary for transcript degradation. This suggests that the degradation machinery targets only those transcripts that are being translated at the ER membrane, providing a mechanism for selection of secretory proteins. However, the means of escape for protein-folding enzymes, which also contain a signal sequence and are translated at the ER membrane, has not yet been explored.

Translation

To reduce the influx of unfolded proteins into the ER, the cell also takes the approach of down-regulating translation during ER stress. In mammalian cells, the UPR is able to inhibit translation in at least two key ways. First, IRE1β promotes the cleavage of 28S ribosomal RNA during ER stress, causing a moderate decline in protein synthesis (82). Although cleavage does require a functional IRE1 ribonuclease domain, it is not yet known whether IRE1 directly cleaves rRNA, or indirectly promotes the cleavage event.

Second, as described in the introduction, PERK activation mediates a translation block during ER stress. When phosphorylated by PERK kinase, eIF2α is unable to

exchange its associated GDP for GTP (83). Since this exchange is an obligate step in translation initiation, PERK-dependent translation inhibition can be quite dramatic, reducing translation to 10 % under certain conditions of ER stress. This inhibition is rapid and precedes the slower transcriptional branches of the UPR pathway. It is therefore considered the "first line of defense" against ER stress (84). *Perk* knockout cells are severely impaired in ER stress survival, and this defect can be rescued by external means of translation inhibition (85).

Budding yeast do not have a *Perk* homologue. However, they do have eIF2α and several eIF2α kinases that are able to repress translation. One of these kinases, Gcn2p seems to function during the UPR (22). Therefore, it is surprising that the yeast UPR does not appear to repress translation (86). We do not yet understand why PERK-mediated translational repression is crucial to the mammalian UPR, but dispensable for budding yeast.

PERK-dependent translational inhibition was initially thought to equally affect mRNAs translated in the cytosol and those translated at the ER membrane. However, recent studies suggest that translation in each compartment is actually affected differently by ER stress (87). In the cytosol, ER stress causes mRNAs to move from a strongly translated polyribosomal fraction, to a nonribosome-associated fraction. By contrast, mRNAs at the ER shift from large polyribosomes to smaller polyribosomes and 80S monosomes. Furthermore, ribosomes at the ER membrane remain ER-associated after induction of the UPR. Thus, ER stress decreases translation in both the cytosol and the ER, but a low level of translation is maintained at the ER membrane. During ER stress,

Bip, *Xbp-1*, and *Atf4* all continue to be translated at the ER. This suggests that while reduced translation serves to decrease the protein-folding load in the ER, the low level of translation at the ER is maintained for the preferential production of those proteins that help the ER resume homeostasis. This preferential translation at the ER membrane extends to proteins, such as XBP-1 and ATF4, that do not contain a signal sequence and are not destined to translocate into the ER (87). How such mRNAs are targeted to the ER membrane, and why this targeting promotes escape from translational repression remain open and provocative questions.

Translocation

In addition to targeting nascent secretory proteins to the translocon, the signal sequence of a nascent peptide actually interacts with the translocon to promote protein translocation into the ER lumen (88). Some signal sequences promote efficient translocation, while others are less efficient, and this variation in translocational ability is conserved (89). One purpose of this signal sequence variation is to provide another means of coupling the influx of proteins into the ER to conditions within the cell. Under conditions of ER stress, proteins containing an inefficient signal sequence undergo co-translocational degradation, whereas efficiently translocated proteins remain unaffected. This process, termed "pre-emptive quality control," may protect the cell from the toxic effects of protein aggregation, as those proteins that tend to aggregate in the ER have a weaker signal sequence, and are therefore substrates for degradation (90, 91). It stands to reason that proteins that reside in the ER and enhance protein folding might contain

strong signal sequences, which would render them resistant to co-translocational degradation during ER stress, but this has not yet been demonstrated.

Degradation of Terminally Misfolded Proteins

ER-Associated Degradation

Despite the fact that protein-folding enzymes outnumber folding substrates in the unstressed ER (92), the protein-folding process is error-prone and a large percentage of secretory proteins permanently misfold. If allowed to escape the ER, these misfolded proteins could be highly toxic to the cell. They are therefore retained in the ER and subsequently recognized and degraded by the ER-Associated Degradation (ERAD) pathway (93). During ER stress, the ER's protein folding machinery is overwhelmed, and permanently misfolded proteins accumulate to especially high levels. The UPR enables the ER to safely clear these accumulated substrates by enhancing ERAD activity (2). This function of the UPR is vital, as overexpression of a misfolded ERAD substrate has little impact on wild type cells, but is lethal to yeast that do not have an intact UPR (86). Furthermore, even in the absence of stress, simultaneously disabling both the ERAD and UPR pathways is synthetically lethal (2).

ERAD begins when components within the ER lumen or ER membrane recognize an unfolded ER substrate to be permanently misfolded, thus distinguishing it from a legitimate folding intermediate that still could achieve its appropriate conformation. This recognition process is complex and incompletely understood. In mammalian cells, EDEM appears to recognize misfolded glycosylated proteins, and HERP helps recognize

misfolded proteins that are not glycosylated (94). In yeast, Yos9p (95, 96) and EDEM's homologue Htm1p (97) have both been implicated in misfolded glycoprotein recognition. Following recognition, misfolded substrates are delivered to an unknown channel, where they are retrotransolocated into the cytoplasm. Once retrotranslocation has begun, the HRD1/HRD3 E3 ubiquitin ligase complex catalyzes the polyubiquitination of the misfolded protein (98, 99). The protein is then completely extracted from the ER by the p97 ATPase complex (Cdc48p in yeast), and delivered to the cytosolic proteasome for degradation (100).

During ER stress in yeast, Hac1p is known to activate *HRD1*, *HRD3*, and *UBC7*, an E2 ubiquitin conjugating enzyme required for Hrd1p/Hrd3p function (2). In the mammalian UPR, XBP1 has been shown to activate *Edem*, *Herp*, *Derlin1* (which is involved in retrotranslocation), and *Hrd1* (7, 70, 71). ATF6 activates *Herp* and *Hrd1* (71). Thus, the UPR takes a broad approach, increasing the efficiency of multiple steps in the ERAD pathway, in order recognize and destroy proteins that cannot achieve their appropriate conformation.

Autophagy

Autophagy is a mechanism of bulk degradation, whereby large portions of the cytosol and its resident organelles are engulfed by a double lipid bilayer. The resulting subcompartment, termed the autophagosome, ultimately fuses with the lysosome (or vacuole in yeast) so that its components can be degraded and recycled. Autophagy is best understood as a means of enduring starvation conditions, when recycled cellular content

can replace nutrient supplementation to provide for the cell's most essential functions. During nutrient deprivation in yeast, the cell initiates autophagy by transcribing the ubiquitin-like gene, *ATG8*. Once translated, Atg8p undergoes a series of modifications, including lipidation, which are required for autophagosome formation. After lipidation, Atg8p co-localizes with, and probably helps to form pre-autophagosomal structures (PASs) in the cytosol. These PASs nucleate autophagosomes, which ultimately fuse with the vacuole, which degrades the autophagosomal content (101).

Recently, it has become evident that autophagy is also activated during ER stress in both yeast and mammals (67, 102-104). This process, termed "ER-phagy," is thought to help the cell withstand the stress. Although we are just beginning to understand how ER-phagy helps the cell cope with ER stress, current data suggest that it supplements the ERAD pathway in clearing unfolded proteins from the ER (105, 106). In addition, it might be used to counterbalance the membrane expansion that is induced by the UPR (67). Most models suggest that during ER stress autophagy causes ER membranes and their resident misfolded proteins to be engulfed, delivered to the lysosome, and degraded. This engulfement might occur indiscriminately, or subcompartments of the ER might be designated for misfolded protein targeting, and ultimate disposal. In support of the idea that ER-Phagy specifically degrades ER, ER-phagy-induced autophagosomes in yeast cells contain membranes that appear to be derived from the ER. Furthermore, inhibiting autophagy interferes with the disposal of certain misfolded mutant secretory proteins (105, 106) and causes the accumulation of potentially toxic protein aggregates (104, 107).

Although little is known about the autophagic mechanism during ER stress, it does appear to overlap somewhat with starvation-induced autophagy. During ER stress, Atg8p is induced and lipidated (103), although other autophagic modifications to the protein have not been examined. Atg8p then co-localizes with cytosolic structures, which appear similar to PASs, although they are more numerous than the PASs formed during starvation. It is thought that these Atg8p-containing structures help nucleate autophagosomes during ER stress because they are juxtaposed to ER-induced autophagosomes and because *ATG8* is required for autophagosome formation during ER stress (67). Although there are some similarities between ER-phagy and starvation-induced autophagy, the autophagosomes produced by each process differ in their content, and therefore must be derived by processes that are somehow distinct. Future studies will seek to understand the similarities between ER-phagy and starvation-induced autophagy, and define mechanistic features of each process.

Precisely how ER stress triggers the activation of autophagy is also poorly understood. In yeast, *IRE1* and *HAC1* are not required for the induction of Atg8p. However, ectopic expression of the spliced form of *HAC1* is sufficient to induce accumulation of Atg8p protein, but not sufficient to induce PAS formation. This suggests that both *HAC1*-dependent and *HAC1*-independent pathways emanate from the ER to regulate various aspects of the autophagic process in yeast (67). However, the precise nature of this regulation remains to be uncovered. In mouse and human cell lines, *Ire1*-/- cells are defective in inducing autophagy during ER stress. However, IRE1 appears to trigger autophagy through its phosphorylation of JNK, rather than by splicing

Xbp-1 (102, 104). Furthermore, expression of dominant negative *Perk*, or an unphosphorylatable mutant of *eIF2α* can inhibit ER-induced autophagy in certain cell types, suggesting that PERK also has the ability to promote autophagy during ER stress (107). However, the mechanism linking PERK to the autophagic pathway is completely unknown.

Apoptosis

In addition to providing a wide array of adaptive responses to help the cell survive ER stress, the UPR can also trigger apoptotic cell death. This outcome is presumably reserved for cases of ER stress when adaptation is not possible or not desired. ER-induced apoptosis depends upon the activation of pro-apoptotic Bcl-2 family members, BAX and BAK (108, 109), which reside in the cytosol, mitochondria, and ER. In response to various apoptotic signals, these proteins oligomerize and insert themselves into the outer mitochondrial membrane, where they trigger cytochrome c release and caspase activation. During ER stress, inhibiting mitochondrial membrane permeabilization and cytochrome c release reduces apoptosis, indicating that the UPR utilizes this mitochondrial apoptotic pathway (110). Some evidence also suggests that BAX and BAK can promote apoptosis directly from their position within the ER. During ER stress, BAX and BAK assume their activated forms within the ER membrane and caspase 12, which is ER-localized, becomes activated in a *Bax*/*Bak*-dependent manner. Furthermore, targeting BAK to the ER is sufficient to activate caspase 12 and trigger apoptosis (111). However, the mitochondrial pathway, rather than the ER-specific

pathway, is probably the dominant means of inducing apoptosis during ER stress, as caspase 12 knockout MEFs are only mildly resistant to UPR-induced apoptosis (112).

During ER stress, the UPR signals the activation of BAX and BAK in at least two key ways. Firstly, all three UPR transcription factors induce the expression of *Chop*, a transcription factor that is partly required for ER-induced apoptosis (113). Upon expression, CHOP downregulates the transcription of *Bcl-2*, a BAX/BAK inhibitor (114) and increases the expression of the BAX-activating protein, DR5 (115). Secondly, during ER stress, IRE1 activates a MAP kinase pathway that results in JNK activation. Cells that cannot activate JNK during ER stress are partially resistant to apoptosis (27). It is not yet known how JNK activates apoptosis during ER stress. However, in response to other apoptotic stimuli, JNK has been shown to inhibit the BAX/BAK inhibitors BCL-2 and BCl-xL and activate the pro-apoptotic proteins, BIM and BMF. Furthermore, JNK activates several transcription factors, which activate a wide variety of genes including some that induce apoptosis. When apoptosis is the appropriate response to ER stress, the UPR pathway clearly relies upon CHOP and JNK activation to communicate this to the apoptotic machinery. However, it remains to be seen whether these two pathways account for all UPR-induced apoptosis, or whether additional pathways exist to promote apoptosis during ER stress.

In response to an unfolded protein stimulus in the ER, the UPR can activate numerous adaptive responses and apoptotic signals, whose combined effects either allow the cell to survive ER stress, or apoptotically kill the cell. We do not yet understand the exact conditions that induce apoptosis over survival, nor do we know the mechanism of

detecting these conditions and integrating them into a cell fate decision. This mechanism must depend upon conditions within the ER, including the type, severity, and duration of ER stress, which are probably sensed through the differential activation and repression of the three molecular UPR sensors. In addition, a cell's fate during ER stress depends upon its broader physiological environment, including cytosolic conditions, cell type, and developmental cues. Current research, focusing on the interplay between cellular context and UPR induction, will shed light on how the UPR arrives at cell fate decisions, and how these decisions are customized to promote survival of the organism.

1.6 PHYSIOLOGICAL UPR

The fundamental circuitry and logic of the UPR pathway were initially discerned with the help of pharmacalogical agents that cause extensive misfolding of bulk proteins in the ER and maximally activate all three branches of the pathway. However, it is now clear that the UPR has been refined to help the cell cope with a wide array of physiological situations that are more subtle than these pharmacalogical conditions of widespread protein misfolding. As expected, many secretory cell types invoke the UPR pathway to cope with their unusually high protein-folding load. Surprisingly, the UPR pathway has also been shown to be active in nonsecretory cells, and to perform nonsecretory functions. Furthermore, emerging evidence suggests that the UPR can sometimes serve a housekeeping function, maintaining an appropriately equipped ER, even when levels of ER stress are low. As discussed below, the tissue-specific nature of

the UPR's involvement in cell function highlights the complexity and flexibility of the UPR pathway.

A Pathway Specialized for Secretion

Tissues that primarily function in protein secretion, such as the liver, pancreas, salivary glands, and skeletal secretory cells, exhibit the most dramatic requirement for UPR components. In these cell types, the UPR is thought to respond to an increased secretory load by expanding the ER's function. Lacking this ability to expand, UPR-deficient cells continue to experience extreme ER stress and ultimately undergo apoptosis.

Ire1α-/- and *Xbp-1*-/- mice die during development at E12.5 with small, apoptotic livers (116, 117), and *Xbp-1*-/- lethality can be rescued by expressing *Xbp-1* selectively in hepatocytes (118). Since enzyme secretion is a primary function of the liver, it has been proposed that the UPR's role in hepatocytes is to support their secretory activity, but the precise nature of this role remains to be discovered.

Mice that express *Xbp-1* only in the liver survive until birth, but soon develop defects of the exocrine pancreas and salivary glands (118), suggesting that the IRE1/XBP-1 branch of the UPR is active in these tissues. This idea is further supported by the fact that wild type mice highly express *Ire1α* and *Xbp-1* in the pancreas and salivary glands (119, 120). In addition to higher expression levels, *Xbp-1* splicing has been detected in the mouse pancreas (121) and *Drosophila* salivary glands (122), indicating activation of IRE1 in these cells. Furthermore, pancreatic acinar cells and salivary gland cells of *Xbp-1* knockout mice contain much less ER than their wild type

counterparts, and fail to secrete important digestive enzymes. As a result, these mice die of malnutrition soon after birth (118). Studies also suggest that PERK plays a role in the function of specialized secretory cells; PERK is activated in the exocrine pancreas and, like *Xbp-1*-/- cells, *Perk* -/- pancreatic cells have an abnormal ER and reduced secretion of digestive enzymes (123, 124).

Xbp-1 and *Perk* mRNA are also highly expressed in chondrocytes and osteoblasts of the developing mouse skeleton (120). These two cell types are the major secretory cells of the skeletal system; chondrocytes are responsible for the secretion of cartilage proteins and osteblasts secrete bone matrix proteins during development. Probably due to defects in the secretory function of these two cell types, *Perk*-/- mice have abnormal skeletal development, with reduced collagen production and defective bone matrix secretion (123). PERK appears to perform a similar function in the human skeletal system, as individuals with a genetic disorder caused by loss of PERK function also suffer from poor skeletal development (125).

Studies in the above secretory tissues have refined our understanding of *in vivo* UPR signaling. It is now clear that activation of a specific branch of the UPR does not necessarily induce that pathway's full repertoire of downstream effects. For example, in pancreatic acinar cells, XBP-1 is activated, but only a subset of XBP-1's target genes are transcriptionally induced (118). This may be because target genes differ in their sensitivities to XBP-1 activation, in which case the level of ER stress and the resulting level of XBP-1 activity might dictate the specific transcriptional program that is appropriate for a given cell type. Alternatively, the UPR pathway might intersect with

other pathways in order to refine its physiological effects on the cell. For example, certain cell types might induce transcriptional activators or repressors that act on the promoters of UPR target genes to enhance or dampen their transcription.

Inducing the UPR to Halt Protein Production

The tissues described thus far illustrate the ability of the UPR pathway to enhance protein secretion. In these cases, to allow for protein production, the cell must invoke some means of preventing or overcoming the translation attenuation that is normally caused by PERK activation. By contrast, in pancreatic β cells, translation attenuation is precisely the purpose of UPR induction. β cells detect high glucose levels in the bloodstream, and respond by secreting insulin. Following secretion, these cells must synthesize large quantities of insulin to replenish their stores and prepare for the next glucose stimulation. This process of insulin replacement is controlled by PERK-mediated eIF2α phosphorylation. In their basal state, β cells activate PERK to maintain high levels of eIF2α phosphorylation and low levels of translation. After glucose stimulation, eIF2α becomes dephosphorylated, allowing large amounts of insulin to be produced and directed to the secretory pathway. When the appropriate amount of insulin has been produced, PERK becomes reactivated by the abundance of insulin in the ER, and shuts off insulin production (123). As a result of their inability to control insulin production, the β cells of *Perk*-/- mice experience significant ER stress, causing them to undergo apoptosis around 4 weeks after birth. Consequently, β cells are depleted from the pancreas, causing deficient insulin production, hyperglycemia, and diabetes in *Perk*

knockout mice (123, 124, 126). Similarly, in humans, mutations in Perk have been linked to Wolcott-Rallinson Syndrome, which is marked by early onset diabetes (125).

Plasma Cells: Two Phases of UPR

In the peripheral immune system, mature B cells that encounter antigen differentiate to become antibody-secreting plasma cells. A role for the UPR in this process has been postulated for a long time, but only recently has experimental evidence supported such a role (127). As plasma cells differentiate, *Xbp-1* becomes transcribed (128) and spliced (129) and ATF6 becomes cleaved and activated (130). Ultimately, chaperones and other trafficking genes are transcriptionally activated (71), and the volume of the ER expands (7), thus allowing the plasma cell to produce and secrete large amounts of Ig. Proving the importance of XBP-1-mediated transcription in plasma cell differentiation, *Xbp-1*-/- B cells proliferate normally, but do not differentiate into plasma cells and do not secrete Ig. The expression of spliced *Xbp-1* restores Ig secretion in *Xbp1*-/- B cells, whereas the expression of an un-spliceable *Xbp-1* does not. Furthermore, expression of *Xbp-1* in an activated B cell line is sufficient to drive cells toward a plasma cell differentiation program (128). We do not yet know the significance of ATF6 activation in plasma cells, as *Atf6* knockout mice have only recently been generated (131, 132). More work will need to be done to characterize the plasma cell differentiation program in hematopoietic stem cells taken from these mice. Interestingly, PERK phosphorylation is not detected during plasma cell differentiation, suggesting that PERK

is not involved in this process. This is probably because translational inhibition would counteract the plasma cell's objective of generating large amounts of Ig (133).

These data all point to a classical model of UPR activation, whereby increased production of Ig crowds the ER and stimulates certain branches of the UPR pathway thus expanding the cell's capacity to secrete Ig. In support of this model, B cells deleted for Ig heavy chain produce less XBP-1 protein than wild type cells during differentiation (129). However, further studies uncovered several surprising aspects of the plasma cell UPR that argue against a simple classical model of activation. First, Ig production is not absolutely required for UPR induction during plasma cell differentiation. In cells deleted for heavy chain, some XBP-1 protein is produced during differentiation. Second, primary B cells that are activated through their B cell receptor are primed to initiate plasma cell differentiation, but do not differentiate and do not produce Ig. However, these cells do induce a modest amount of *Xbp-1* splicing, activate the transcription of chaperones, and expand their ER (134). Finally, the initiation of *Xbp-1* splicing, ATF6 cleavage, and chaperone expression during the course of plasma cell differentiation actually precede the production of Ig light and heavy chains (130, 135). Thus, in plasma cells the UPR appears to be active before an increased secretory load would mandate its activation.

Therefore, it is currently thought that the UPR is activated in two phases during plasma cell differentiation. First, in an "anticipatory phase," XBP-1 and ATF6 are activated prior to Ig production, to induce an initial expansion of the secretory pathway. Second, once Ig production begins, this imposes an increased secretory load that signals

further activation of the UPR and further expansion of the cell's secretory capacity. The discovery of an anticipatory UPR was unexpected, and the mechanism of activation during this phase is still entirely unknown. Perhaps, the UPR sensors have adjustable sensitivities, and within certain physiological settings such as the developing plasma cell, the threshold for activation is reduced. This would allow UPR induction in the plasma cell when unfolded protein levels are still relatively low. Another possibility is that certain types of unfolded proteins, which are specifically present in the developing plasma cell, can signal UPR activation even if they are not abundant and the ER is not overloaded.

Beyond the UPR's Secretory Function

In yeast, the UPR pathway activates the transcription of 381 genes, 208 of which have a known function. Half of these functionally characterized UPR target genes function in protein processing, secretion, or lipid metabolism, and are presumably activated to expand the cell's secretory capacity during ER stress. The other half of these UPR target genes act in non-secretory processes such as signaling, gene regulation, metabolism, and DNA repair (2). Similarly, of the hundreds of genes bound by XBP-1 in skeletal myotubes, plasma cells, and pancreatic β cells, approximately 40% perform non-secretory physiological functions, including cell growth and differentiation, RNA processing, signal transduction, and gene regulation (79).

Interestingly, in the mammalian system, this extra-secretory ability of the UPR manifests itself in a tissue-specific manner. A growing number of cell types require UPR

signaling for their specific differentiation programs and to perform their normal, non-secretory physiological functions. For example, in the developing liver, XBP-1 induces the expression of α1-antitrypsin, α-fetoprotein, transthyretin, and apoplipoprotein A1, all of which promote hepatic proliferation, but not secretory function (116). During neuronal development, *Xbp-1* is spliced and this splicing promotes axonal growth and branching (136). When expressed in myoblasts, spliced XBP-1 actually inhibits myotube differentiation through its activation of the myogenesis inhibitor, *Mist1* (79).

Reconstitution of *Rag2*-/- mice with *Ire1*-/- hematopoietic stem cells has revealed that *Ire1* is required in the pro B cell stage of early B lymphopoiesis for VDJ recombination, a process that does not require secretion (117). Furthermore, in the developing plasma cell, spliced XBP-1 induces a dramatic expansion of the ER and the broader secretory pathway, but it also regulates the increase in cell size, mitochondrial mass, and lysosomal content that are characteristic of terminally differentiated plasma cells (7). Moreover, spliced XBP-1 activates the transcription (137) and translation (69) of Ig heavy chain in the plasma cell, thus promoting Ig secretion even before it enters the secretory pathway. XBP-1 also enhances IL6 production (129), decreases CD44 expression, and increases Syndecan-1 expression (128), all changes that mark plasma cell differentiation but do not enhance secretory function.

Proper tissue development often depends upon reduced proliferation or apoptosis of selected cells. Surprisingly, in some cases, the UPR is responsible for triggering this inhibition in tissue growth. For example, during mammary acinar morphogenesis, loss of adhesion activates the PERK pathway, which downregulates translation. As a result, cell

proliferation is reduced, CHOP is activated, and apoptosis is modestly enhanced. Mammary acinar cells expressing a dominant negative *Perk* form abnormally large and amorphous acini, indicating that UPR-induced growth inhibition is a key component of mammary morphogenesis (138). Similarly, during the development of a mature muscle fiber, myoblasts fuse to form multi-nucleated myotubes, a process that requires a modest degree of myoblast apoptosis. ATF6 and caspase 12 are activated specifically in those myoblasts that are undergoing apoptosis, and preventing ATF6 cleavage prevents apoptosis and proper differentiation of the myotube. This indicates that the apoptosis signal that is necessary for proper myotube development is generated by the UPR (139). Therefore, in the mammary acinus and myotube, the UPR is selectively activated, not to enhance secretory function or to relieve ER stress, but to control cell growth and promote proper tissue differentiation. The surprising ability of the UPR to perform in this capacity emphasizes current gaps in our understanding of the upstream signals that activate the UPR and how cells can tailor downstream UPR signals to their specific physiological needs.

The UPR as a Housekeeping Pathway

The UPR is best-known for its role in responding to conditions of extreme ER stress, such as those imposed by the production of massive amounts of secretory protein or by pharmacalogical agents that cause widespread misfolding. Recently, it has become evident that the UPR also has the ability to regulate ER function under normal conditions, when ER stress levels are low. For example, during unstressed growth in diploid yeast,

basal *HAC1* mRNA splicing appears to inhibit meiosis and pseudohyphal growth, two differentiation programs that are only induced in response to nitrogen starvation (140). Basal *HAC1* splicing also supports efficient cytokinesis in yeast. In the absence of ER stress, *hac1Δ* cells display a modest cytokinesis defect, and this defect is exacerbated when ER stress is applied (141). This implies that during normal cell growth, basal UPR signaling provides a higher level of ER function, which is required for efficient cytokinesis. Furthermore, in unstressed skeletal muscle cells, XBP-1 binds the promoters of 118 genes, most of which are involved in protein folding and trafficking (79). Since skeletal muscle cells have no apparent secretory function, and presumably do not experience ER stress, this XBP-1 binding represents a basal UPR activity, which most likely helps these cells maintain normal ER function.

The discovery that the UPR functions in unstressed cells has two possible non-mutually exclusive explanations. Firstly, constitutive low-level UPR activity may enhance the ER's basal function in a constant manner. In this case, the UPR would not have to be modulated to achieve its function, it would simply provide a constant level of support to the ER. If this is true, cells without a functional UPR would always have decreased ER function, but this might only be evident when examining processes that require maximal ER capacity. Secondly, the UPR might monitor basal fluctuations in ER functional demand, becoming slightly active when the cell calls for incremental increases in ER capacity, and then shutting off when this need is met. In this way, the cell could fine-tune the ER to its changing environment, and perhaps even avoid the dangers of sudden and extreme ER stress.

1.7 PERSPECTIVES

In the past, researchers have taken drastic measures to induce the UPR pathway and detect its activity. These measures included adding DTT to cells to reduce all protein disulfide bonds, adding tunicamycin to inhibit N-linked glycosylation, adding thapsigargin to inhibit ER calcium import, or overexpressing a misfolded mutant protein. Because these methods strongly activate all three branches of the UPR pathway and induce the UPR's full repertoire of cellular consequences, they allowed scientists to identify the pathway's molecular components and describe their breadth of cellular effects. Furthermore, the ability to detect UPR activity only after causing widespread protein misfolding allowed an appreciation of the pathway's potential as a "stress response pathway," inactive until a stress is encountered, then activated to cope with conditions of ER stress. In this chapter, I have highlighted some of the more recently discovered roles for the UPR in normal cell physiology. Physiological studies have begun to reveal that the specific nature of the UPR's activation can be quite different for different cell types, and that the pathway's function can range from stress response to general housekeeping.

During physiological instances of its activation, the UPR can be modulated on several different levels to achieve results that are fine-tuned to specific cellular contexts. One way that the UPR can be modulated is at the level of sensor activation. Although pharmacological agents lead to rapid and strong induction of all three UPR signaling branches, many physiological studies, including one study that measured several different levels of PERK activity in different mouse tissues (123), indicate that activation of a

given branch within a cell is not an "all or none" event. Only by moving away from strong external stressors have we begun to appreciate the pathway's potential for achieving intermediate levels of activity, operating more like a dimmer switch than an on/off switch. Furthermore, in many physiological cases, each UPR signaling branch appears to be tuned separately. For example, in the plasma cell, XBP-1 and ATF6 are activated strongly (128-130), but PERK activity has not been detected (133). Another layer of physiological fine-tuning of the UPR occurs subsequent to activation, where individual UPR branches can selectively activate portions of their downstream response. For example, pancreatic acinar cells induce *Xbp-1* splicing, but only activate a subset of XBP-1's target genes. Therefore, under physiological conditions the cell can utilize several strategies to modulate the UPR pathway according its specific requirements, thus lending the pathway enormous versatility and flexibility. One of the challenges now is to dissect the precise mechanisms that allow this modulation.

Certain physiological instances of UPR activation confirm the pathway's role as a stress response pathway that becomes active when it senses high levels of unfolded proteins in the ER. For example, high levels of collagen synthesis in chondrocytes or Ig production in plasma cells can activate the UPR pathway, which in turn increases the secretory capacity of these cell types and allows them to achieve their secretory function. However, more recent studies indicate that the UPR pathway also has a role to play in cells that do not appear to be experiencing ER stress. For example, even before they begin to produce Ig, plasma cells seem to induce the UPR pathway (130, 134, 135), indicating that some mechanism must be in place to induce the pathway when stress

levels are low. Even in some nonsecretory cell types, the UPR pathway is active at low levels. This basal UPR activity probably performs the housekeeping function of helping the ER sustain its basal protein-folding capacity. As of yet, this basal UPR activity has only been detected in a few circumstances. For example, in the unstressed skeletal muscle, XBP-1 binds to a subset of its promoters (79), and during unstressed growth in budding yeast, cytokinesis requires UPR signaling (141). However, studies of the UPR's potential housekeeping function have been hindered by a lack of sensitive methods to detect low levels of UPR activation. It is likely that the development of more sensitive assays will uncover a broad role for basal UPR signaling in helping many cell types maintain normal cellular function. This housekeeping role of the UPR, though subtle, may be a key aspect of the UPR's physiological function. In fact, other signal transduction pathways might also serve housekeeping functions that have been overlooked due to subtle activation levels. The model of a single pathway serving both a housekeeping function and a stress response function could be utilized for multiple aspects of cellular regulation, and may turn out to be a common mode of signal transduction.

ACKNOWLEDGEMENTS

Chapter 1 is modified from material that has been accepted for publication in *Handbook of Cell Signaling, 2nd Edition*, 2009, Elsevier, Ralph A. Bradshaw and Edward A. Dennis (Eds.). Alicia A. Bicknell and Maho Niwa. I was the primary author of this chapter under the direction of Maho Niwa.

Chapter 2: A novel role in cytokinesis reveals a housekeeping function for the unfolded protein response

2.1 ABSTRACT

The Unfolded Protein Response (UPR) pathway helps cells cope with endoplasmic reticulum (ER) stress by activating genes that increase the ER's functional capabilities. We have identified a novel role for the UPR pathway in facilitating budding yeast cytokinesis. Though other cell cycle events are unaffected by conditions that disrupt ER function, cytokinesis is sensitive to these conditions. Moreover, efficient cytokinesis requires the UPR pathway, even during unstressed growth conditions. UPR-deficient cells are defective in cytokinesis, and cytokinesis mutants activate the UPR. The UPR likely achieves its role in cytokinesis by sensing small changes in ER load and making according changes in ER capacity. We propose that cytokinesis is one of many cellular events that require a subtle increase in ER function, and that the UPR pathway has a previously uncharacterized housekeeping role in maintaining ER plasticity during normal cell growth.

2.2 INTRODUCTION

The endoplasmic reticulum (ER) plays a crucial role in several important aspects of eukaryotic cell physiology. It assists in the folding and maturation of all nascent secretory proteins and initiates their distribution to the broader secretory pathway (142). In addition, the ER influences the overall composition of the cellular proteome by

mediating the ER-associated degradation (ERAD) pathway, a pathway that destroys permanently misfolded proteins and also responds to specific degradation signals to regulate the levels of certain native proteins (93). The ER also houses many lipid biosynthetic enzymes, which impact the relative composition and overall abundance of lipids throughout the cell (143).

Genes involved in protein folding, protein trafficking, ERAD, and lipid metabolism are all transcriptionally activated by a conserved, ER-initiated signal transduction pathway, called the Unfolded Protein Response (UPR) (2, 6, 144-146). In budding yeast, the UPR pathway begins with an ER transmembrane protein, Ire1p (9, 147). The N-terminus of Ire1p lies in the lumen of the ER where it senses the ER's condition. When Ire1p detects a need for increased ER function, it transmits a signal across the ER membrane to activate its own cytosolic kinase and endoribonuclease domains (9, 10, 12, 147). Activated Ire1p then initiates the unconventional, splicesome-independent splicing of *HAC1* mRNA (11, 12). Only the spliced form of *HAC1* mRNA can be translated, making the splicing step a critical point of regulation (19, 148). Upon translation, Hac1p localizes to the nucleus, where it acts as a transcription factor to upregulate a wide array of UPR target genes (11, 149), thus increasing the ER's capacity to serve its many functions (2).

Northern analysis, measuring the relative abundance of spliced *HAC1* mRNA in the cell, is currently the most commonly used method of detecting UPR activation (11). Using this technique, previous studies have detected UPR activation only during extreme conditions of ER stress. For example, *HAC1* mRNA splicing has been detected in cells

treated with pharmacological agents that cause widespread protein misfolding (11, 149), or in cells overexpressing mutant proteins that fold improperly (86). The inability to detect *HAC1* mRNA splicing during normal growth has led to the designation of the UPR pathway as a "stress response pathway." However, it is likely that cellular demand for ER function is dynamic, even during unstressed growth conditions. This evokes the intriguing possibility that the UPR pathway, in addition to responding to conditions of extreme stress, manages the everyday challenges of fluctuating ER demand. This housekeeping function for the UPR has been previously unnoticed, perhaps because it induces a level of Ire1p activity that is too subtle to be detected by conventional *HAC1* northern analysis.

Because progression through the cell cycle requires dramatic molecular and cellular changes, we hypothesized that cell cycle progression requires fluctuations in ER capacity. To isolate a cell cycle event that requires particularly high ER functionality, we used ER stress as a tool to disrupt ER function. We then asked whether any particular cell cycle event was sensitive to this reduction in ER capacity. Most cell cycle events that we examined did not require exceptionally high ER activity, as they occurred normally during ER stress. However, cells experiencing ER stress were specifically defective in cytokinesis, suggesting that elevated ER functionality is required for cells to carry out efficient cytokinesis.

Since cytokinesis required a greater ER capacity than other cell cycle events, we tested the possibility that the UPR plays a role in achieving an increased ER capacity during normal, unstressed cytokinesis. Indeed, we found that UPR-deficient cells were

unable to carry out efficient cytokinesis, even in the absence of external ER stress. This is the first time the UPR pathway has been shown to function in cells that are growing optimally, expressing no misfolded mutant proteins, exposed to no protein misfolding agents, and not differentiating into high volume secretory cells. Our study, therefore, supports the concept of a UPR that continuously fine-tunes the ER to accommodate everyday fluctuations in ER functional demand.

2.3 RESULTS

HAC1 mRNA splicing occurs during unstressed growth

Because previous *HAC1* northern analysis has not uncovered HAC1 mRNA splicing in unstressed cells (11), we carried out a *HAC1* northern with 30 μg of RNA, rather than the 10 μg of RNA that are traditionally assayed. Under these conditions, we could clearly detect the spliced form of *HAC1* in unstressed, optimally grown, wild type cells. This spliced form constituted 7.4 +/-0.6% of total *HAC1* mRNA (Fig. 2.1). Basal splicing was *IRE1*-dependent, suggesting the presence of a bona fide UPR signal in unstressed cells. The results of our northern analysis, which we confirmed by RT-PCR (Fig. 2.2), prompted us to seek a functional relevance for basal UPR induction.

ero1-1 cells are delayed in the cell cycle with high DNA content, large buds, and divided nuclei

To determine whether this low level of UPR activity has a role in cell cycle progression, we used the *ero1-1* temperature sensitive allele to identify cell cycle stages

that are sensitive to ER perturbations. In the yeast ER, the essential proteins Ero1p (Endoplasmic Reticulum Oxidoreductin 1) and Pdi1p (Protein Disulfide Isomerase 1) work together to catalyze oxidative protein folding (77, 150, 151). For cells carrying the *ero1-1* temperature sensitive allele, growth at the restrictive temperature rapidly induces ER stress (76, 152).

In asynchronous cultures, restrictive growth of *ero1-1* cells caused an accumulation of cells with a 2C or greater DNA content (Fig. 2.3). This suggests that ER stress delays cell cycle progression at a point subsequent to DNA replication. To specifically define this ER sensitive stage of the cell cycle, we induced ER stress in α factor synchronized *ero1-1* cells (Fig. 2.4A). When grown at the restrictive temperature, synchronized *ero1-1* cells experienced severe ER stress, as measured by *HAC1* splicing (Fig. 2.4B & C). Compared to wild type cells, these ER-stressed cells proceeded normally through the initial stages of the cell cycle. By 30 min following temperature shift, both cell types completed DNA replication, thus adopting a 90-95% 2C DNA content (Fig. 2.4D and quantitated in Fig. 2.4E). After 1 h of growth at 37º C, wild type cells began to divide and re-enter G1 phase. By contrast, only a small percentage of *ero1-1* cells divided at 37ºC. Instead, ER-stressed cells retained a 2C DNA content or began to acquire abnormally high amounts of DNA (Fig. 2.4D).

Microscopic examination of synchronized wild type and *ero1-1* cells revealed that ER-stressed cells were delayed with large buds and divided nuclei. After 30 min of 37º C growth, 90% of cells of each cell type had initiated bud formation (Fig. 2.4F & H). After 45 min, both cell types remained budded, and by this time, 60-70% of both cell

populations had divided nuclei (Fig. 2.4G). After 1 h, wild type cells began to divide and become newly divided unbudded cells with a single nucleus. By contrast, *ero1-1* cells did not divide, but remained budded with divided nuclei for the remainder of the time course (Fig. 2.4F & G), suggesting that ER stress slows the cell cycle at a point after nuclear division, probably during late M phase, or cytokinesis. In fact, many *ero1-1* cells began to adopt a multi-budded morphology after 1.5 h of 37º C growth (Fig. 2.4H). This multi-budded morphology was never seen in wild type cells. The appearance of extra buds coupled with the appearance of 3C/4C DNA peaks strongly suggests that *ero1-1* cells initiate a new round of the cell cycle, despite a block or delay in the previous cell division.

Tunicamycin-treated cells are delayed in the cell cycle with high DNA content, large buds, and divided nuclei

In order to confirm that ER stress is specifically responsible for delaying the cell cycle in *ero1-1* cells, we examined the effects of another well-characterized ER stress inducer, tunicamycin (Tm), on cell cycle progression. Tm inhibits N-linked glycosylation in the ER, which causes the accumulation of unfolded proteins. Consistent with previous reports, (153, 154), we found that Tm inhibits the budding process when added immediately after α factor release (Fig. 2.5). Budding inhibition is known to activate the morphogenesis checkpoint and induce a G2/M delay (155), which would likely obscure a subsequent ER-induced delay. Therefore, we introduced Tm to

synchronized cultures 30 minutes after G1 release, after cells had already initiated the budding process (Fig. 2.5).

Tm treatment recapitulated the cell cycle effects of the *ero1-1* mutation. As expected, Tm-treated cells displayed 90% *HAC1* mRNA splicing 1 h after α factor release (Fig. 2.6A & B) and retained maximal UPR induction for the entire 3 h time course. Both Tm-treated and untreated synchronized cultures contained approximately 90% 2C cells after 1 h, indicating that they had progressed through S phase and into G2/M phase (Fig. 2.6C & D). After 1.25 h of growth, untreated cells began to divide, as indicated by the return to a 1C DNA content, then continued through the next cell cycle, ultimately losing synchronicity. Like *ero1-1* cells, Tm-treated cells failed to divide and instead began to attain a 3C or 4C DNA content (Fig. 2.6C).

Untreated and Tm-treated cells were approximately 90% budded after 1 h of synchronized growth (Fig. 2.6E). After 1.5 h of growth, untreated cells divided and became unbudded before re-entering the next cell cycle. Tm-treated cells remained 80%-90% budded for the entire duration of the time course. Furthermore, after 1.75 h of growth, Tm-treated cells began to attain a multi-budded morphology (Fig. 2.6G).

We also examined the timing and integrity of nuclear division in Tm-treated cells. In addition to following the segregation of DAPI bodies in these cells, we expressed a GFP fusion protein that localized to both copies of chromosome IV (see Materials and Methods). This allowed us to visualize sister chromatids segregating to separate nuclei during nuclear division (156) to confirm that DNA segregation was occurring appropriately. We found that nuclear division occurred with the same kinetics in Tm-

treated cells as in untreated cells, as both conditions allowed approximately 45% of cells to divide their nuclei after 1 h of growth and approximately 75% of cells to divide their nuclei after 1.25 h of growth (Fig. 2.6F). After 1.5 h of growth, untreated cells divided to become unbudded cells with a single nucleus. Tm-treated cells continued to contain 70%-80% divided nuclei for the remainder of the time course. Furthermore, we never observed DAPI bodies separating with improperly segregated sister chromatids, indicating that mitosis occurred properly in these Tm-treated cells (Fig. 2.6G, white arrows denote GFP-marked chromosomes). Therefore, similar to *ero1-1* cells grown at the restrictive temperature, cells experiencing ER stress due to Tm treatment were delayed with a budded morphology after nuclear division.

Tm treatment and *ero1-1* restrictive growth had very similar effects on the cell cycle, strongly suggesting that these effects are the specific result of ER stress, rather than ER-independent effects of Tm treatment or the *ero1-1* allele. To verify that the cell cycle is sensitive specifically to ER stress, we examined the effects of Tm treatment on the cell cycle of synchronized *hac1*Δ cells. Since *HAC1* is required for recovery from ER stress, *hac1*Δ cells should be unable to recover from any specific effect of ER stress, but should respond normally to ER-independent stimuli. Indeed, the absence of *HAC1* rendered cells incapable of recovering from the Tm-induced appearance of cells with a high DNA content. The percentage of 3C/4C cells in the wild type, Tm-treated populations peaked at 40% after 2 h of growth (Fig. 2.8A & B), then began to decline, reaching 25% after 3 h of growth. By contrast, *hac1*Δ cells continued to be 40%-45% 3C/4C for the entire 3 h time course.

ER stress induces cytokinesis delay

To distinguish between the possibilities of a late M phase delay or a delay in cytokinesis, we examined the effect of ER stress on several mitotic events: Clb2p production/degradation, Cdc14p release, and mitotic spindle formation/depolymerization. Clb2p is a major regulator of cell cycle progression. Its levels increase as cells enter mitosis and decrease as cells exit mitosis. Cells delayed in mitotic exit typically display sustained high levels of Clb2p (157). Directly following temperature shift (0 h time point) both wild type and *ero1-1* cells contained very low levels of Clb2p (Fig. 2.7A), consistent with most cells' being in G1 or S phase. In both cell types, Clb2p levels began to increase 30 min after temperature shift, marking mitotic entry 15 min before nuclear division (Figs. 2.6F & 2.7A). Similarly, Clb2p degradation, marking mitotic exit, occurred at the same time (60 min) in wild type and *ero1-1* cells. In wild type cells, this Clb2p decrease correlated well with the onset of cytokinesis (Figs. 2.6E & 2.7A), but in *ero1-1* cells, cytokinesis did not occur.

The key events of mitotic exit are signaled by the phosphatase Cdc14p, which is only active during anaphase. During all other times in the cell cycle, Cdc14p is kept inactive by virtue of its nucleolar localization. After nuclear division, Cdc14p is released into the nucleus and cytoplasm where it signals multiple key cell cycle events, including the completion of Clb2 degradation, the breakdown of the mitotic spindle, and cytokinesis (158, 159).

Ten minutes after temperature shift, for both wild type and *ero1-1* cells, Cdc14p-GFP co-localized with a portion of the nucleus, consistent with the expected nucleolar

localization of Cdc14p (Fig. 2.7B). After 55 min of 37°C growth, both cell types released Cdc14p-GFP into their nucleus and cytoplasm, demonstrating that these conditions of ER stress did not delay Cdc14p release. After 70 min of 37°C growth, wild type cells divided and resumed nucleolar localization of Cdc14p. *ero1-1* cells also reabsorbed Cdc14p into the nucleolus after 70 min of growth, but these cells did not divide and eventually assumed a multi-budded morphology (Figs. 2.6G & 2.7B).

Finally, we used a *TUB1*-GFP fusion gene (160) to examine the formation and breakdown of the mitotic spindle during ER stress. By 45 min after temperature shift, both wild type and *ero1-1* cells exhibited fully formed mitotic spindles between their two spindle pole bodies, indicating that ER stress did not delay spindle formation. Spindle breakdown also occurred at the same time (75 min) in both cell types. Again, *ero1-1* cells did not divide and in the absence of cell division, some *ero1-1* cells re-replicated their spindle pole bodies, re-budded, and re-formed a mitotic spindle, thus forming the unusual cells depicted in Fig. 2.7C (150' panel).

We also examined Clb2 fluctuations, Cdc14p release, and mitotic spindle formation and breakdown in synchronized untreated and Tm-treated cells. We found that, like *ero1-1,* Tm had no effect on these mitotic markers (Fig. 2.8). Therefore, ER stress delays cell division, but does not affect mitotic entry, mitosis, or mitotic exit, suggesting that ER stress specifically inhibits cytokinesis or cell separation.

Cytokinesis creates a membrane barrier between mother and daughter cell. After cytokinesis, the septum continues to hold the two cells together; the septum must be degraded for cell separation to occur (161). Experimentally, lyticase can be used to

degrade the septum of delayed cells, thus differentiating between a cytokinesis defect, and a defect in cell separation.

Lyticase treatment demonstrated that ER-stressed cells fail to divide because of incomplete cytokinesis, rather than incomplete cell separation. We collected *ero1-1* cells 2.5 h after temperature shift, as described in Fig. 2.4A, except α factor was added back to the medium 45 min after G1 release to prevent initiation of a second cell cycle. As before, most cells were delayed with a budded morphology at this time point. Their delay was clearly caused by a cytokinesis defect, as 79% of these budded cells were resistant to cell separation by lyticase treatment (Fig. 2.7E). Confirming that lyticase treatment only separated cells that had completed cytokinesis, wild type cells in M phase (collected 1 h after α factor release) remained 96% budded after lyticase treatment. In addition, *cts1Δ* cells, which are known to be defective in cell separation (162), were 43% budded 1.5 h after α factor release (data not shown). Of the budded *cts1Δ* cells, 86% were separated by lyticase (Fig. 2.7E), confirming that the experimental conditions used here were sufficient to dissociate the majority of separation-defective cells.

Successful cytokinesis requires that cortical actin patches become polarized to either side of the bud neck late in the cell cycle (163-167). We followed actin patch localization in synchronized cells and found that wild type and *ero1-1* cells displayed bud localized cortical actin patches throughout S phase, G2 phase, and most of M phase (Fig. 2.7D). Just prior to cytokinesis, the actin patches of *ero1-1* cells redistributed to the bud neck in a manner indistinguishable from wild type cells (Fig. 2.7D). Therefore, the ER

stress-induced cytokinesis defect is not caused by a delay or alteration in actin patch redistribution.

Unfolded Protein Response signaling facilitates cytokinesis during normal cell growth

The induction of ER stress in synchronized cell populations revealed that cytokinesis is highly sensitive to the state of the ER. This suggests that ER capacity increases during cell division, a process that might be facilitated by UPR signaling. To determine whether UPR signaling affects cytokinesis during normal cell growth, we examined cytokinesis in *hac1*Δ strains. In the absence of any external ER stressor, wild type cell populations never exhibited cells with a greater than 2C DNA content. By contrast, after 1.5 h of normal synchronized growth, 15% of untreated *hac1*Δ cells were greater than 2C. This number increased to 20% after 2 h of growth and remained approximately 20% until the end of the 3 h time course (Fig. 2.9A). Untreated *hac1Δ* cells were almost as cytokinesis deficient as wild type cells treated with Tm (Fig. 2.9A compare wt +Tm to *hac1*Δ -Tm). Furthermore, we examined *hac1Δ* and *ire1Δ* strains for the multi-budded morphology that is indicative of cells with a cytokinesis defect. We found that a small percentage of cells (<1%) did display this multi-budded morphology, whereas we never observed multi-budded cells in wild type populations (Fig. 2.9C). A complete cytokinesis block should cause a much higher percentage of cells to attain multiple buds. Therefore, UPR mutants are delayed in cytokinesis, rather than blocked.

To further investigate the link between UPR signaling and the cytokinesis process, we measured basal UPR activity in various cytokinesis mutants using a 4xUPRE-GFP reporter construct (77). *MLC2*, *CHS2*, *HOF1*, *CYK3*, and *BNI1* all participate in cytokinesis (see Discussion). Of the cytokinesis mutants tested, *mlc2Δ* and *chs2Δ* strains did not exhibit basal UPR activity (Fig. 2.9D). However, in the absence of any external ER stress induction, *hof1Δ*, *cyk3Δ* and *bni1Δ* strains exhibited 3-6 fold UPR reporter gene expression, compared to wild type cells. This level of reporter activity reflects a true link between the UPR and cytokinesis, as *hrd1Δ*, and *doa10Δ* mutants, which are ERAD-deficient and known to induce functionally significant levels of UPR activity (2, 168), exhibited similar levels of reporter gene expression. The finding that some cytokinesis mutants exhibit UPR activation is quite novel; the detection of basal UPR activity has been previously limited to mutants with specific ER defects.

2.4 DISCUSSION

A Housekeeping Function for the UPR: How the ER Adapts to Normal Fluctuations in Cellular Demand

In eukaryotic cells, critical cellular functions are organized and carried out by functionally specialized organelles. This compartmentalization of function eases the maintenance of cellular homeostasis, as each organelle can separately control its own function in accordance with the complex requirements of the cell. The endoplasmic reticulum (ER), for example, has a vital role in the production of lipids and proteins that make up the secretory pathway, plasma membrane, and, in yeast, the cell wall. Even

during normal, unstressed growth, different internal cellular conditions, such as different stages of the cell division cycle, probably require different levels of ER functionality. However, the precise mechanism of adapting ER function to suit physiological fluctuations in internal cellular conditions is unknown. Because such a mechanism would be capable of sensing the condition of the ER and adjusting the ER's capacity, the UPR pathway is an excellent candidate for a mechanism of ER adaptation.

In our study, we have shown that cytokinesis requires higher levels of ER functionality than other cell cycle events. This finding implies that ER functionality increases during cytokinesis, and allowed us to examine the UPR's role in achieving this functional increase. We found that UPR-deficient strains were cytokinesis defective. In addition, several cytokinesis-defective strains displayed elevated basal UPR activity. Taken together, our data establish a function for the UPR pathway in facilitating cell division during normal cell growth. The UPR presumably achieves this function by adapting ER capacity.

The UPR's role in cytokinesis, revealed by this study, represents a novel type of UPR activity, as it can be detected during optimal, unstressed growth conditions. All previous studies of UPR mutants describe their inability to respond to unusually stressful growth conditions such as inositol starvation (9, 169), drug treatments that induce widespread protein misfolding (9, 147), overexpression of a misfolded mutant protein (86, 170-172), or development into a specialized secretory cell (128-130, 135). Each of these known UPR-requiring conditions imposes a massive load on the ER. The newly discovered importance of UPR signaling during normal cell growth uncovers a novel

housekeeping function for the UPR pathway. In addition to responding to stressful growth conditions, the UPR must monitor and manage the cell's fluctuating ER requirements.

The UPR's ability to serve a housekeeping function sheds new light on the mode of UPR activation. In theory, the UPR pathway might operate according to one of two modes of activation. It could activate in a manner similar to an "on/off switch." In this case, the pathway remains "off" until a threshold level of stress is experienced, at which point the pathway "turns on" and becomes highly active. Alternatively, the UPR pathway might operate as a "dimmer switch," in which the "off state" and "on state" actually represent two extremes on a continuum. Previous studies have investigated the UPR pathway by inducing crisis levels of ER stress. If the UPR pathway could fine-tune the level of ER function, this could actually prevent such an ER crisis by allowing gradual adaptation of ER capacity.

Data from previous studies provide support for both modes of activation. In support of the "on/off switch" mode of activation, *HAC1* mRNA remains unspliced during normal cell growth, but becomes rapidly and efficiently spliced upon treatment with DTT or Tm, or overexpression of misfolded proteins (11). In addition, certain modest amounts of ER stress have been shown to not activate the UPR pathway at all. For example, expression of the misfolded mutant protein, CPY*, from its genomic locus does not activate UPR signaling, and ER-associated degradation of genomic CPY* does not require UPR components (170, 171). However, data is also accumulating to support the "dimmer switch" mode of UPR activation. For example, certain mutations in the

ERAD pathway have been shown to induce intermediate levels of UPR activity (2, 11, 170, 171). Our study further supports the "dimmer switch" mode of UPR activation, as we have shown that subtle activation of the UPR pathway contributes to efficient cytokinesis.

The ER's Role in Cytokinesis

Although DNA replication, mitotic entry, spindle formation, nuclear segregation, Cdc14p release, mitotic exit, spindle disassembly, and actin patch repolarization all occur normally during ER stress, cytokinesis does not (Summarized in Figure 2.10). Therefore, we have found that ER stress specifically disrupts cytokinesis, and we have ruled out the possibility that this disruption is due to a defect in actin patch relocalization. This disruption could be due to a stress-induced attenuation of any of the ER's many functions, including secretion, ERAD, or phospholipid metabolism.

Despite the ER's well-characterized role in initiating protein secretion, it remains unknown whether ER stress inhibits the entire secretory pathway. If it does, there are several reasons that this may impact cytokinesis. Cytokinesis begins with the assembly and contraction of an actomyosin ring. In animal cells, it has been shown that membrane deposition at the cleavage furrow must accompany actomyosin ring contraction, for proper cytokinesis to occur (173, 174). The extra membrane, which is delivered in the form of secretory vesicles, presumably relieves the tension created by membrane constriction. Perhaps, like in animal cells, the yeast secretory pathway assists in

cytokinesis by providing new membrane to the site of ring contraction, and it is lack of membrane at the bud neck that prevents cytokinesis under conditions of ER stress.

Regardless of whether membrane addition *per se* is required for yeast cytokinesis, it is clear that Golgi-derived vesicles are targeted to the yeast bud neck at the end of the cell cycle, and that these vesicles assist in the process of cytokinesis. Firstly, vesicles carry cargo that is necessary for actomyosin ring contraction. Cells that are defective in vesicle fusion assemble an actomyosin ring normally, but the assembled ring is unstable and does not properly contract (175). Secondly, during cytokinesis, secretory vesicles provide the yeast bud neck with the enzymes responsible for septum formation, a process that is essential for yeast cytokinesis (175-177). Therefore, if ER stress disrupts vesicle trafficking, this could slow membrane deposition, ring contraction, and/or septation, and thereby delay cytokinesis, thus explaining the results of our study. This explanation implies that during normal cytokinesis, the UPR manifests its housekeeping function by increasing the cell's secretory capacity, thus fulfilling the enhanced secretory requirements of cytokinesis.

Despite expectations that ER stress would broadly inhibit secretion, some studies find that ER stress has a minimal impact, if any, on the overall secretory pathway (86, 172). This suggests that the ER might play a role in cytokinesis through one of its cellular functions besides protein folding and trafficking. This possibility is especially intriguing, as it implies that the UPR pathway can detect ER functional cues other than the simple accumulation of unfolded proteins in the ER. Though previous studies have

not tested this prospect directly, UPR target genes represent the entire spectrum of ER functions (2).

In addition to functioning in protein folding and secretion, the ER has the task of regulating phospholipid metabolism. Since cytokinesis entails a membrane fusion event and the creation of a membrane barrier between mother cell and daughter cell, it is not surprising that certain phospholipids are necessary for its proper completion. Phosphatidylethanolamine and phosphatidylinositol 4,5-bisphosphate become locally concentrated to the cleavage furrow during cytokinesis in various eukaryotic cell types. Interfering with the production of either of these two phospholipids results in a cytokinesis defect (178-181). Therefore, the disruption of cytokinesis by ER stress may be due to the effects of ER stress on phospholipid metabolism. If this is the case, the UPR's role during normal cytokinesis may be to upregulate genes involved in phospholipid metabolism.

Three cytokinesis mutants *bni1Δ, hof1Δ*, and *cyk3Δ* exhibit constitutive UPR activity. Strains deleted for *MLC2* or *CHS2*, which are involved in the cytokinesis processes of actomyosin ring disassembly and septum formation respectively (176, 182), did not activate the UPR. During yeast cytokinesis, *BNI1* promotes actomyosin ring assembly (183), *HOF1* coordinates ring contraction with septum formation (182, 184), and *CYK3* mediates septum formation (185). There is no indication that any of these mutants are defective in protein secretion or any other aspect of ER function. This is the first instance of UPR activity in mutants that are not directly defective in an ER-associated function. Furthermore, unlike previous cases of basal UPR activity in

mutants, none of these three genes is a UPR target gene (2). Therefore, the UPR induction in these mutants does not represent the cell's attempt to transcriptionally activate the specific gene that is absent. Increased UPR activity in *hof1Δ*, *cyk3Δ*, and *bni1Δ* strains probably helps these cells partially overcome their cytokinesis defect. This implies that the UPR pathway can directly or indirectly sense and modify the cell's cytokinesis efficiency.

Our data highlight a new role for the UPR pathway in cytokinesis. Cytokinesis probably represents only one of many normal cellular functions that invoke a moderate level of UPR induction. Though difficult to detect, these instances of moderate UPR induction could help the ER constantly maintain an appropriate capacity in a fluctuating cellular environment.

ACKNOWLEDGEMENTS

We are grateful to Randy Hampton, Arshad Desai, and Lorraine Pillus for reagents and for scientific discussion. We also thank Randy Hampton for critical reading of this chapter and Steven Reed for scientific advice.

Chapter 2 is modified from material that was published in *The Journal of Cell Biology*, 2007, Vol. 177, No. 6, 1017-1027. Alicia A. Bicknell, Anna Babour, Christine M. Federovitch, and Maho Niwa. I was the primary investigator and author of this paper under the supervision of Maho Niwa. Anna Babour conducted experiments depicted in Figures 2.7B-D and Figures 2.8B-D and Christine M. Federovitch conducted experiments depicted in Figure 2.9D.

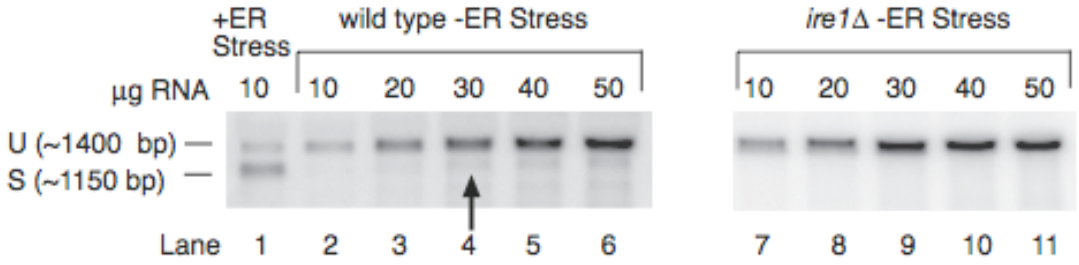

Figure 2.1 *HAC1* mRNA splicing occurs during unstressed growth: Wild type cells (MNY1002) were treated with 1 µg/ml tunicamycin for 1.5 h to induce UPR. 10µg of RNA were loaded on northern gel (Lane 1). Indicated amounts of RNA from untreated asynchronous wild type (MNY1002) cells (Lanes 2-6) and *ire1Δ* (MNY1011) cells (Lanes 7-11) were loaded on northern gel. Gel was probed with *HAC1* specific probe to detect unspliced (U) and spliced (S) forms. Arrow indicates presence of spliced *HAC1* in unstressed sample.

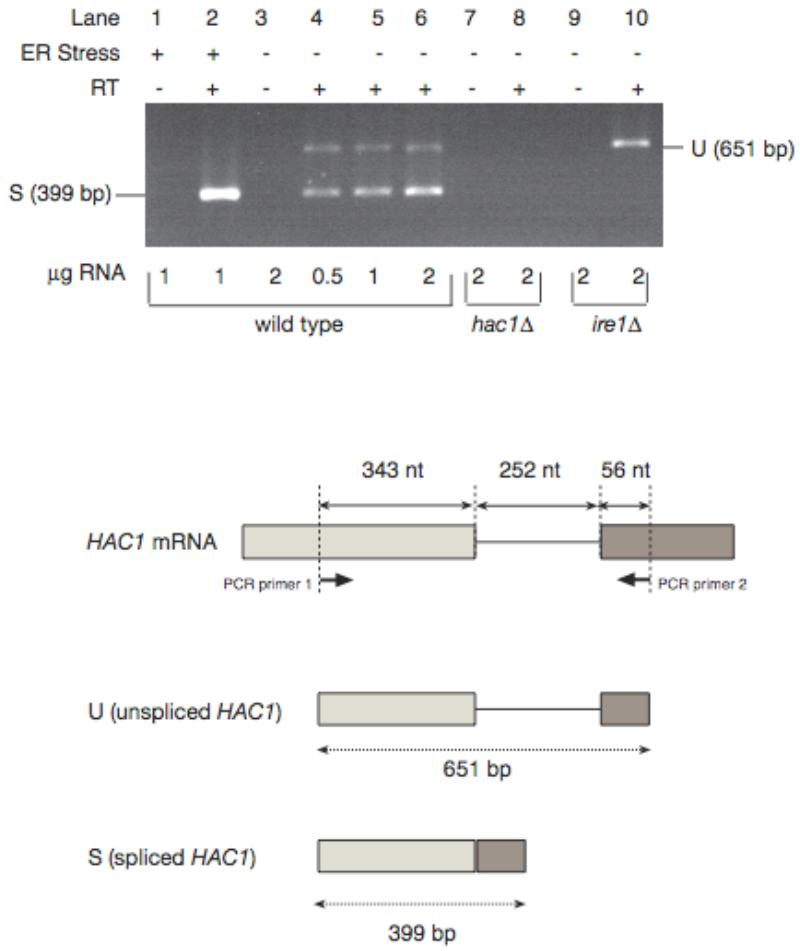

Figure 2.2 RT-PCR detects spliced *HAC1* mRNA in unstressed cells: RNA was isolated from wild type (MNY1002), *ire1Δ* (MNY1011), and *hac1Δ* (MNY1010) cells, grown in the absence (lanes 3-10) or presence (lanes 1-2) of 1 µg/ml Tm, and RT-PCR was performed. Indicated amounts of RNA were added to initial cDNA synthesis reaction, +/- RT indicates whether or not reverse transcriptase was added to reaction. 1/10 of this reaction volume was subjected to 25 cycles of PCR amplification, using PCR primers that recognize *HAC1* cDNA 343 bp upstream of the intron (forward), and 56 bp downstream of the intron (reverse). Because the *HAC1* intron is 252 bp in length, unspliced *HAC1* PCR product (U) is 651 bp and spliced *HAC1* PCR product (S) is 399 bp. Due to its significantly smaller size, spliced *HAC1* was amplified with a greater efficiency than unspliced *HAC1*. Therefore, although this assay clearly establishes that spliced *HAC1* mRNA is present in unstressed cells, it overrepresents the extent of basal *HAC1* splicing.

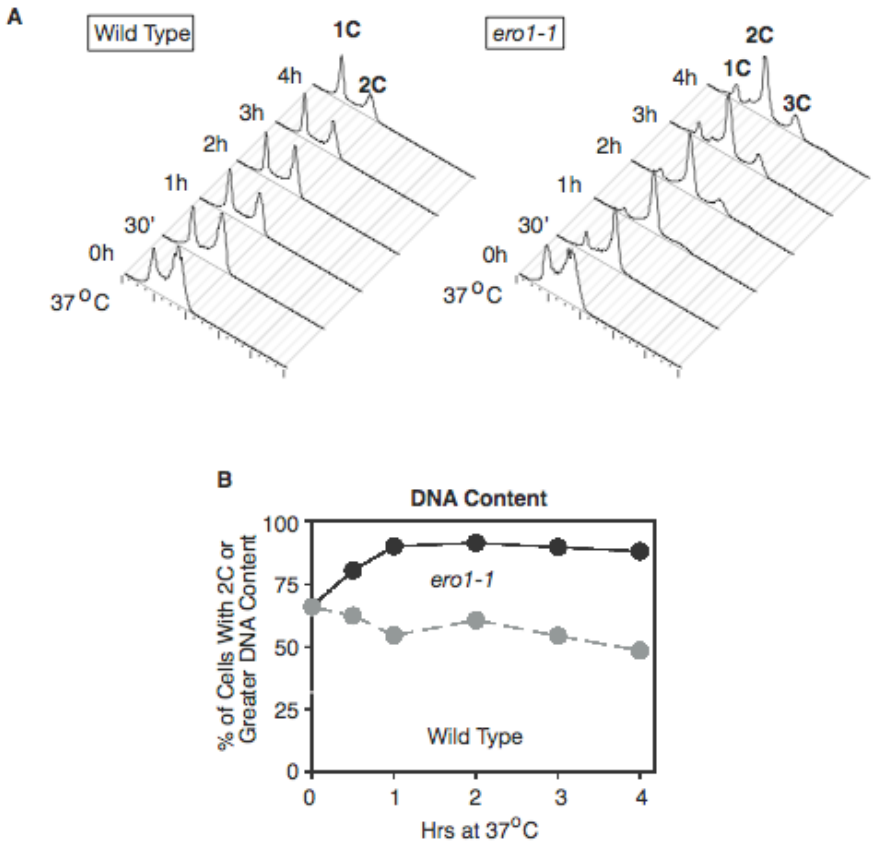

Figure 2.3 ER stress, induced by Ero1p inactivation, causes G2, M, or cytokinesis delay: Wild type (MNY1001) and *ero1-1* (MNY1002) asynchronous cells were grown at the permissive temperature, and then shifted to the restrictive temperature (0 h) to induce ER stress in *ero1-1* cells. (A) Flow cytometric analysis of cells stained with Sytox Green to measure total DNA content. (B) Quantitation from (A) of the percentage of cells in the population that were 2C or greater. During growth at the permissive temperature, wild type and *ero1-1* cells both displayed an asynchronous distribution of 34% G1 or S phase cells (1C or between 1C and 2C) and 66% G2 or M phase (2C) cells. Following shift to 37° C growth 30 min & 1 h time points), the percentage of wild type cells in G1 transiently increased (shown as decrease in % 2C/3C cells), presumably due to the well-characterized (186) heat shock-induced G1 to S phase cell cycle delay. Following recovery from heat shock, at later time points, wild type cells once again accumulated in G1 phase, probably due to a gradual depletion of nutrients in the growth medium (187). In contrast to wild type cells, *ero1-1* cells did not experience the normal accumulation of G1 phase cells in response to heat shock or nutrient deprivation. After 30 minutes of ER stress, induced by growth at the restrictive temperature, the percentage of *ero1-1* cells exhibiting a 2C DNA content increased from 66% to 80%. By one hour of 37° C growth, 90% of *ero1-1* cells had a 2C DNA content. Interestingly, a small population of 3C *ero1-1* cells appeared at this time point. For the remaining four hours of growth at 37° C, *ero1-1* cells never resumed normal cell cycle progression. Error bars represent standard deviation of three repeats.

Figure 2.4 *ero1-1* cells are delayed in the cell cycle with high DNA content, large buds and divided nuclei: Wild type (MNY1002) and *ero1-1* (MNY1003) cells were shifted to 37°C following α factor synchronization and 25 min of recovery at 25°C. The 25 min after α factor removal prevented cells from undergoing the heat-specific G1/S phase delay that was observed in asynchronous experiments (Fig. 2.3), thus allowing examination of subsequent, ER-specific cell cycle effects. (A) Schematic representation of experiment. Note 0 h time point is defined as the time of shifting to 37º C growth. (B) Northern analysis with *HAC1* specific probe shows the conversion of unspliced *HAC1* mRNA (U) to spliced *HAC1* mRNA (S) in *ero1-1* cells experiencing ER stress upon growth at 37°C. (C) Quantitation of (B) calculated as spliced *HAC1* mRNA divided by total *HAC1* mRNA. (D) Flow cytometric analysis of cells stained with Sytox Green, a fluorescent dye that binds DNA quantitatively and emits fluorescence with an intensity corresponding to cellular DNA content (188). First peak in histogram (indicated as 1C) represents pre-replication cells and the second peak (2C) represents post-replication cells. Arrow indicates appearance of 3C cells, represented by a third peak. (E) Quantitation from (D) of the percentage of cells in the population that contained 2C or greater DNA content combined. (F) 200 cells per time point were scored as + or – bud. Graph represents the percentage of total cells that contained a bud. (G) Cells were stained with DAPI to visualize nuclei and 200 cells per time point were scored as + or – divided nuclei. Graph represents the percentage of total cells that contained divided nuclei. (H) Cells were stained with DAPI. Red arrow indicates additional bud. All error bars represent standard deviation of three repeats.

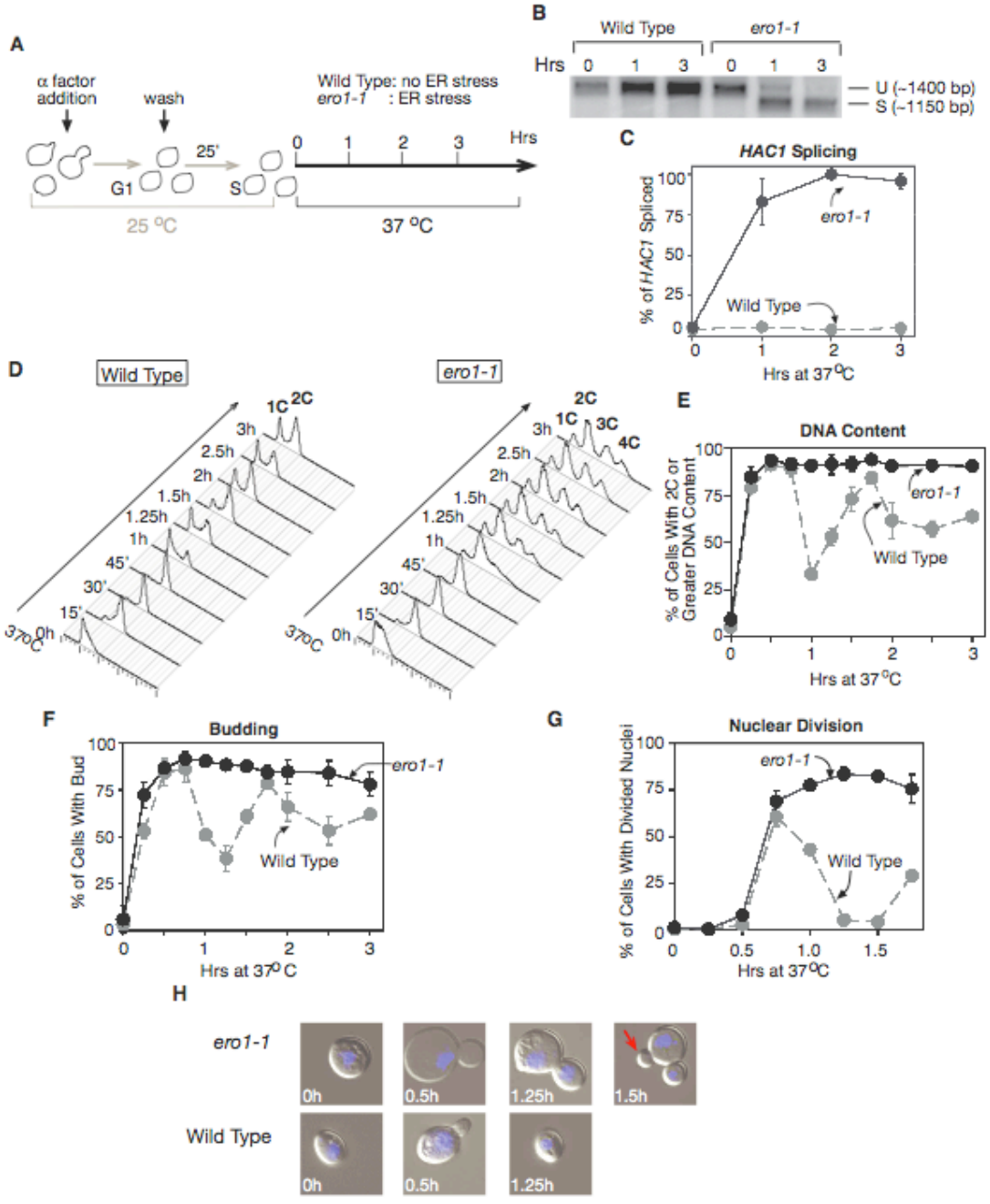
A
α factor addition
wash
25'
G1
S
25 °C
37 °C
Wild Type: no ER stress
ero1-1 : ER stress
0 1 2 3 Hrs
B
Wild Type
ero1-1
Hrs 0 1 3 0 1 3
U (~1400 bp)
S (~1150 bp)
C
HAC1 Splicing
% of HAC1 Spliced
ero1-1
Wild Type
Hrs at 37°C
D
Wild Type
ero1-1
1C 2C
2C 1C 3C 4C
3h
2.5h
2h
1.5h
1.25h
1h
45'
30'
15'
0h
37°C
E
DNA Content
% of Cells With 2C or Greater DNA Content
ero1-1
Wild Type
Hrs at 37°C
F
Budding
% of Cells With Bud
ero1-1
Wild Type
Hrs at 37°C
G
Nuclear Division
% of Cells With Divided Nuclei
ero1-1
Wild Type
Hrs at 37°C
H
ero1-1
Wild Type
0h
0.5h
1.25h
1.5h

Figure 2.5 Tunicamycin treatment inhibits budding when added immediately after α factor release, but does not affect budding when added 30 minutes after α factor release: Wild type (MNY 1005) cells were synchronized in G1 by α factor treatment and treated with Tm either immediately after α factor release (+Tm at 0') or 30' after α factor release (+Tm at 30'). (A) Schematic representation of two conditions of synchronized Tm treatment. (B) Percentage of total cells that contained a bud during all three treatments. Note that cells treated with Tm immediately after α factor release were budding-delayed (no significant budding until 60' after α factor release) compared to untreated cells. Tm treatment 30' after α factor release did not affect budding. (C) Flow cytometric analysis of cells stained with Sytox Green to measure DNA content for the first hour after α factor release for all three treatments. Note that under both conditions of Tm treatment, cells replicated their DNA at the same rate as untreated cells. Therefore, the delayed budding in cells treated immediately with Tm represents a direct block in bud formation, rather than a delay in S phase entry. All error bars represent standard deviation of three repeats. Because addition of Tm at 30' after α factor release did not affect the budding process, we used this condition in subsequent experiments to characterize the effects of Tm treatment on cell cycle events after bud formation.

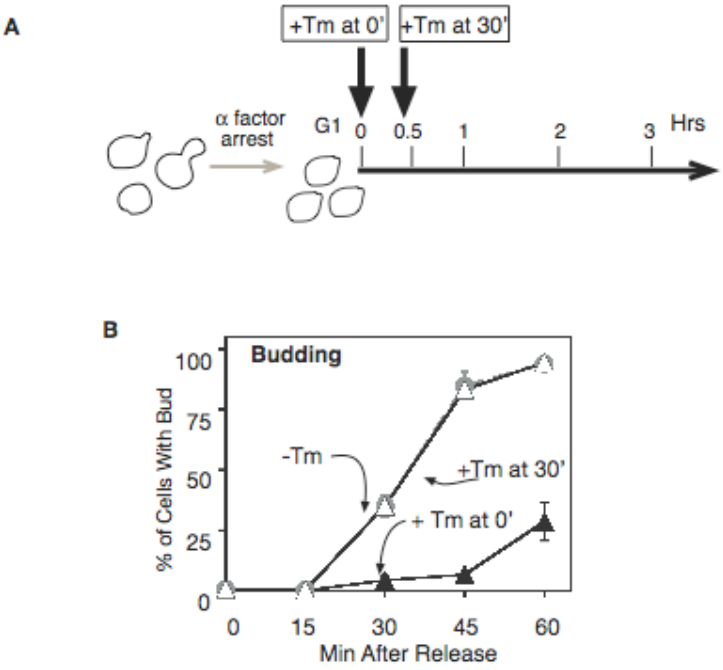
A
+Tm at 0'
+Tm at 30'
α factor arrest
G1
0
0.5
1
2
3
Hrs
B
Budding
% of Cells With Bud
100
75
50
25
0
-Tm
+Tm at 30'
+ Tm at 0'
0
15
30
45
60
Min After Release
C
1h
45'
30'
15'
0h
-Tm
+ Tm at 0'
+ Tm at 30'

Figure 2.6 Tunicamycin-treated cells are delayed in the cell cycle with high DNA content, large buds and divided nuclei: Wild type (MNY1005) cells were synchronized with α factor and treated with +/- Tm 30' after α factor release (See Fig. 2.5). Indicated time points refer to time after α factor release. (A) Northern analysis with *HAC1* specific probe shows the conversion of unspliced *HAC1* mRNA (U) to spliced *HAC1* mRNA (S) in cells experiencing ER stress. (B) Quantitation of (A) calculated as spliced *HAC1* mRNA divided by total *HAC1* mRNA. (C) Flow cytometric analysis of cells stained with Sytox Green to measure DNA content. Arrow indicates appearance of 3C cells. (D) Quantitation from (C) of the percentage of cells in the population that contained 2C or greater DNA content. (E) Percentage of total cells that were budded during synchronized growth +/– Tm. (F) Percentage of total cells that contained divided nuclei, with properly segregated sister chromatids, during synchronized growth +/- Tm. (G) Pictures show DAPI-stained nuclei (blue) and GFP-marked sister chromatids (indicated by white arrows). Red arrow indicates additional bud. All error bars represent standard deviation of three repeats. The 15 minute difference in wild type cell division time (1.25h vs 1.5h), as assayed by flow cytometry vs. budding index (compare B & C), is likely due to differences in the cell fixing protocol for the different assays (see Materials and Methods).

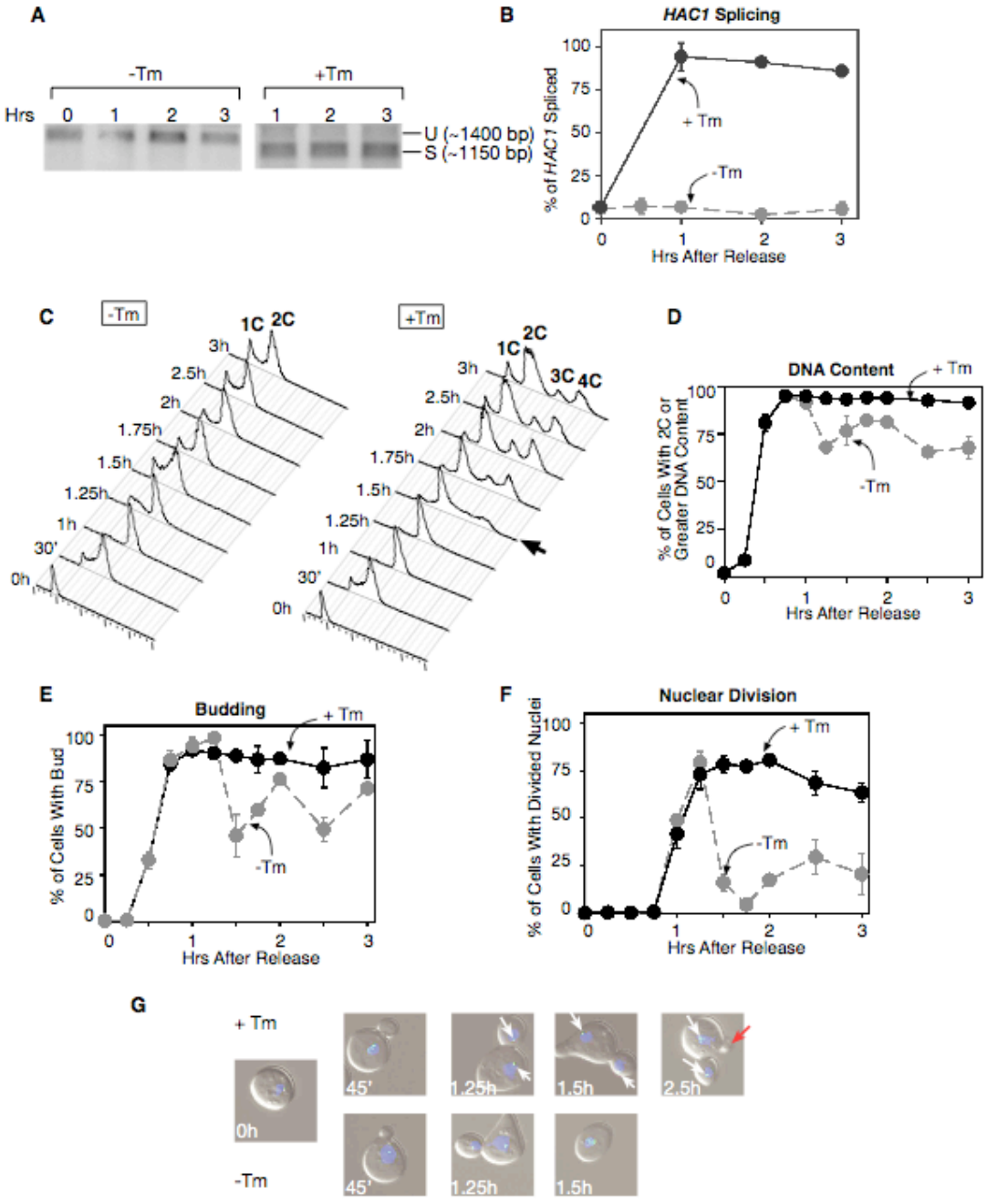
A
-Tm
+Tm
Hrs 0 1 2 3 1 2 3
U (~1400 bp)
S (~1150 bp)
B
HAC1 Splicing
% of HAC1 Spliced
+ Tm
-Tm
Hrs After Release
C
-Tm
+Tm
1C 2C
3C 4C
3h
2.5h
2h
1.75h
1.5h
1.25h
1h
30'
0h
D
DNA Content
+ Tm
-Tm
% of Cells With 2C or Greater DNA Content
Hrs After Release
E
Budding
+ Tm
-Tm
% of Cells With Bud
Hrs After Release
F
Nuclear Division
+ Tm
-Tm
% of Cells With Divided Nuclei
Hrs After Release
G
+ Tm
-Tm
0h
45'
1.25h
1.5h
2.5h

Figure 2.7 Ero1p inactivation causes cytokinesis delay: Experiments were done according to schematic in Fig. 2.1A and cells were collected for immunoblot analysis, probing for Pgk1p (loading control) and Clb2p (A), Cdc14p-GFP visualization (B), Tub1p-GFP visualization (C), and AlexaFluor546 Phalloidin staining to visualize actin patch localization (D). Blue indicates DAPI staining. All scale bars represent 2 μm. (E) Wild type (MNY1002), *cts1Δ* (MNY1012), and *ero1-1* (MNY1003) cells were α factor synchronized and then released at 30°C (wt and *cts1Δ*) or 37°C (*ero1-1*). Cells were grown for the indicated time and α factor was added back to the medium to prevent second cell cycle initiation. Cells were fixed and budding index was calculated before and after lyticase treatment. Graph depicts lyticase resistance, calculated as budding index after lyticase treatment divided by budding index before lyticase treatment. Error bars represent standard deviation of three repeats.

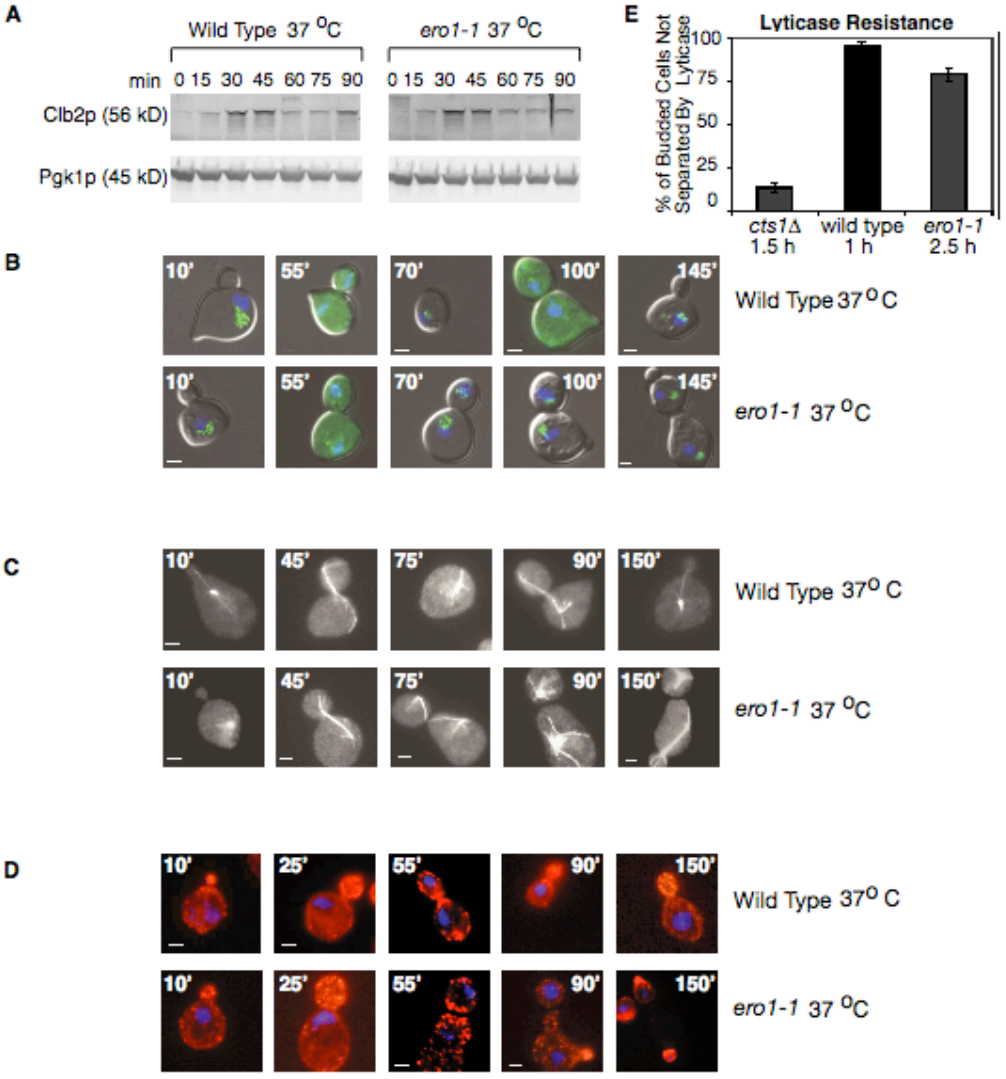
A
Wild Type 37 °C
ero1-1 37 °C
min 0 15 30 45 60 75 90
0 15 30 45 60 75 90
Clb2p (56 kD)
Pgk1p (45 kD)
E
Lyticase Resistance
% of Budded Cells Not Separated By Lyticase
100
75
50
25
0
cts1Δ 1.5 h
wild type 1 h
ero1-1 2.5 h
B
10'
55'
70'
100'
145'
Wild Type 37 °C
ero1-1 37 °C
C
10'
45'
75'
90'
150'
Wild Type 37° C
ero1-1 37 °C
D
10'
25'
55'
90'
150'
Wild Type 37° C
ero1-1 37 °C

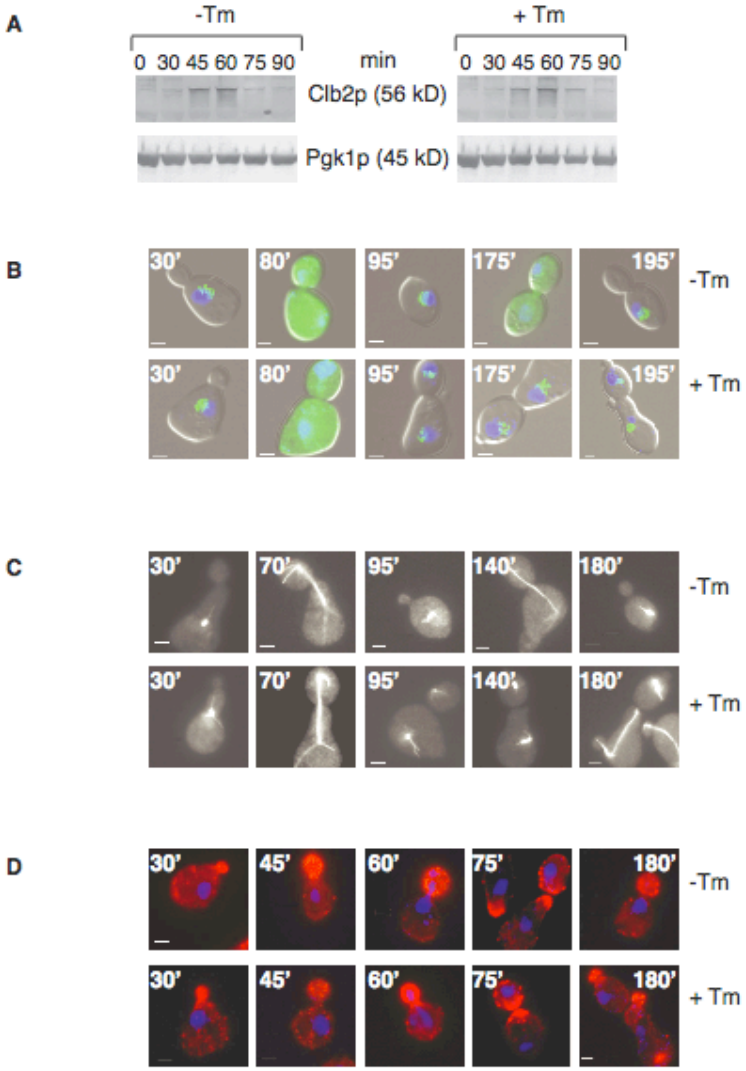

Figure 2.8 Tm treatment causes cytokinesis delay: Experiments were done according to schematic in Fig. 2.5A and cells were collected for immunoblot analysis, probing for Pgk1p (loading control) and Clb2p (A), Cdc14p-GFP visualization (B), Tub1p-GFP visualization (C), and AlexaFluor546 Phalloidin staining to visualize actin patch localization (D). Blue indicates DAPI staining. All scale bars represent 2 μm.

Figure 2.9 Unfolded Protein Response signaling facilitates cytokinesis during normal cell growth: (A) Wild type (MNY1002) and *hac1*Δ (MNY1010) cells were treated with +/- Tm 30 minutes after α factor release. Cells were fixed, stained with Sytox Green and analyzed by flow cytometry. (B) Quantitation of (A). (C) Wild type (MNY1002), *hac1*Δ (MNY1010), and *ire*Δ (MNY1011) were released from α factor arrest for 3 hours before fixation and microscopic examination. (D) Wild type (RHY2724), *hrd1Δ* (RHY5088), *hof1Δ* (RHY5954), *chs2Δ* (RHY5955), *cyk3Δ* (RHY5956), *mlc2Δ* (RHY5957), *doa10Δ* (RHY5958), and *bni1Δ* (RHY5959), which expressed a 4xUPRE-GFP reporter construct, were analyzed by flow cytometry to measure UPR activity in the absence of externally induced ER stress. Graphs represent fold induction compared to wild type cells. All error bars represent standard deviation of three repeats.

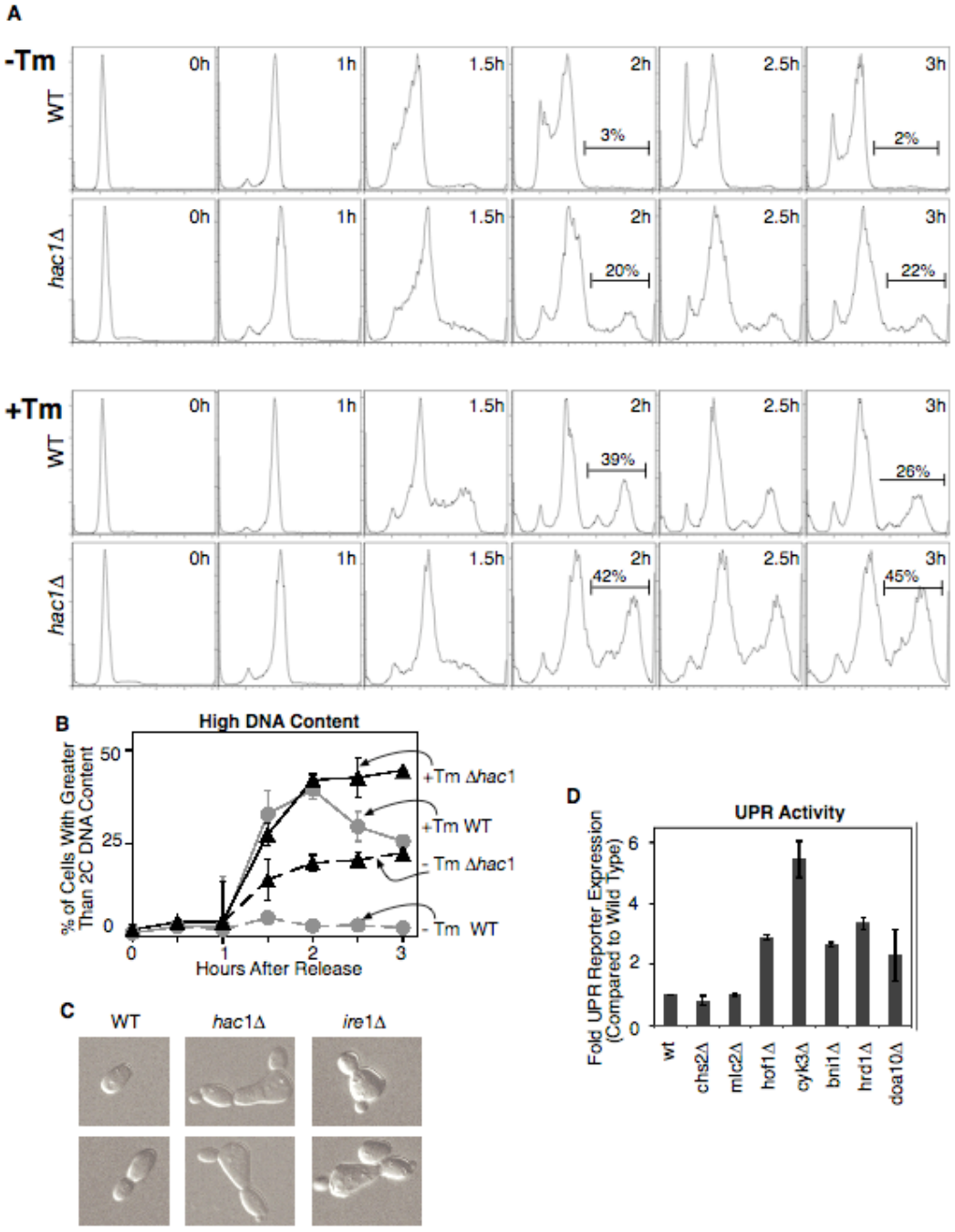
A
-Tm
WT
hac1Δ
+Tm
0h
1h
1.5h
2h
2.5h
3h
3%
2%
20%
22%
39%
26%
42%
45%
B
High DNA Content
% of Cells With Greater Than 2C DNA Content
Hours After Release
+Tm Δhac1
+Tm WT
- Tm Δhac1
- Tm WT
C
WT
hac1Δ
ire1Δ
D
UPR Activity
Fold UPR Reporter Expression (Compared to Wild Type)
wt
chs2Δ
mlc2Δ
hof1Δ
cyk3Δ
bni1Δ
hrd1Δ
doa10Δ

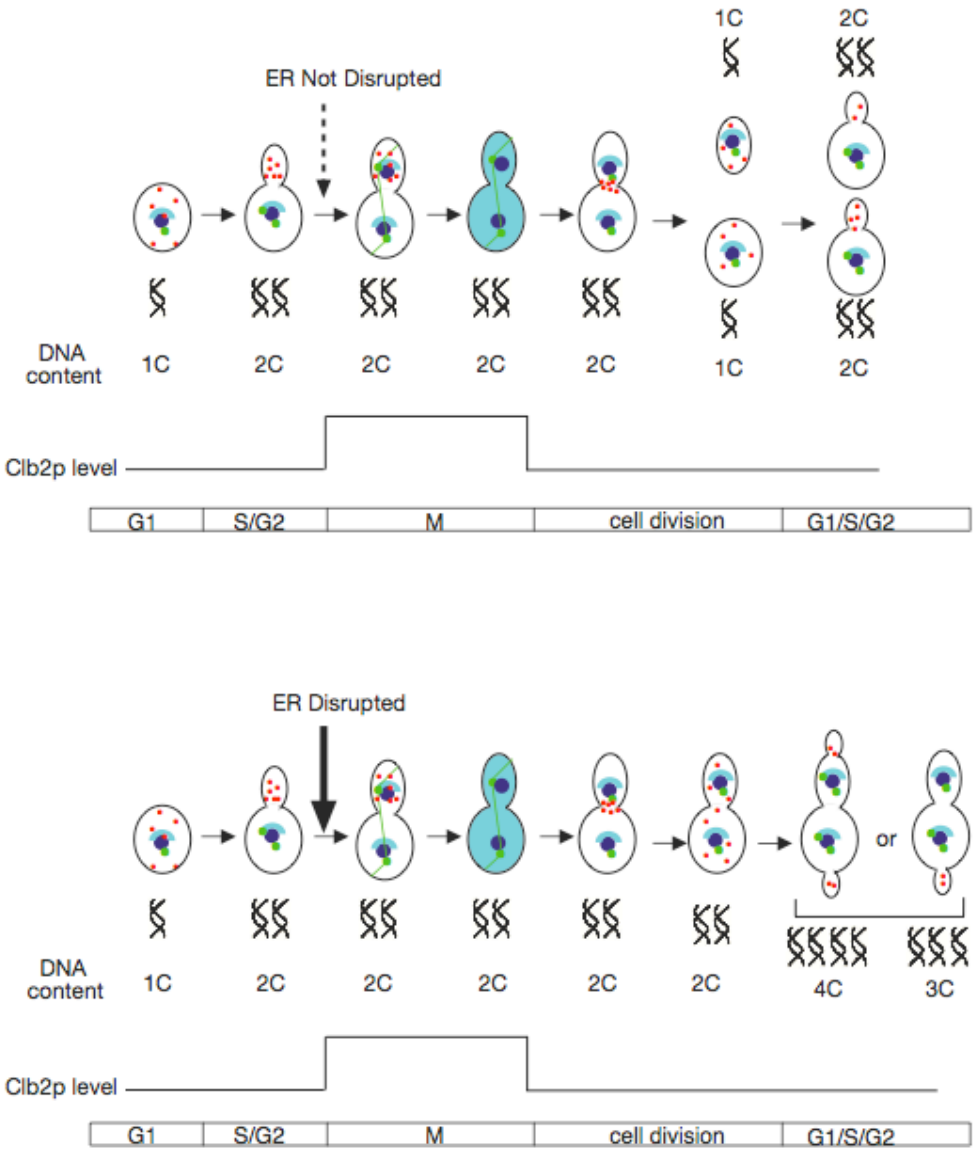

Figure 2.10 Summary of Results: When the ER is perturbed (*ero1-1* restrictive growth or Tm treatment), budding, DNA replication, Clb2p synthesis, spindle formation, nuclear division, Cdc14p release, Clb2p degradation, spindle breakdown, and actin repolarization occur at the same time as unstressed cells. However, *ero1-1* restrictive growth and Tm treatment delay cytokinesis, resulting in the formation of cells with extra buds and high DNA content. Green: Tubulin, Red: Actin, Dark Blue: Nucleus, Light Blue: Cdc14p.

Chapter 3: ER surveillance (ERSU) pathway monitors functional fitness of the endoplasmic reticulum during the cell cycle in yeast

3.1 ABSTRACT

The endoplasmic reticulum (ER) is a vital organelle, important for the production of both lipids and secretory pathway proteins. To accommodate the changing needs of the cell, the ER must be capable of altering its physical size and functional capacity. As the ER cannot be generated *de novo*, it must be faithfully transmitted to the daughter cell each time the cell divides. It is not known whether the cell monitors the functionality of the ER during the cell cycle, and regulates ER inheritance accordingly. We report that interfering with ER function in *S. cerevisiae* activates the MAP kinase Slt2, which then coordinates septin complex stabilization, inhibition of ER inheritance, and a delay in cytokinesis. *slt2Δ* cells, in which the septin complex is unaffected, stressed ER enters the daughter cell, and cytokinesis is undelayed, cannot sustain growth, and this appears to be the direct result of inheriting stressed ER. These data suggest that Slt2 mediates an ER surveillance (ERSU) mechanism that assures a correct ER functional capacity before cell division can proceed.

3.2 INTRODUCTION

Proper segregation of cellular components is the essence of cell division, and is critical to sustain life. In addition to the accurate replication and separation of genetic material, organelles and cytoplasmic proteins must also be separated properly so that newly generated daughter cells can autonomously carry out cellular events immediately

after cell division. The endoplasmic reticulum (ER), for example, must be properly inherited during the cell cycle, as it cannot be synthesized *de novo*.

The ER constitutes a nursery where newly synthesized secretory or membrane polypeptides fold into their native functional structures. In addition, the ER is a major storage site for intracellular calcium, a ubiquitous second messenger vital to cell signaling, and is the primary site of lipid biosynthesis (143). One critical aspect of the ER's function is its ability to adjust its own capacity according to changing environmental and developmental cues. It does this is through the Unfolded Protein Response (UPR) pathway, which senses the build-up of unfolded proteins in the ER (a condition known as ER stress), and up-regulates the transcription of genes encoding ER chaperones and other protein folding enzymes, thus increasing the ER's protein folding capacity (2, 189).

Morphologically, the ER is membranous network, comprised in budding yeast of two subdomains: the perinuclear ER, which surrounds the nucleus, and the cortical ER (cER), which is found near the plasma membrane or the cortex of the cell. ER tubules, approximately 50-100 nm in diameter, connect the cER to the perinuclear ER (190, 191). Most ER proteins analyzed to date can migrate freely between perinuclear ER and cortical ER. cER inheritance begins near the G1/S phase transition, when tubular ER elements appear from preexisting structures at the bud tip and begin to extend along the mother-bud axis, in a manner dependent on the actin cytoskeleton, and the type V mysosin, Myo4. The tubules then spread along the cortex of the bud, thus forming the new cER. In contrast, distribution of the perinuclear ER into the bud is microtubule-

dependent and occurs at the same time as nuclear division (192). Although the key steps of ER inheritance have been described, and many of the molecular players are known, very little is known about how this inheritance might be regulated in response to different conditions within the cell, such as ER stress

In mammalian cells, ER stress leads to temporary arrest at the G1/S phase transition (193), and during this arrest, a decision between apoptosis and survival is thought to take place. Similarly, we have shown that in yeast, ER stress results in a delay in cytokinesis (141), which we hypothesize functions to ensure inheritance of a minimal threshold of ER functional capacity during each cell cycle. In the current study, we show that the cytokinesis delay is part of a multi-faceted cell cycle response to ER stress, which also includes a delay in cER inheritance, and alterations in the morphology of the septin ring. The septin ring is a complex that localizes to the bud neck and regulates cytokinesis, thus the cytokinesis delay is likely to be a direct result of changes to the septin structure. All three ER stress-induced events, cytokinesis delay, septin alterations, and ER inheritance delay, were signaled by the MAP kinase Slt2, and were independent of the UPR. Therefore, a novel pathway, the ER surveillance (ERSU) pathway, is activated by Slt2 and links the functional state of the ER to cell cycle progression.

3.3 RESULTS

ER stress alters the localization and morphology of the septin ring

The most prominent effect on the cell cycle when a cell encounters ER stress is a cytokinesis delay (141). To probe the molecular basis of this delay, we set out to examine

the septin complex, which normally forms at the bud neck from five subunits Cdc3, 10, 11, 12, and Shs1, and establishes the septation site for cytokinesis. Using two previously characterized septin reporters, Shs1-GFP and Cdc11-GFP, we found that three distinct ways of inducing ER stress, tunicamycin (Tm) treatment which inhibits glycosylation, DTT treatment which disrupts disulfide bonds, and *ero1-1* restrictive growth which prevents oxidative protein folding, all caused changes in the morphology of the septin complex (Figure 3.1A). To determine the timing of these changes, and confirm that they reflect changes to the whole septin ring rather than just Shs1 and Cdc11, we examined Cdc10-GFP in α-factor-synchronized cells. During Tm treatment, the septin ring formed normally at the bud neck and converted normally into an hourglass structure as the cell cycle progressed (194, 195). In untreated cells, the septin ring dispersed at the end of the cell cycle as cells underwent cytokinesis. By contrast, during Tm treatment, the septin ring persisted and assumed an aberrant morphology and localization (Figure 3.1B, 60 min; compare –Tm to + Tm), and cytokinesis did not occur.

The morphology of the septin ring can be regulated by post-translational modifications that affect the stability of interactions between septin subunits, and thus impact the dynamic properties of the ring (196). To test the possibility that ER stress regulates septin dynamics, thus accounting for the morphological changes that we observed, we took advantage of a temperature sensitive allele of the *CDC12* septin subunit (197). This mutation destabilizes interactions between septin subunits and thus causes dispersal of the septin ring, and formation of elongated cells that do not undergo cytokinesis (196, 198). Remarkably, addition of Tm to these cells caused septins to

resume their normal morphology, thus rescuing cell shape, cytokinesis (Figure 3.1C, 30ºC +Tm), and overall cell growth (Figure 3.1D, 30ºC +Tm). Since the *cdc12-6* defect specifically destabilizes the septin structure, this rescue suggests that ER stress provides stability to the septin complex. Since stabilization of the septin complex has previously been shown to block cytokinesis (196), it is likely that ER stress-induced septin stabilization accounts not just for the unusual septin morphology depicted in Figures 3.1A & B, but also for the cytokinesis block that we have previously observed in wild type cells (141).

Secretory proteins perform many functions throughout the cell. Therefore, ER stress may affect septin dynamics by inducing a global secretory block, thus preventing upstream septin regulators from being targeted to their appropriate locations within the cell. To test this possibility, we used the well-characterized *sec1-1* temperature sensitive allele to induce a secretory block (Figure 3.2A) that was independent of ER stress (Figure 3.2B). Although shifting to the restrictive temperature blocked secretion, as expected, septin morphology and localization appeared normal in these cells (Figure 3.2C). Thus, a secretory block is not sufficient to affect septin morphology, and it is unlikely that the ER-stress induced stabilization of the septin ring is the indirect consequence of a secretory defect.

ER stress induces a delay in cER inheritance

Since ER stress delays cell cycle progression, we asked whether inheritance of the ER was affected by ER stress. Using the previously-characterized ER marker, Hmg1-

GFP (199, 200), we examined ER distribution between mother and daughter cells in the presence and absence of ER stress. As expected, in the absence of stress, cER was delivered to the daughter cell very early in the cell cycle. As soon as the bud was formed, 96% of cells contained some cER in the bud (Figures 3.3A & B, Class I). As the bud grew, the cER began to spread along the periphery of the daughter cell (Figure 3.3A, -ER Stress, Middle and Right Panels). Perinuclear ER was inherited along with the replicated nucleus later in the cell cycle (192). When ER stress was induced with Tm, DTT, or the *ero1-1* allele, cER entry into the daughter cell was significantly delayed. Early in the cell cycle, prior to nuclear division, only 13% of cells with small buds (defined as Class I) and 30% of cells with medium buds (defined as Class II) contained any cER (Figure 3.3A, +DTT, +Tm, *ero1-1*, Left and Middle panels; quantified for DTT in Figure 3.3B). Even late in the cell cycle, after the nucleus had divided (defined as Class III), 27% of cells contained no cER in the bud (Figure 3.3A, +DTT, +Tm, *ero1-1*, Right panel; quantitated for DTT in Figure 3.3B). By contrast, perinuclear ER was inherited normally during ER stress. This cER inheritance delay was also seen during Tm treatment with another ER reporter, HDEL-DsRed, which marks the lumen of the ER (Figure 3.3C), demonstrating that the effect is not specific to the ER reporter used.

The UPR does not signal septin stabilization, cytokinesis delay, or ER inheritance delay during ER stress.

Thus far, we have found that ER stress impacts the cell cycle in three ways: it alteres septin structures, it inhibits cER inheritance, and it delays cytokinesis. To

determine whether these events are part of a coordinated surveillance mechanism to prevent propagation of a compromised ER, we sought to identify a common upstream signal for all three events.

To date, the only known signaling pathway initiated from the ER is the Unfolded Protein Response (UPR) pathway. The UPR up-regulates the ER's protein folding capacity when ER stress is detected (189). In budding yeast, the UPR is set in motion by Ire1p, an ER transmembrane receptor kinase/riboendonuclease (RNase) that senses ER stress, and signals the transcriptional activation of genes that help cells cope with the stress (9, 10, 12, 147). We examined a potential role for Ire1 in inducing septin stabilization, cytokinesis delay, and ER inheritance delay during ER stress. During Tm treatment in synchronized cells, *ire1Δ* cells, like wild type cells, adopted a 3C/4C DNA content, which we have previously shown indicates a cytokinesis delay (Figure 3.4A). Furthermore, *ire1*Δ cells co-expressing the septin reporter, CDC10–mCherry, and the ER reporter Hmg1-GFP displayed both an aberrant septin morphology and delay in cER inheritance, very similar to wild type cells (Figure 3.4B). These results indicate that ER stress induces a cytokinesis delay, septin stabilization, and ER inheritance block through a mechanism independent of the *IRE1*-mediated UPR pathway.

Slt2 MAP kinase mediates septin alterations, cytokinesis delay, and ER inheritance delay during ER stress

Previously, it has been shown that the MAP Kinase Slt2 is activated during ER stress (201, 202), although its precise function remains unclear. Because genetic links have been found between Slt2 and septins (203) and Slt2 activation has been shown to delay ER inheritance (204), we tested the possibility that Slt2 activates septin stabilization, cytokinesis delay, and ER inheritance delay during ER stress. Using an antibody specific for the phosphorylated form of Slt2, we found a robust increase in Slt2 phosphorylation upon incubation with Tm (Figure 3.5A). Tm treatment also induced an increase in total Slt2 levels. However, Slt2 phosphorylation was independent of this increase in total levels, as we could still detect phosphorylation in cells lacking *RLM1*, the transcription factor driving *SLT2* expression (Figures 3.5A and B and (205)). Furthermore, Slt2 phosphorylation was completely independent of *IRE1* (Figure 3.5A), making it a good candidate mediator of the putative ER surveillance mechanism.

If Slt2 mediates the ER surveillance mechanism, *slt2Δ* cells should be unable to induce cytokinesis delay, septin alterations, and cER inheritance delay in response to ER stress. In fact, synchronized *slt2Δ* cells did not attain a 3C/4C DNA content after Tm treatment (Figure 3.5C; *slt2Δ* +Tm), indicating that cytokinesis was not delayed. In addition, unlike wild type cells, the septin ring of *slt2Δ* cells appeared normal after Tm treatment (Figure 3.5D). Furthermore, ER inheritance was delayed considerably less in *slt2Δ* cells than in wild type cells during ER stress (Figures 3.5 E & F). The failure to signal each of these three events was not caused by an inability of tunicamycin to induce

ER stress in *slt2Δ* cells, as *slt2Δ* cells efficiently activated the UPR pathway (Figure 3.5G).

ER surveillance (ERSU) signaling is necessary for survival of ER stress

During ER stress, septin alterations, cytokinesis block, and ER inheritance delay are all mediated by Slt2. This points to a mechanism of coordinated regulation of these three processes, which we have termed the ER Surveillance (ERSU) pathway. ERSU activation appears to be vitally important during ER stress, as *slt2Δ* cells cannot sustain growth on plates containing Tm (Figure 3.6B, +Tm). To confirm that this sensitivity was the result of an inability to induce the ERSU pathway, we treated *slt2Δ* cells with the actin depolymerization agent latrunculin B (LatB) (206). Since cER movement and septin morphology are both actin-dependent (207, 208), LatB treatment prevented ER inheritance in *slt2Δ* cells (Figure 3.6A, Hmg1-GFP) and disrupted septin structures (Figure 3.6A, Shs1-GFP), thus mimicking the effects of ERSU signaling in *slt2Δ* cells. Remarkably, LatB treatment rescued the Tm-sensitivity of *slt2Δ* cells (Figure 3.6B, compare Tm to Tm+LatB), suggesting that ERSU signaling is important for sustaining viability during ER stress. Taken together, these data support the idea that the ERSU pathway is in place to prevent the deleterious consequences of inheriting a stressed ER.

Slt2 phosphorylation and kinase activity are essential for ERSU signaling

Slt2 is a MAP kinase that becomes phosphorylated in the ERSU pathway. We therefore tested the importance of phosphorylation and kinase activity in ERSU signaling using the kinase dead K54R mutation, and the phosphorylation site T190A/Y192F mutation (209) . We found that neither of these mutants could rescue growth of *slt2Δ* cells on Tm plates (Figure 3.7A).

Since phosphorylation and kinase activation of Slt2 were important for ERSU signaling, we sought to identify the upstream mediators of Slt2 phosphorylation during ER stress. Under previously characterized conditions of Slt2 activation, Slt2 is directly phosphorylated by two redundant MEKs, Mkk1 and Mkk2. Mkk1/2 can be activated by the MEKK, Bck2, which can be activated by Pkc1. However, different types of stress can feed into this linear activation pathway at different levels (210). To determine how the ERSU pathway activates Slt2, we examined Tm-induced phosphorylation (Figure 3.7B) and Tm sensitivity (Figure 3.7C) in the absence of each of these kinases and found that each of them is important for ERSU, indicating that the pathway is activated upstream of Pkc1. Since cell wall stress also activates Slt2 via Pkc1, we tested Tm sensitivity of each mutant in the presence of the osmotic stabilizer, sorbitol. Sorbitol did not prevent Tm sensitivity, indicating that Tm is not activating the pathway indirectly by damaging the cell wall (Figure 3.7C).

The ERSU pathway is activated by Wsc1

Slt2 can be activated by various upstream stimuli. Therefore, we asked whether Slt2 activation would always lead to septin stabilization, or whether this effect was

specific to the type of stimulus. We found that the chitin antagonist, calcoflour white (CFW) did not affect septins, while alkaline treatment (KOH) and treatment with the antifungal drug caspofungin (CP) did induce an altered septin morphology (Figure 3.8A). Since each of these treatments induced Slt2 phosphoryation (Figure 3.8B) as reported previously (205, 211-213), this indicates that Slt2 phosphorylation is not sufficient to induce septin stabilization.

The Pkc1-Slt2 pathway can be activated by six sensors that reside on the plasma membrane, Wsc1-4, Mid2, and Mtl1. Different types of stress activate different combinations of sensors (212, 214-217) and septin alterations correlated with the use of the Wsc1 sensor to activate Slt2 (211). Thus, we predicted that Tm-induced Slt2 phophorylation might be *WSC1*-dependent. In fact, when we examined knockouts strains of each sensor, only *wsc1Δ* cells displayed reduced Slt2 phosphorylation and enhanced Tm sensitivity (Figures 3.8C & D). Furthermore, *wsc1Δ* cells did not display an aberrant septin morphology during Tm treatment (Figure 3.8E), confirming that ERSU relies on Wsc1 activation.

In certain cases, Wsc1 is known to collaborate with the other five sensors (210). Therefore, we examined strains with *WSC1* deleted in combination with other sensors. We found that the *wsc1Δ wsc2Δ* double deletion strain was more Tm-sensitive than the *wsc1Δ* strain alone (Figure 3.8F), suggesting that both sensors are involved in ERSU signaling.

During cell wall stress, Wsc1's function in sensing the stress relies on its localization to sites of polarized growth on the plasma membrane. This localization requires constitutive endocytosis of Wsc1 from the cell surface. Thus, *wsc1* mutants defective in endocytosis are incapable of establishing polarized localization and of sensing cell wall stress, and are therefore hypersensitive to cell wall stress (218). In contrast, cells bearing the *wsc1*^{AAA} endoyctosis-defective mutation were not sensitive to Tm treatment (Figure 3.8G), indicating that Wsc1 function sensing ER stress does not rely on endocytosis. Thus, cell wall stress and ER stress are sensed through distinct mechanisms by Wsc1, indicating that the activation of Slt2 during ER stress is not caused by effects of ER stress on cell wall integrity.

ERSU promotes mother cell viability during ER stress

We have shown that Slt2's function in linking the cell cycle with ER stress is important for long-term survival during ER stress. To determine whether this survival was achieved through the specific preservation of either the mother or daughter cell, we stained both WT and *slt2Δ* cells FUN-1 vital dye following Tm treatment (Figure 3.9B). This dye generates differential staining patterns in metabolically active and inactive cells: live metabolically active cells exhibit red-fluorescent cylindrical intravacuolar structures (CIVSs; Figure 3.9A upper panels), whereas dead cells display a diffuse bright cytoplasmic green and red fluorescence, which appears yellow when merged (Figure 3.9A, lower panels).

During ER stress in wild type cells, 22% of cells were metabolically inactive, suggesting cell death (Figure 3.9B). When cell death was seen in a budded cell, the mother cell remained metabolically active, whereas the daughter cell appeared dead (Figure 3.9B). By contrast, in *slt2Δ* cells. ER stress caused apparent cell death in both the mother and daughter cells, suggesting that ERSU signaling specifically promotes mother cell viability, perhaps at the expense of the daughter cell.

3.4 DISCUSSION

We report here the identification of an ER surveillance (ERSU) pathway that monitors the functional capacity of the ER, and delays both ER inheritance and cytokinesis when the ER is stressed. The cytokinesis delay correlates with, and is probably caused by, altered dynamics of the septin complex. All three events, cytokinesis delay, septin alterations, and ER inheritance inhibition, are independent of UPR signaling, and instead rely upon the MAP kinase *SLT2*. By delaying both ER inheritance and cell cycle progression when ER stress is detected, we hypothesize that the *SLT2*-mediated ERSU pathway ensures that only functional ER is transmitted to daughter cells.

One outstanding question is how signals from the ER are communicated to Slt2. Since disruption of the cell wall can activate Slt2 via the cell wall integrity (CWI) pathway (210), a simple explanation may be that ER stress perturbs the delivery of protein(s) to the plasma membrane, thus leading to cell wall stress and induction of the CWI pathway. However, blocking the delivery of secretory vesicles to the plasma

membrane in a *sec1-1* mutant failed to trigger the ERSU pathway. Furthermore, cell wall stress does not seem to be the upstream stimulus for ERSU activation, as osmotic stabilizer in the media does not prevent the pathway from being triggered. In addition, during ER stress, the mechanism for Wsc1 activation is distinct from cell wall stress, as it does not require endocytosis or polarized localization of Wsc1 (218).

An intriguing possibility for ERSU activation involves the regulation of Wsc1 localization. It has been shown that in certain cases, Wsc1 and Wsc2 can be activated from within the secretory pathway, rather than from their usual position at the cell surface (219). Therefore, a signal preferentially retaining Wsc1 and Wsc2 within the secretory pathway might actually allow them to directly detect ER stress.

The ERSU pathway causes stressed ER to be preferentially retained in the mother cell. This type of mother cell retention has also been seen for factors that contribute to cell aging, such as extrachromosomal rDNA circles (ERCs) and carbonylated proteins. These toxic factors, which accumulate from generation to generation, ultimately leading to cell death, are retained in the mother cell to increase the lifespan of the newly generated daughters (220-222). Recently, it has been shown that mother cell retention of ERCs requires a septin-dependent diffusion barrier within the nuclear envelope (223). Moreover, the inheritance of carbonylated proteins is controlled by Spa2 (224), a protein known to regulate the localization of Slt2 (225). Our data show that Slt2 regulates both septins and cER inheritance. We do not yet know whether the ER inheritance delay depends upon the regulation of septins, but previous studies have found genetic links between ER inheritance components and the septin complex (226). Taken together, these

data point to a general mechanism, controlled by septins and Slt2, that regulates asymmetric distribution of components between mother and daughter cells.

One key difference between ER stress and aging is that ER stress is reversible, whereas aging factors accumulate permanently. Furthermore, unlike aging, the ERSU pathway specifically promotes mother cell viability, while allowing the daughter cell to die. Perhaps retaining the ER in the mother cell affords the cell more time to reverse the stress, and resume normal ER function, before continuing to propagate the ER. Although the first daughter dies, probably due to insufficient levels of ER in the cell, the mother can recover and provide fully functional ER to subsequent generations of daughter cells, thus allowing propagation of the species.

Studies with a specific ER stress reporter have recently shown that ER stress is not transmitted to daughter cells (227). When combined with our data, this suggests a very interesting distinction between perinuclear ER and cER. Since perinuclear ER is inherited normally during ER stress, but ER stress is not inherited, the perinuclear ER must not be a major site of ER stress. Instead, ER stress must be somehow partitioned to the cER, which is retained in the mother cell. In the future, it will be very interesting to explore the mechanism and functional implications of this distinction between the two subdomains of the ER.

The failure to regulate ER functional capacity is increasingly recognized as contributing to the pathophysiology of a number of human diseases, including certain cancers. Thus, further understanding of the cellular mechanisms of ER Stress Surveillance Response (ERSU) assuring the maintenance and transmission of a

functionally competent ER will be invaluable for developing previously unrecognized strategies for therapeutic intervention.

ACKNOWLEDGEMENTS

We thank David Levin for *bck1Δ*, *mkk1Δ mkk2Δ*, and *pkc1Δ* strains, as well as for plasmids p2188, p2190, and p2193 and Enrique Herrero for *pkc1Δ* strains. We also thank Peter Novick for providing the *sec1-1* strain, Yves Barral for providing the *cdc12-6* strain, and Randy Hampton for plasmids pRH475 and pRH1827.

Chapter 3 is modified from material that has been submitted for publication. Anna Babour, Alicia A. Bicknell, Joel Tourtelotte, and Maho Niwa. I was the secondary investigator and secondary author of this paper. The specific experiments that I conducted are depicted in Figures 3.1D, 3.4A, 3.5A, 3.7A-C, 3.8B-D, and 3.8F-G. Joel Tourtelotte conducted experiments depicted in Figures 4.2A, 4.2B, 4.5B, and 4.5G; Anna Babour conducted the remaining experiments and Maho Niwa supervised the work.

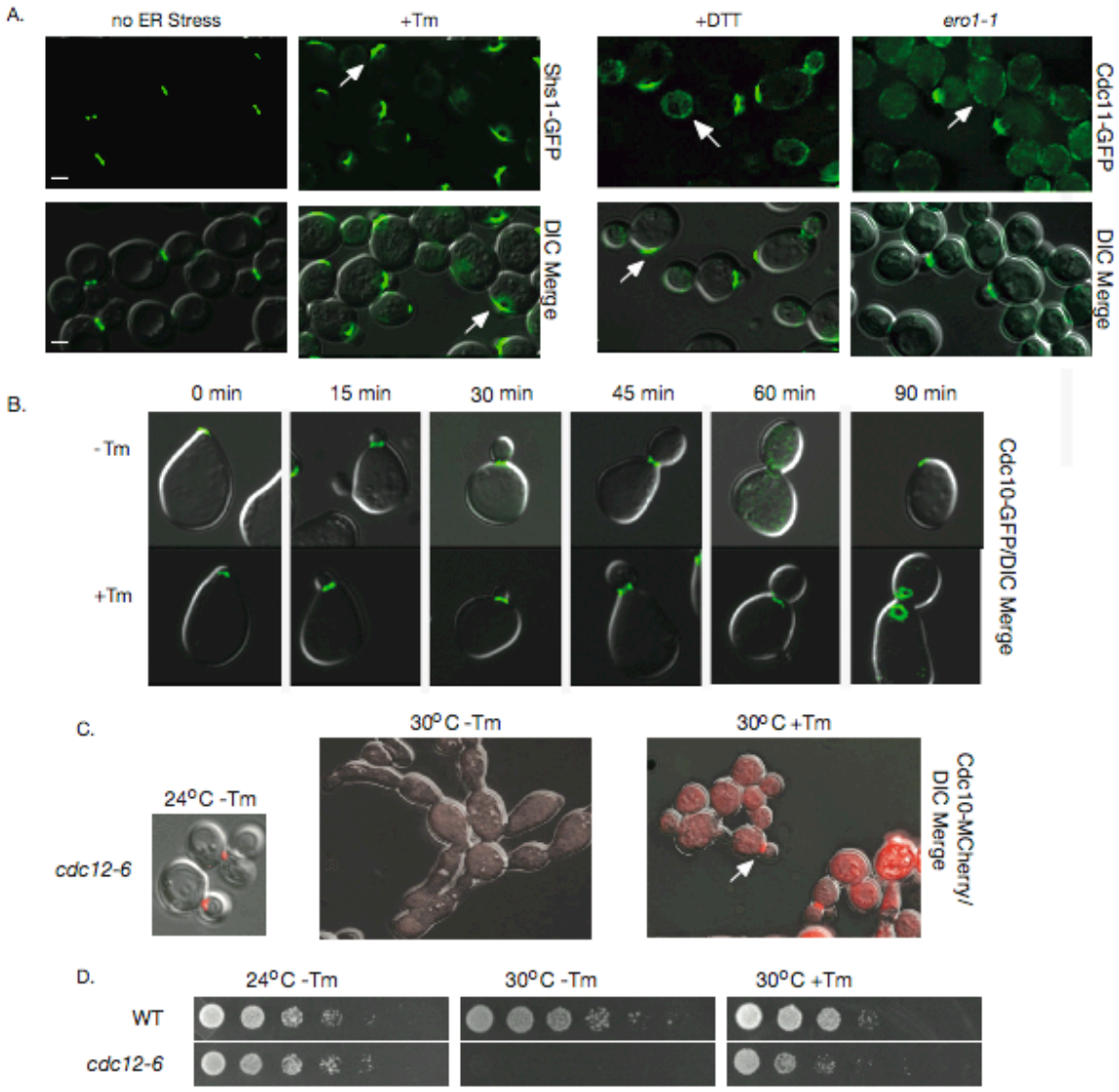

Figure 3.1 ER stress alters the localization and morphology of the septin ring: (A) Genomic loci of septin subunits *SHS1* and *CDC11* were C-terminally tagged with GFP. ER stress was induced with 1 μg/ml Tm or 2 mM DTT, or shift to 37°C in *ero1-1* strains. Arrows indicate abnormal septin morphology observed during ER stress: crescent structures along the plasma membrane and away from the bud neck, crescents accompanied by an adjacent ring, rings around the entire daughter cell, or patches along the plasma membrane. Bars, 2 μm. (B) Cells expressing genomically GFP-tagged *CDC10* were synchronized in G1 with α-factor, allowed 15 minutes to recover from α-factor arrest, and then treated with or without Tm for the indicated amount of time. (C) *CDC10*-mCherry was integrated at the genomic locus in *cdc12-6* cells grown in YPD or YPD+Tm at the indicated temperature. (D) Five fold serial dilutions of wild type and *cdc12-6* cells spotted on YPD or YPD+Tm plates.

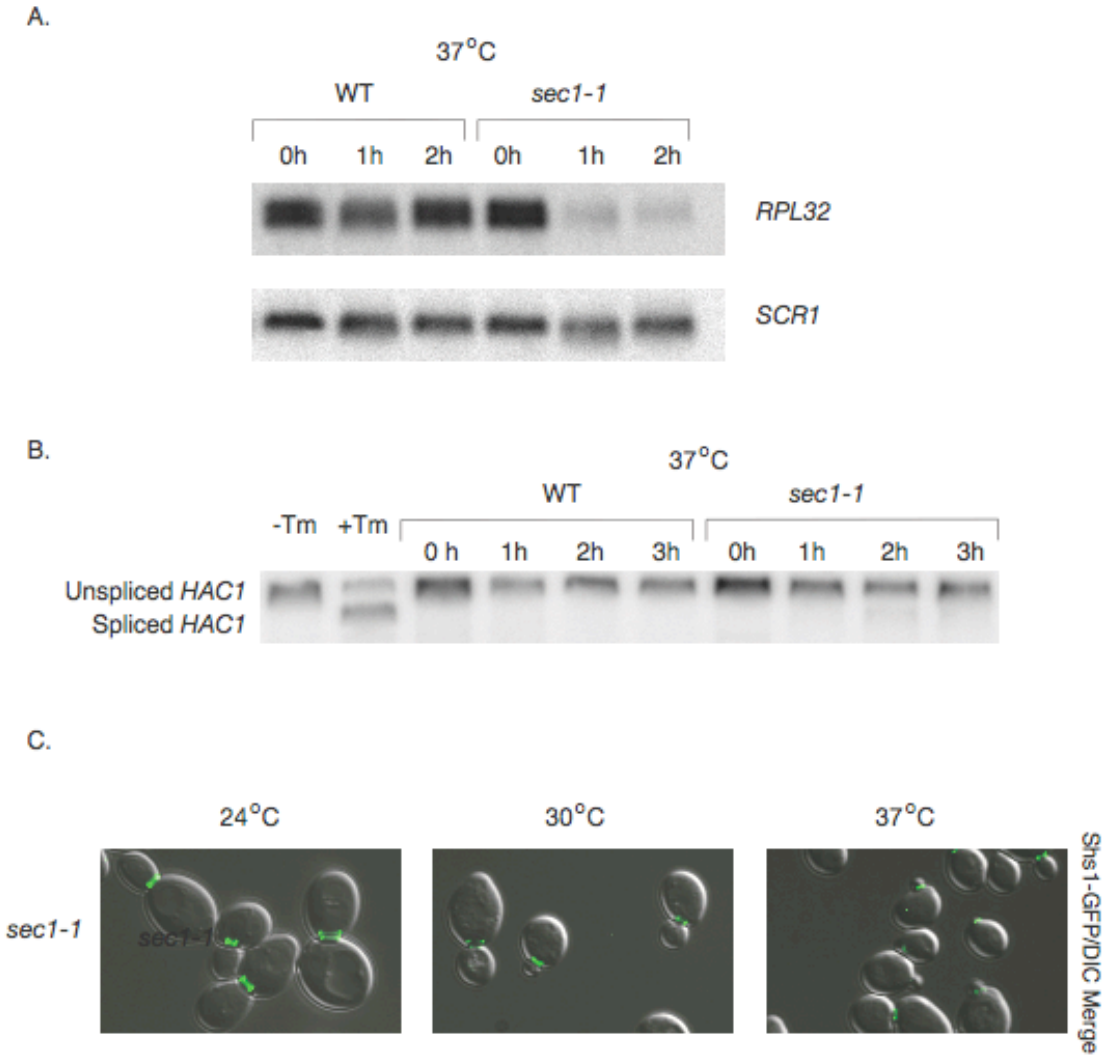

Figure 3.2 *sec1-1* mutation induces secretory block, but no ER stress and no septin alterations: (A) Secretory block is known to repress *RPL32* transcription through the arrest of secretion response. *RPL32* northerns confirmed that secretory block was induced upon shift to 37°C in *sec1-1* cells. (B) The UPR pathway, which activates splicing of *HAC1*, is induced during ER stress. The lack of *HAC1* splicing during the secretory block induced in *sec1-1* cells indicates that ER stress is not induced. (C) *sec1-1* cells expressing *SHS1*-GFP at their genomic locus were cultured at the indicated temperatures to show that a secretory block does not alter septin structures.

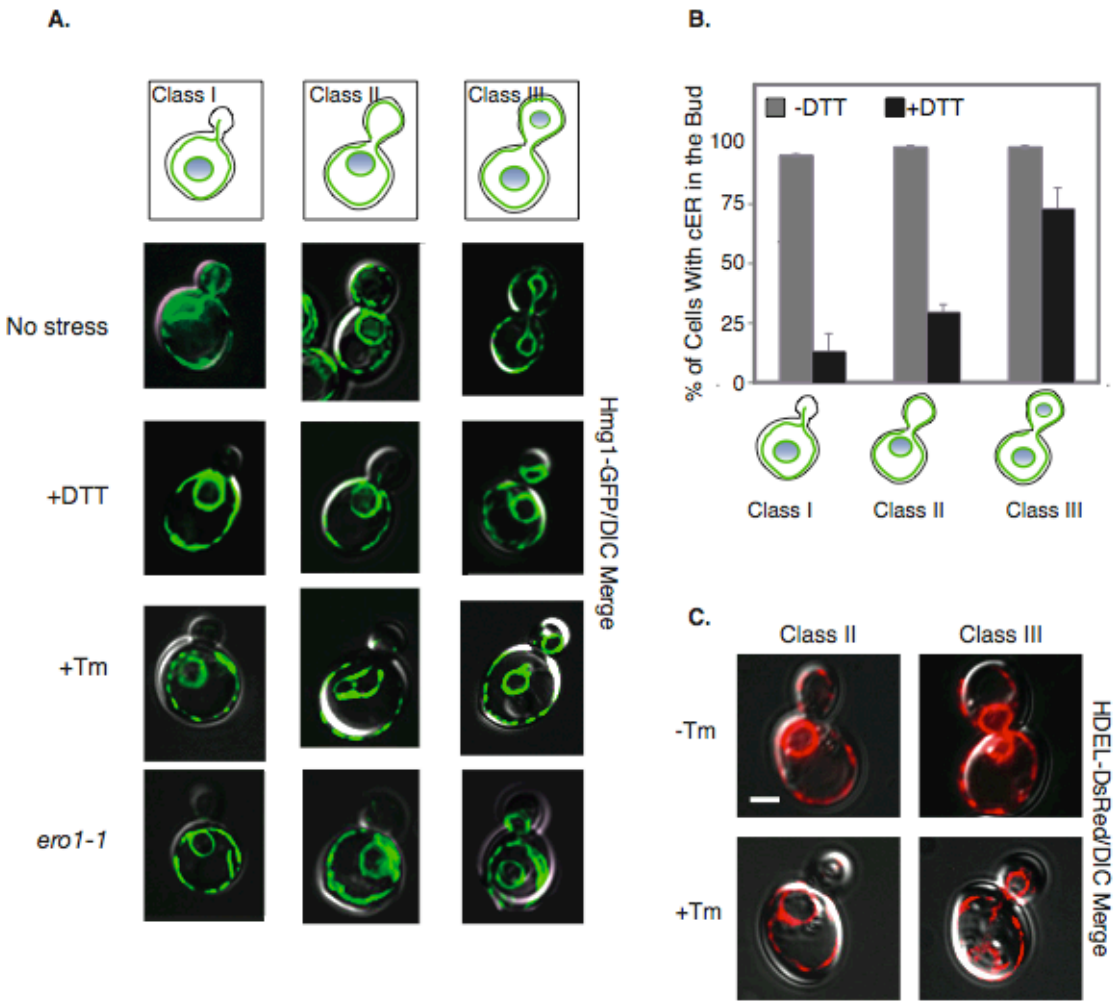

Figure 3.3 ER stress induces a delay in cER inheritance: (A) ER stress was induced in cells expressing the ER membrane marker, Hmg1-GFP, and cells were examined by fluorescence microscopy. In wild type cells, 1 μg/ml Tm, 2mM DTT was added to cultures. In *ero1-1* cells, cultures were shifted to growth at 37°C. Three categories of cells are depicted: cells with a small bud (class I), cells with a large bud containing no nucleus (class II) and cells with a large bud containing a nucleus (class III). (B) For each of the three classes of cells, the number of cells containing elements of cER in the daughter cell was counted (n=300) during growth under normal conditions (grey bars) or in the presence of 2 mM DTT (black bars). The average of 3 independent experiments is depicted, error bars represent SD. (C) Visualization of Ds-Red-HDEL in wild-type cells grown in YPD (left panel) or YPD+Tm (right panel).

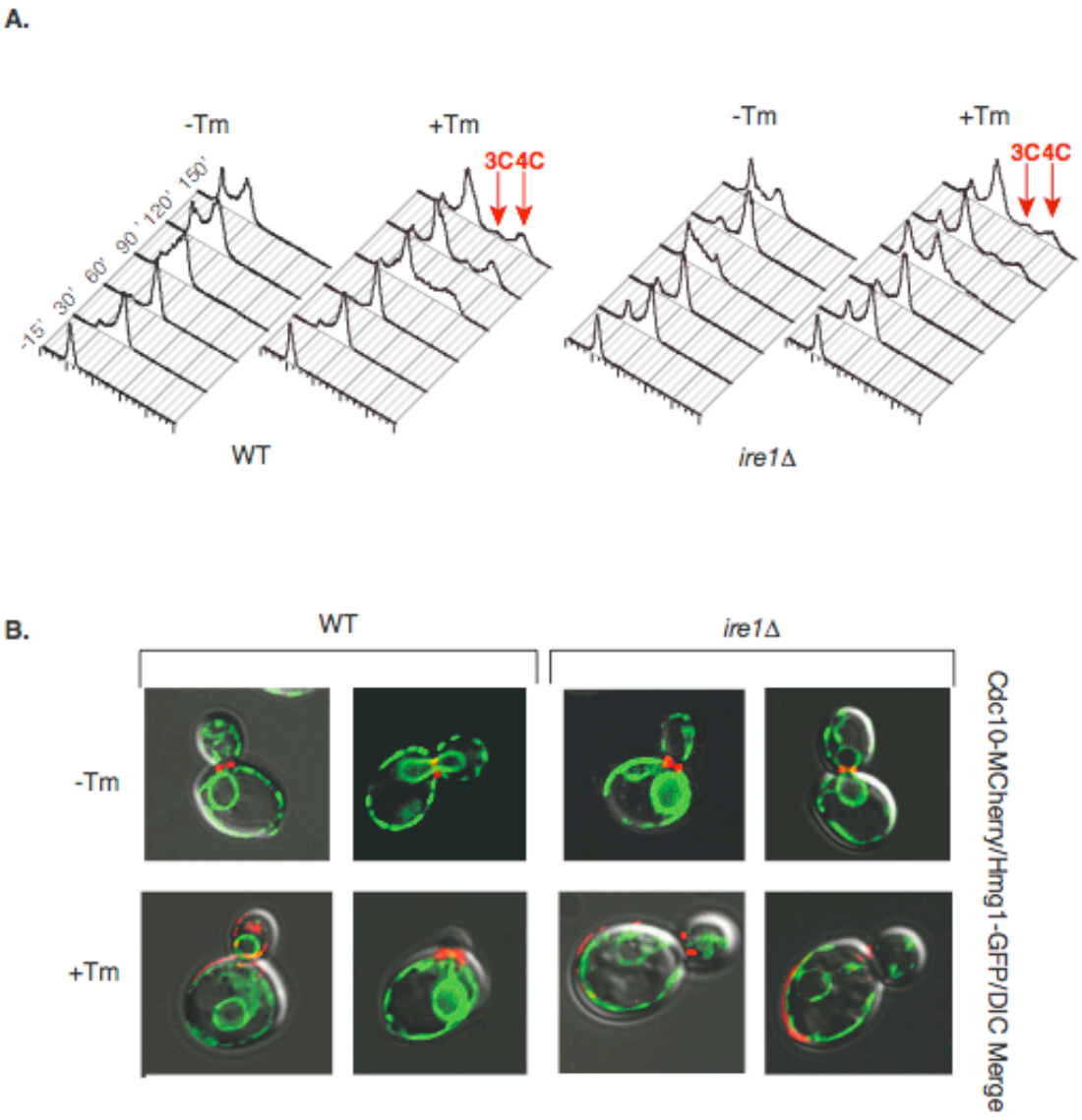

Figure 3.4 The UPR does not signal septin stabilization, cytokinesis delay, or ER inheritance delay during ER stress: (A) Wild-type and *ire1*Δ cells were synchronized with a factor, allowed to recover for 15 minutes, and then treated with or without 1 μg/ml Tm. To monitor the cell cycle, DNA was stained with Sytox Green, and fluorescence intensity was measured by flow cytometry. After 90 minutes, populations of both cell types adopted with 3C or 4C DNA content (red arrows), which we have previously shown indicates a cytokinesis delay. (B) Visualization of the ER reporter, Hmg1-GFP, and Septin reporter, Cdc10-mCherry, in wild type (upper panels) or *ire*Δ (lower panels) cells, grown with (right panels) or without (left panels) 1 μg/ml Tm.

Figure 3.5 Slt2 MAP kinase mediates septin alterations, cytokinesis delay, and ER inheritance delay during ER stress: (A) Wild type, *ire1Δ*, or *rlm1Δ* cells were treated with Tm for 2 h and prepared for immunoblot analysis, probing for phospho-Slt2, total Slt2 or Pgk1 (loading control). (B) Northern blots, probing for *SLT2* or *SCR1* (loading control) after 2 h of Tm treatment in wild type and *rlm1Δ* cells. (C) Wild-type and *slt2*Δ cells were synchronized with a factor, allowed to recover for 15 minutes, and then treated with or without 1 μg/ml Tm. To monitor the cell cycle, DNA was stained with Sytox Green, and fluorescence intensity was measured by flow cytometry. Arrows indicate 3C/4C DNA peaks indicative of a cytokinesis delay, which are absent in *slt2*Δ cells. (D) Visualization of Cdc10-GFP in wild-type (left) and *slt2*Δ cells (right) grown at with or without 1 μg/ml Tm as indicated. Blue indicates DAPI staining. (E) Wild-type and *slt2*Δ cells expressing Hmg1-GFP were grown in the presence or absence of 1 μg/ml Tm and examined by fluorescence microscopy. Three categories of cells are depicted: cells with a small bud (class I), cells with a large bud containing no nucleus (class II) and cells with a large bud containing a nucleus (class III). (F) For wild type and *slt2*Δ cells, the number of cells in each class containing elements of cER in the daughter cell was counted (n=300) during growth under normal conditions or in the presence of 2 mM DTT. The average of 3 independent experiments is depicted, error bars represent SD. (G) equivalent *HAC1* splicing in wild type and *slt2Δ* cells during Tm treatment indicates that ER stress in sensed in both cell types.

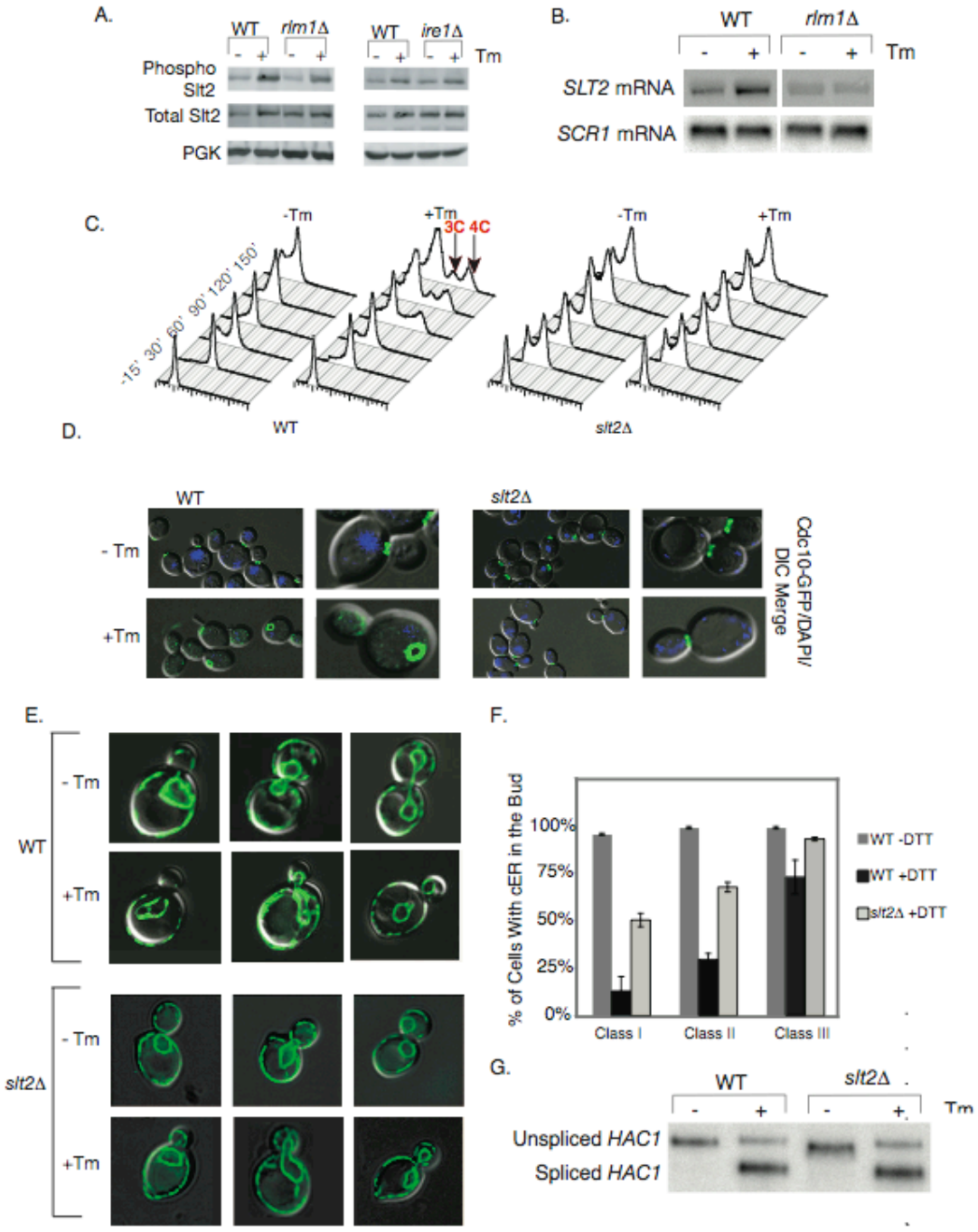
A.
WT
rlm1Δ
WT
ire1Δ
- + - + - + - +
Tm
Phospho Slt2
Total Slt2
PGK
B.
WT
rlm1Δ
- + - +
Tm
SLT2 mRNA
SCR1 mRNA
C.
-Tm
+Tm
3C 4C
-15' 30' 60' 90' 120' 150'
WT
slt2Δ
D.
WT
slt2Δ
- Tm
+Tm
Cdc10-GFP/DAPI/ DIC Merge
E.
WT
- Tm
+Tm
slt2Δ
- Tm
+Tm
F.
% of Cells With cER in the Bud
100%
75%
50%
25%
0%
Class I
Class II
Class III
WT -DTT
WT +DTT
slt2Δ +DTT
G.
WT
slt2Δ
- + - +
Tm
Unspliced HAC1
Spliced HAC1

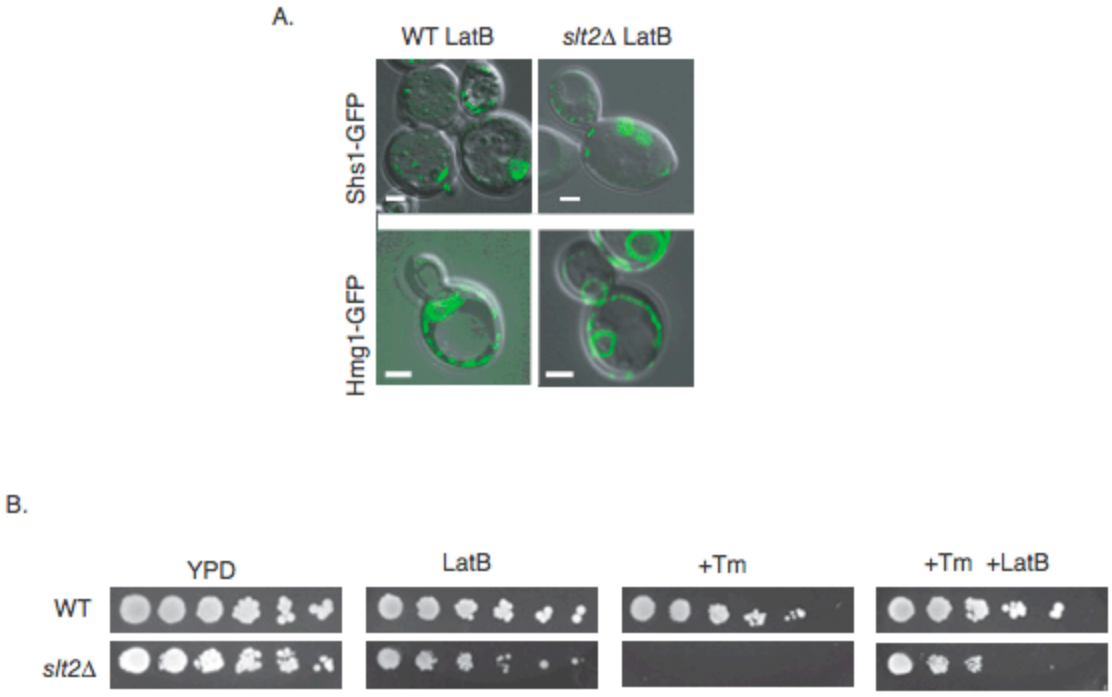

Figure 3.6 ER Surveillance (ERSU) signaling is necessary for survival of ER stress: (A) Effect of latrunculin B on ER and septin distribution. Septin reporter, Shs1-GFP (upper panel) and ER reporter, Hmg1-GFP (lower panel) were visualized in wild-type (right) or *slt2*Δ cells (left) treated with 400 μM Latrunculin B. In both cell types, septin morphology was altered and ER inheritance was delayed. (B) 5 fold serial dilutions of wild type and *slt2*Δ cells on plates containing no drug, Tm alone, 6 μM LatB, or Tm+6 μM LatB.

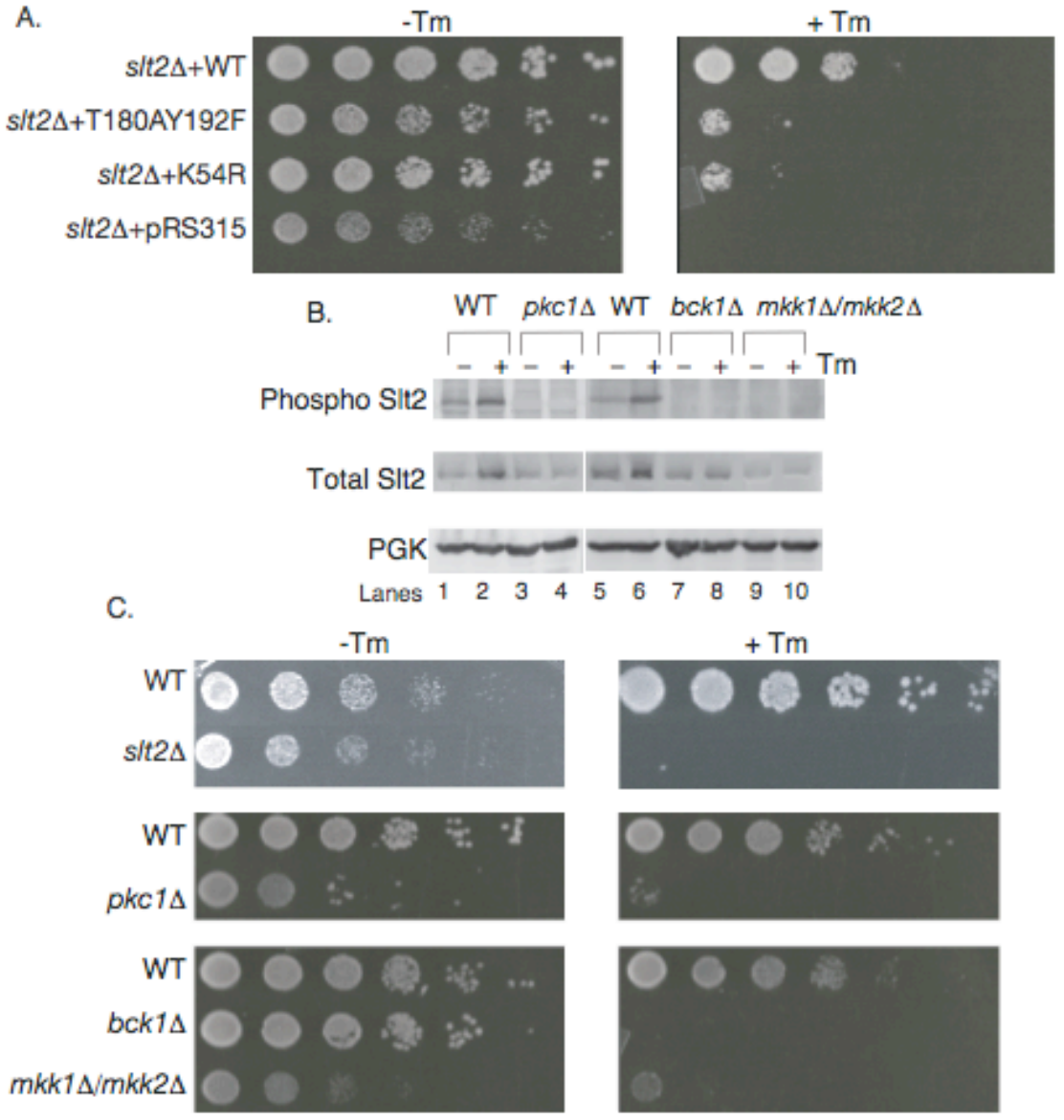

Figure 3.7 Slt2p phosphorylation and kinase activity are essential for ERSU: (A) *slt2Δ* cells were transformed with empty plasmid, or plasmid containing wild type *SLT2*, T180AY192F *slt2*, or K54R *slt2*. Cells were grown to log phase in SC-leu medium, diluted serially 5 fold, and spotted onto plates with or without 0.1 μg/ml Tm. (B) *pkc1Δ* and corresponding wild type cells were grown in the presence of 1M sorbitol, while *bck2Δ, mkk1Δ /mkk2Δ,* and corresponding wild type cells were grown in the absence of sorbitol. Cells were treated with 1 μg/ml Tm for 2 h, and cell extracts underwent immunoblot analysis to detect levels of phospho Slt2, total Slt2, and PGK (loading control). (C) Cells of indicated genotype were grown to log phase in YPD + 1M sorbitol, diluted serially 5 fold, and spotted onto plates containing 1M sorbitol or 1M sorbitol + 0.2 μg/ml Tm.

Figure 3.8 The ERSU pathway is activated by Wsc1: (A) Wild-type cells expressing indicated septin fusion genes were visualized after 2 hours of treatment with 10μg/ml calcofluor white (CFW), 10ng/ml caspofungin (CP), 35mM KOH (pH 8.2) or 1 μg/ml tunicamycin (Tm). (B) Samples from the experiment described in A were collected and analyzed by western blot for Slt2 phosphorylation (top), total Slt2 (middle) and Pgk (loading control, bottom) (C) The indicated mutants in the BY4741 backgrounds were grown in YPD and treated with 1 μg/ml Tm for two hours. Samples were collected and analyzed by western blot for Slt2 phosphorylation (top), total Slt2 (middle) and Pgk (loading control, bottom). (D) 5 fold serial dilutions of the indicated mutants in the BY4741 background were spotted onto plates with and without Tm. Growth was monitored after 2 days. (E) Septin structures were monitored in *wsc1Δ* cells expressing a Cdc10-mCherry fusion protein upon growth in YPD (left) or YPD + 1 μg/ml Tm. (F) 5 fold serial dilutions of the indicated double mutants in the BY4741 background were spotted onto plates with and without Tm. Growth was monitored after 2 days. (G) 5 fold serial dilutions of wild type cells, and cells with the genomic copy of *WSC1* replaced by the endocytosis mutant, *wsc1-AAA* were spotted onto plates with and without Tm and CP. Growth was monitored after 2 days.

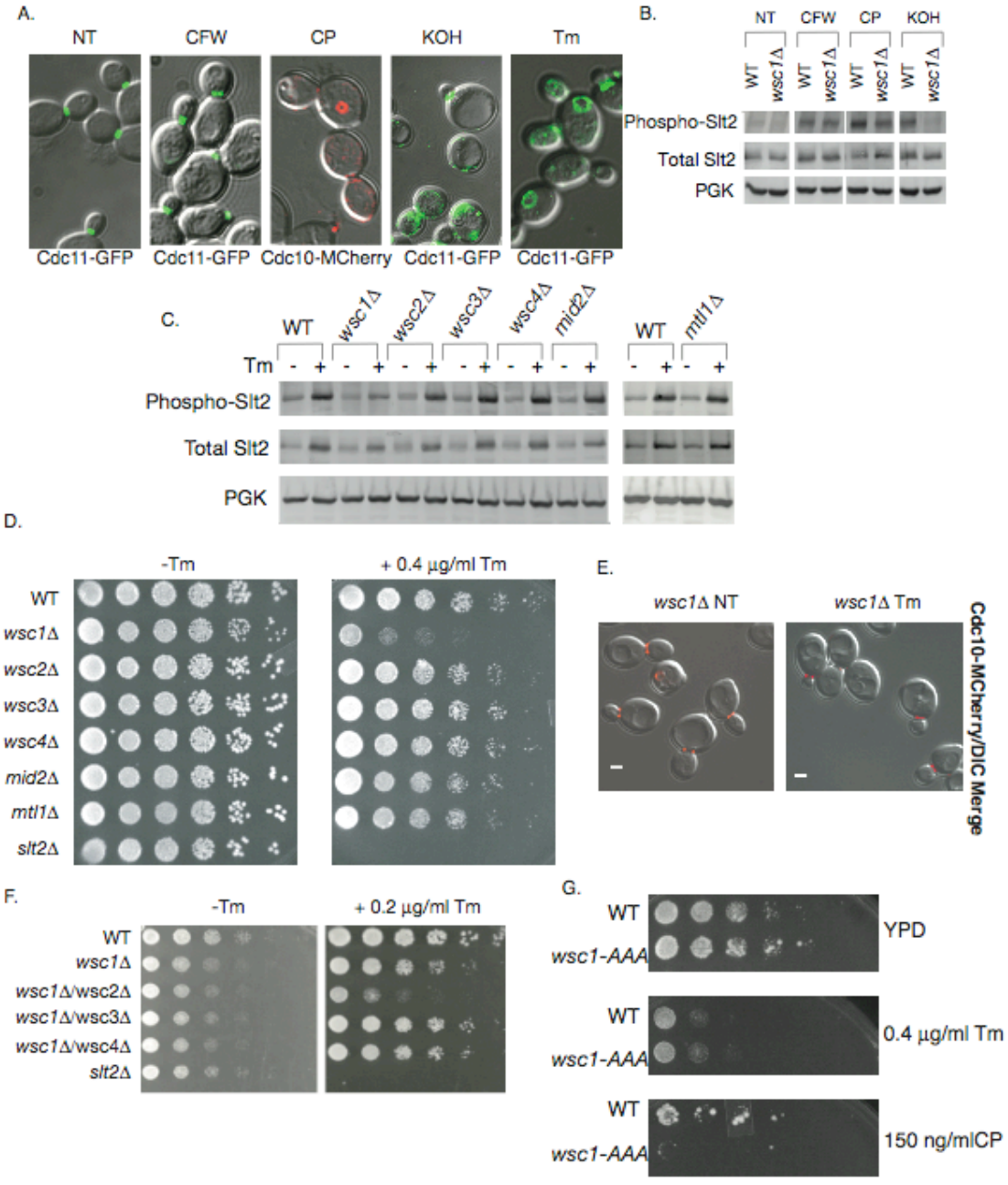
A.
NT
CFW
CP
KOH
Tm
Cdc11-GFP
Cdc11-GFP
Cdc10-MCherry
Cdc11-GFP
Cdc11-GFP
B.
NT
CFW
CP
KOH
WT
wsc1Δ
Phospho-Slt2
Total Slt2
PGK
C.
WT
wsc1Δ
wsc2Δ
wsc3Δ
wsc4Δ
mid2Δ
WT
mtl1Δ
Tm
Phospho-Slt2
Total Slt2
PGK
D.
-Tm
+ 0.4 µg/ml Tm
WT
wsc1Δ
wsc2Δ
wsc3Δ
wsc4Δ
mid2Δ
mtl1Δ
slt2Δ
E.
wsc1Δ NT
wsc1Δ Tm
Cdc10-MCherry/DIC Merge
F.
-Tm
+ 0.2 µg/ml Tm
WT
wsc1Δ
wsc1Δ/wsc2Δ
wsc1Δ/wsc3Δ
wsc1Δ/wsc4Δ
slt2Δ
G.
WT
wsc1-AAA
YPD
WT
wsc1-AAA
0.4 µg/ml Tm
WT
wsc1-AAA
150 ng/mlCP

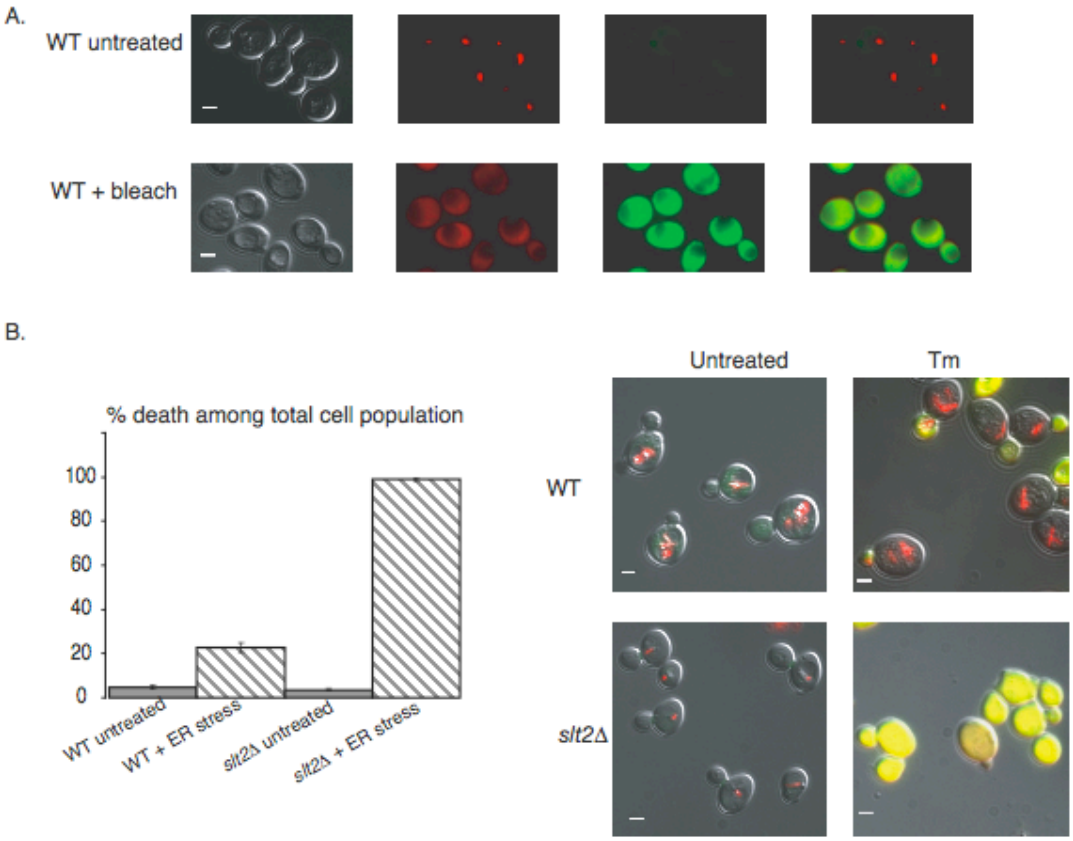

Figure 3.9 ERSU promotes mother cell viability during ER stress: (A) Vital dye assay. Log phase wild-type cells were stained for 30 minutes with FUN-1 after growth in YPD (top) or after the addition of 10% bleach to the medium before microscopic observation. (B) Exponentially growing wild type or slt2D cells were treated for 2 hrs with 1 μg/ml Tm or DMSO (vehicle) and subsequently stained with FUN-1 to monitor cell viability. % Death was calculated as number of yellow cells divided by total number of cells.

Chapter 4: Hog1 map kinase plays a central role in a late-phase endoplasmic reticulum stress response pathway

4.1 ABSTRACT

When unfolded proteins accumulate in the endoplasmic reticulum (ER), the unfolded protein response (UPR) is quickly activated to alleviate the stress. However, little is known about how cells cope with ER stress that persists after the UPR is activated. We have found that long-term ER stress activates Hog1, a p38-type MAP kinase, and that Hog1 activation provides resistance to the stress. Activation of Hog1 depends on both UPR-dependent and independent signals. Upon activation, Hog1 translocates to the nucleus to regulate transcription. It later returns to the cytoplasm where it helps activate autophagy by enhancing production of Atg8, a critical autophagy protein. Thus, Hog1 MAP kinase mediates a heretofore undefined, multi-faceted late-phase ER stress response.

4.2 INTRODUCTION

In eukaryotic cells, plasma membrane proteins, proteins that are secreted, and proteins that reside within the secretory pathway all begin their maturation within the endoplasmic reticulum (ER). The ER is contains chaperones, glycosylation enzymes, and oxidoreductases that make it an ideal environment for the folding of nascent proteins. Secretory proteins leave the ER for their targeted locations only after they have achieved their appropriate conformation, making the ER a gateway to the secretory pathway. In

response to environmental or developmental changes, the demand for protein folding can increase dramatically, and overwhelm the ER's protein-folding machinery, thus leading to an accumulation of unfolded proteins within the ER. This condition, known as ER stress, is deleterious to cells and has been implicated in many human pathologies, including Alzheimer's, Parkinson's, and Huntington's diseases (228). Therefore, when ER stress is detected, cells react in multiple coordinated ways to alleviate the stress. At the center of this stress response is the unfolded protein response (UPR), a conserved pathway that activates a transcriptional program that helps expand the ER's protein-folding capacity (9, 147). In budding yeast the UPR is initiated when Ire1p, an ER transmembrane protein, detects stress within the ER lumen and activates its cytoplasmic ribonuclease domain (12). The ribonuclease removes a UPR-specific intron from *HAC1* mRNA, thus initiating its splicing. *HAC1* encodes a transcription factor that activates UPR target genes (11), but only the spliced form of *HAC1* can be translated (19, 23), making Ire1 activation a key regulatory step for the UPR pathway.

Within 15 minutes of ER stress induction in yeast, 381 genes are activated in an *IRE1*/*HAC1*-dependent manner (2). Much work has been done characterizing these UPR target genes, which appear to be the "first responders" to ER stress. However, relatively little is known about how the cell responds if ER stress persists after these genes are activated. We analyzed data from previous microarray studies (2) and found that approximately 250 genes that are not part of the initial wave of transcription become activated when ER stress persists for two hours. Autophagy, a process of bulk cytoplasmic degradation, is also induced after two hours of persistent ER stress (67, 103).

It is currently unknown what signals control these two late processes and how those signals interface with the UPR. However, the contemporaneous nature of the transcriptional response and autophagy induction suggests that these two processes might be regulated in a coordinated manner, as part of a late-phase ER stress response. This late-phase response would presumably help cells cope with conditions of ER stress that persist after UPR activation.

A genetic screen revealed that deletion of *HOG1* (High Osmolarity Glycerol) mitogen activated protein kinase (MAPK) decreases resistance to ER stress (201). *HOG1* has unique functional properties that suggest it could regulate both aspects of the late-phase ER stress response. First, it has the ability to control a broad transcriptional program, which has been exemplified during its response to osmotic stress (229-231). Second, it has the potential to regulate autophagy. Although a physiological role in autophagy has not yet been identified, when Hog1 activation is primed by osmotic stress, this enhances the level of starvation-induced autophagy (232). Moreover, *HOG1*'s mammalian homologue p38 regulates autophagy during physiological conditions, such as the innate immune response in macrophages (233) or following exposure to chemotherapeutics in human cancer cells (234-236). Therefore, Hog1 is a candidate to mediate a late-phase ER stress response, comprised of transcriptional activation and autophagy induction.

HOG1 is one of five MAPKs encoded in the yeast genome. MAPKs are serine/threonine-specific protein kinases that respond to various stimuli, including stressors such as DNA damage, heat shock, and osmotic stress. These kinases are

activated by a conserved cascade of phosphorylation events; the stimulus causes activation of a MAPK/ERK Kinase Kinase (MEKK), which in turn phosphorylates a MAPK/ERK Kinase (MEK), which then phosphorylates the MAPK on neighboring tyrosine and threonine residues, causing its activation. Once activated, MAPKs regulate a wide array of cellular events, from cell proliferation and apoptosis to short-term homeostatic control and stress management (237).

Hog1 directs the cellular response to osmotic stress. In its absence, high levels of solute in the extracellular environment causes cells to rapidly lose viability (238). During osmotic stress, two distinct MAPK activation modules converge to activate Hog1 by phosphorylation of neighboring threonine and tyrosine residues. Either one of the upstream modules is sufficient for activation of the pathway (239). Upon activation, Hog1 translocates into the nucleus. Nuclear translocation requires phosphorylation on both residues, but does not require Hog1 kinase activity (240). Within the nucleus, Hog1 regulates multiple transcription factors, and also interacts directly with promoters of target genes to regulate the cell's transcriptional response to osmotic stress (241-246). Following adaptation, Hog1 becomes dephosphorylated by three different phosphatases, Ptc1, Ptp2, and Ptp3 (247-249). Hog1 exits the nucleus at the same time that it is dephosphorylated, but nuclear exit does not require dephosphorylation (250).

Most previous studies have focused on Hog1's transcriptional function. Yet, Hog1 also has cytoplasmic targets, including Rck1, Rck2, and Hsl1, that it phosphorylates during osmotic stress (251, 252). Since Hog1 activation correlates with nuclear localization, it is not clear how these cytoplasmic proteins are targeted by Hog1.

They might be phosphorylated by a very small pool of Hog1 that remains in the cytoplasm while activated. Alternatively, they might become phosphorylated just prior to Hog1's nuclear import, or in a narrow window subsequent to nuclear export but prior to dephosphorylation.

In this study, we show that Hog1 becomes activated during the later stages of ER stress, in a manner that depends upon *IRE1* and *HAC1,* as well as components of both Hog1 MAPK cascades. Hog1 activation plays a role both in the nucleus and cytoplasm, regulating transcription and autophagy respectively. Thus, Hog1 regulates a coordinated response that is specifically reserved for the later stages of ER stress. We therefore refer to this response as the late-phase ER stress response.

4.3 RESULTS

Hog1 protects cells from ER stress

To determine whether Hog1 plays a role in the ER stress response, *hog1Δ* cells were plated on media containing tunicamycin (Tm) or dithiothreitol (DTT), two drugs that are widely used to induce ER stress. Tm is an inhibitor of N-linked glycosylation in the ER and DTT disrupts intramolecular and intermolecular disulfide bonds, thus both treatments lead to an accumulation of unfolded proteins in the ER, but by different mechanisms. Consistent with a previous genome-wide DTT sensitivity screen (2), *hog1Δ* cells were found to be impaired in their ability to grow in the presence of either of these drugs (Figure 4.1A), indicating that *HOG1* contributes to cell survival during prolonged ER stress.

The UPR pathway is activated at a level commensurate with the amount of stress in the ER. Therefore, *HAC1* mRNA splicing, a proximal marker of UPR activation, can be used to assay the extent of ER stress. To confirm a role for *HOG1* in alleviating ER stress, we measured *HAC1* mRNA splicing in wild type and *hog1Δ* cells. In the absence of stress-inducing drugs, *hog1Δ* cells exhibited the same low level of splicing as their wild type counterparts, indicating that under normal growth conditions *HOG1* is not necessary for proper ER function. When DTT was added to the media, *HAC1* mRNA became 75% spliced within the first hour of treatment for both wild type and *hog1Δ* cells (Figure 4.1B). However, *hog1Δ* cells retained a high level of splicing longer than wild type cells, suggesting that the ER in *hog1Δ* cells is impaired in regaining homeostasis. Very similar results were seen when Tm was used to induce ER stress. Because the continued presence of Tm induces prolonged *HAC1* mRNA splicing even in wild type cells (data not shown), Tm was added for 45 minutes, and then washed out of the medium. As cells recovered from this insult, the state of the ER was monitored by measuring *HAC1* mRNA splicing. Once again, *hog1Δ* cells were impaired in their recovery from ER stress (Figure 4.1C).

To determine whether Hog1 could affect the ER during the induction phase of ER stress, osmotic stress was used to pre-activate Hog1 in wild type cells. Cultures were first treated with 0.8 M NaCl for 10 minutes, which is known to activate Hog1 phosphorylation through the osmotic stress response pathway (238). Immunoblotting with a phospho-specific p38 antibody confirmed that Hog1 was highly phosphorylated after this pre-treatment (Figure 4.1D). Cells were then exposed to DTT and the induction

of *HAC1* mRNA splicing was monitored. The addition of NaCl alone did not induce any measurable *HAC1* splicing (Figure 4.1E, lane 1, top and bottom panels). However, pre-treatment with osmotic stress did dramatically slow the kinetics of *HAC1* splicing following the addition of DTT (Figure 4.1E compare top and bottom panels), suggesting that prior activation of Hog1 can mitigate the severity of ER stress.

Hog1 is activated during ER stress

Since Hog1 appears to play a role in coping with ER stress, the possibility that ER stress induces Hog1 phosphorylation was examined. Both DTT and Tm treatments resulted in increased levels of phosphorylated Hog1 protein (Figure 4.2A). 0.4 M NaCl is known to induce Hog1 phosphorylation within 5 minutes (238). During DTT treatment, Hog1 was phosphorylated slightly more than during NaCl treatment, while Tm treatment induced slightly less phosphorylation than NaCl. The kinetics of this ER-induced Hog1 phosphorylation event were markedly different from the kinetics of UPR activation. As measured by *HAC1* mRNA splicing, UPR activation occurred within 15 minutes of drug exposure (Figure 4.1E bottom panel). By contrast, Hog1 phosphorylation was not observed until 2 hours after DTT or Tm treatment. Therefore, Hog1 phosphorylation appears to be part of a previously undefined late-phase ER stress response.

During osmotic stress, Hog1 phosphorylation results in its immediate import into the nucleus, where it interacts with various transcription factors to mediate a transcriptional response. To determine whether this was also true during ER stress, the

localization of Hog1-GFP was examined during ER stress and osmotic stress. As expected, Hog1-GFP localized to both the nucleus and cytoplasm during normal growth, but became exclusively nuclear after 5 minutes of osmotic stress induced by 0.4 M NaCl treatment (Figure 4.2B). Similarly, after 2 hours of DTT or Tm treatment, the timepoint at which Hog1 phosphorylation was initially seen, Hog1-GFP was imported into the nucleus. This suggests that one of Hog1's roles in alleviating ER stress might be through its function as a transcriptional regulator. Therefore, transcript levels of four of Hog1's known target genes: *HSP12*, *ENA1*, *CTT1*, and *STL1* (229, 246, 253) were examined. During osmotic stress, all four transcripts were induced in a *HOG1*-dependent manner, as expected. By contrast, during ER stress only *HSP12,* which encodes a small heat shock protein with unknown biochemical activity, was induced (Figure 4.2C). The kinetics of *HSP12* induction correlated with the kinetics of Hog1 phosphorylation and nuclear import. Furthermore, *HSP12* induction was dramatically reduced in *hog1Δ* cells. Like osmotic stress, ER stress did induce a small amount of *HSP12* transcription even in *HOG1*'s absence, suggesting that an additional factor collaborates with Hog1 to regulate *HSP12* transcription during both types of stress.

ER stress utilizes both *SSK1* and *STE11* Hog1 activation branches

MAPK upstream activation modules play a key role in regulating the cellular response to various types of stress in all eukaryotic cell types. Often, different types of stress will feed into different modules to activate the same MAPK, and the nature of the response is conferred partly by the specific module(s) that are activated (254). In the case

of Hog1, two modules can stimulate activation of the MAPK (239, 255, 256). In one pathway, a two component phospho-relay mechanism comprised of Sln1, Ypd1, and Ssk1 (239, 255, 257, 258) stimulates the activation of two redundant MEKKs, Ssk2 and Ssk22 (Figure 4.3A, depicted in white). In the second branch, two putative osmosensors, Msb2 and Hkr1 (259) activate Sho1 at the plasma membrane (239, 256), which signals the downstream activation of a third MEKK, Ste11 (Figure 4.3A, depicted in black). Any one of these three MEKs can phosphorylate Pbs2, a MEK (238), which in turn phosphorylates Hog1 (Figure 4.3A, depicted in grey).

To determine the role of the two MAPK pathways in the ER stress response, Hog1 phosphorylation was examined following DTT treatment in strains lacking the MEK, *PBS2*, and each of the three MEKK's, *STE11*, *SSK2*, and *SSK22*. *PBS2* was absolutely necessary for DTT-induced Hog1 activation, suggesting that Hog1 is directly phosphorylated by Pbs2 during ER stress, as it is during osmotic stress (Figure 4.3B, lanes 2 & 6). Of the three MEKK's examined, *STE11* was not necessary for DTT-induced Hog1 phosphorylation, whereas *SSK2* and *SSK22* were partly necessary (Figure 4.3B, lanes 3-6). To determine whether the two pathways acted redundantly, each upstream activation branch was removed individually, and in combination. Removal of the *SSK1* branch substantially reduced DTT-induced Hog1 phosphorylation (Figure 4.3C, compare lanes 2 & 4). Furthermore, although removal of *STE11* by itself had no effect on Hog1 phosphorylation (Figure 4.3C, compare lanes 2 & 3), it did result in further decrease of Hog1 phosphorylation when combined with removal of *SSK1* (Figure 4.3C, compare lanes 4 & 5). In fact, with both branches deleted, no Hog1 phosphorylation was

observed during DTT treatment (Figure 4.3C, lane 5). This indicates that both upstream branches contribute to ER-induced Hog1 phosphorylation, and that the two branches are partly redundant; activation of the *SSK1* branch can completely compensate for the loss of *STE11*, whereas *STE11* can only partly compensate for the loss of *SSK1*.

To determine whether the signal from the ER to the MAPK activation modules is mediated by the plasma membrane, as it is during osmotic stress, *SHO1* was deleted individually and in combination with *SSK1*. Sho1 was chosen to test plasma membrane involvement because it sends a positive signal to the Hog1 activation cascade, whereas Sln1 sends a negative signal and cannot be tested by a simple loss of function assay. Like *STE11*, removal of *SHO1* alone had no effect on DTT-induced Hog1 phosphorylation (Figure 4.3D, compare lanes 2 & 5). However, when combined with the deletion of the parallel pathway component *SSK1*, deletion of *SHO1* dramatically reduced Hog1 phosphorylation (Figure 4.3D, compare lanes 3 & 4). Therefore, both known Hog1 activation branches are activated during ER stress, and at least one of these branches is activated via a component on the plasma membrane.

To confirm that both branches are involved in the ER stress response, growth during ER stress was examined for cells lacking each of the pathway components. As expected, *pbs2Δ* cells were equally sensitive to growth on Tm plates as were *hog1Δ* cells (Figure 4.3E). Furthermore, the removal of both Hog1 activation branches, either through the deletion of *SSK1* along with *STE11* or *SSK1* along with *SHO1,* also caused the same level of Tm sensitivity as removal of *HOG1*. Confirming the partial redundancy between the two branches, removal of *STE11* or *SHO1* alone did not increase

Tm sensitivity, but deletion of *SSK1* had an intermediate effect on Tm sensitivity. This intermediate effect of removing *SSK1* during ER stress is particularly interesting, as it distinguishes the pathway from the osmotic stress pathway, where the two pathways appeared completely redundant and removal of *SSK1* had no effect (Figure 4.3E middle panel).

Role of UPR signaling in activation of Hog1 during ER stress

ER stress utilizes the same upstream activation components as osmotic stress, but it is still not clear how the ER communicates with these components. Since the signal to activate Hog1 from the ER travels through the plasma membrane, one potential way of linking Hog1 to the ER is through a general block of the secretory pathway. Although a general block in secretion has not been reported during ER stress (86), if such a block were to occur it could prevent the targeting of key regulators to the plasma membrane, thus causing Hog1 activation. Strains bearing the *sec61-2* temperature sensitive allele were used to test this possibility. At the restrictive temperature, strains bearing this allele are known to experience a block in secretion within one hour (260). This particular strain was selected because, unlike many secretion-deficient strains, its secretion block is not accompanied by an increase in ER stress, which by itself would induce Hog1 phosphorylation. To verify that secretion was blocked in the *sec61-2* strain, transcription of the ribosomal protein gene *RPL32* was examined. This gene is known to be specifically downregulated when secretion is blocked (261). After one hour of growth at 37°C, significant downregulation of *RPL32* was observed (Figure 4.4A), verifying that

secretion was blocked. However, even after four hours of growth at the restrictive temperature, Hog1 phosphorylation was not detected in *sec61-2* cells (Figure 4.4B), indicating that a secretory block is not sufficient to cause Hog1 phosphorylation, and some other mechanism must exist to link Hog1 to the ER.

Currently, Ire1 is the only known direct sensor of ER stress in yeast. In *ire1Δ* cells, DTT-induced Hog1 phosphorylation was dramatically reduced, but not completely eliminated (Figure 4.4C). Therefore, at least two distinct mechanisms exist to activate Hog1 during ER stress: one that is *IRE1*-dependent, and one that is not. Furthermore, the *IRE1*-dependent branch is specific to ER stress, as *ire1Δ* cells exhibited wild type levels of Hog1 phosphorylation during osmotic stress.

The presence of an *IRE1*-dependent Hog1 activation branch confirms that a secretory block is not sufficient to induce Hog1 phosphorylation (Figure 4.4A). Previous studies have been unable to detect a block in secretion in wild type cells during ER stress, but have detected a block in *ire1Δ* cells, presumably because these cells are not capable of compensating for the increased ER load. Therefore, if Hog1 phosphorylation were simply the result of a secretory block, more phosphorylation would be expected in *ire1Δ* cells, rather than less.

To determine whether Ire1 promotes Hog1 phosphorylation through its activation of Hac1, or through some distinct mechanism, DTT-induced Hog1 phosphorylation was examined in *hac1Δ* cells. Like *IRE1*, *HAC1* was partly necessary for phosphorylation (Figure 4.4C), suggesting that canonical UPR signaling is involved in regulating Hog1 activation. To determine whether activation of Hac1 is sufficient to induce Hog1

phosphorylation, the activated form of *HAC1*, lacking the inhibitory intron, was expressed from a promoter containing the glucocorticoid responsive element. Expression from this promoter can be induced by the addition of deoxycorticosterone (DOC) to the medium, as long as a mammalian glucocorticoid receptor is constitutively expressed in the cells (262). Previously, expression of spliced *HAC1* from this promoter has been shown to induce UPR target gene transcription (2). By one hour after treatment with DOC, the activated form of Hac1 was expressed at similar levels to those observed during DTT treatment (Figure 4.4D, top panel, compare lanes 3 & 11). Furthermore, this expression was sufficient to induce UPR-dependent gene activation (Figure 4.4E), as measured by Unfolded Protein Response Element (*UPRE)-lacZ* reporter expression (11). However, spliced *HAC1* expression was not sufficient to induce Hog1 phosphorylation (Figure 4.4D, middle panel, lanes 10-13). Therefore, for Hac1 to have an effect on Hog1 phosphorylation, an unknown second signal must be present in the cell; the UPR's role during ER stress is most likely to potentiate this unknown signal.

To determine which of Hog1's two upstream activation branches is potentiated by the UPR, a genetic analysis was conducted. First, DTT-induced Hog1 phosphorylation was examined in an *ire1Δ ssk1Δ* double deletion strain. As before, single deletion of these genes reduced Hog1 phosphorylation by approximately 50% (Figure 4.5A, lanes 2-4). Deleting both genes in combination caused an even further reduction in DTT-induced Hog1 phosphorylation (Figure 4.5A, lane 5), indicating that Ire1 acts, at least partly, in parallel with Ssk1. Therefore, Ire1 probably activates components of the Ste11 Hog1 activation branch. However, activation of the Ste11 branch cannot be Ire1's only

contribution to Hog1 phosphorylation; deleting *STE11* has no effect on Hog1 phosphorylation (Figure 4.5B, compare lanes 2 & 3), but deleting *IRE1* has a substantial effect (Figure 4.5B, compare lanes 2 & 4). Therefore, Ire1 most likely acts on Hog1 phosphorylation by potentiating both branches of the Hog1 activation cascade, although we cannot rule out the possibility that Ire1 acts on Hog1 independently of either of Hog1's activation branches.

Since the downstream effect of UPR signaling is transcriptional activation, the possibility that the UPR potentiates Hog1 activation by increasing the abundance of Hog1 signaling components was examined. The transcript levels of *PBS2*, *SSK1*, and *STE11* were examined. *STE11* was induced in an *IRE1*-dependent manner after two hours of ER stress, while *PBS2* and *SSK1* were not (Figure 4.5C & D and data not shown). In addition, *SSK22*, a key mediator of Hog1's second activation module, has been shown by genome-wide analysis to be induced at that time. The activation of these two genes most likely accounts, at least partly, for the UPR-dependent potentiation of Hog1 phosphorylation. These data are consistent with a model in which an unknown primary signal activates both Hog1 activation branches during ER stress, and the UPR enhances this activity by increasing the expression of *STE11* and *SSK22* (Figure 4.5E).

Autophagy requires Hog1 phosphorylation during ER stress

During the later stages of ER stress, yeast cells induce autophagy (67, 103), which is a mechanism of targeting large portions of the cytoplasm to the vacuole for degradation and recycling. It is presumed that the function of ER stress-induced autophagy is to

degrade some portion of the ER. However, the mechanism of inducing autophagy during ER stress is not known.

When autophagy is induced, the small ubiquitin-like protein Atg8 increases in abundance (263, 264). Atg8 helps to form the autophagosome (263), which ultimately fuses with the vacuole to deliver cytoplasmic components (265). During autophagosome formation, some Atg8 molecules become trapped within the autophagosome, and are subsequently delivered to the vacuole and degraded (264). A *GFP-ATG8* fusion gene, expressed from the *ATG8* promoter, is widely used to monitor three distinct steps of autophagy (266-268). First, this marker allows the use of GFP immunoblotting to measure Atg8 protein levels, which increase during the early induction of autophagy. Second, when autophagy is induced, structures termed pre-autophagosomal structures (PASs, also called phagophore assembly sites) are created to nucleate the autophagosome (267). Because Atg8 is targeted to these structures, the GFP-Atg8 reporter may be used to observe their formation. Finally, when GFP-Atg8 is ultimately delivered to the vacuole, the Atg8 portion of the chimeric protein is degraded by the proteases in the vacuole, whereas the GFP portion of the protein is resistant to degradation and remains intact. Therefore, when a smaller form of GFP is detected on an SDS-PAGE gel (Figure 4.6A, top panel, bottom band), this marks the fusion of the autophagosome with the vacuole and the degradation of its contents.

During Tm treatment in wild type cells, an increase in GFP-Atg8 levels was observed after two hours. At four hours, the release of the smaller, stable GFP was detected, indicating that Atg8 was delivered to the vacuole and degraded (Figure 4.6A).

In *hog1Δ* cells, levels of GFP-Atg8 did increase, but this increase was considerably diminished compared to wild type cells. Corresponding to the lower GFP-Atg8 levels, *hog1Δ* cells also exhibited lower levels of the cleaved GFP fragment during the later timepoints. This role of Hog1 in regulating GFP-Atg8 accumulation was dependent on its phosphorylation; *pbs2Δ* and *ste11Δ ssk1Δ* cells, which cannot phosphorylate Hog1 (Figures 4.3B & C), were also defective in Tm-induced accumulation of GFP-Atg8 (Figure 4.6B). To confirm a role for Hog1 in autophagy, GFP-Atg8 was also examined during DTT treatment. Like Tm, DTT induced an increase in total GFP-Atg8 levels at 2 hours, and the release of the small GFP fragment at 4 hours. Both the increase and the release were significantly reduced in *hog1Δ* cells (Figure 4.6C).

Autophagy is also strongly induced by starvation, during which cytoplasmic degradation allows cells to recycle essential nutrients (269, 270). To determine the specificity of Hog1's role in regulating Atg8 during ER stress, GFP-Atg8 induction in wild type and *hog1*Δ cells was examined during starvation, induced by nitrogen removal from the medium (Figure 4.6D). Before autophagy induction, GFP-Atg8 levels were 1.5 fold higher in wild type cells than in *hog1*Δ cells (Figures 4.6A, C, & D, lanes 1 & 5). During starvation, this ratio remained constant as GFP-Atg8 levels increased (Figure 6E). In contrast, during both DTT and Tm treatment, GFP-Atg8 levels were induced significantly more in wild type cells than in *hog1*Δ cells, suggesting that Hog1 plays a role in activating Atg8 during ER stress, but not during starvation.

The increase in Atg8 protein levels and the formation of PASs during autophagy are parallel processes (267), both of which depend upon an upstream autophagy induction

signal (263). Therefore, to determine whether Hog1 specifically regulates Atg8 protein levels, or broadly regulates the induction phase of autophagy, PAS formation was examined in *hog1Δ* and wild type cells. As expected, cells expressing GFP-Atg8 formed discrete PAS-like puncta following DTT and Tm treatment. However, the appearance of these structures did not depend upon *HOG1*. Therefore, Hog1's function in regulating autophagy occurs at a step that specifically regulates Atg8 levels (Figure 4.6F).

Modulating Atg8 protein levels has previously been shown to directly affect the amount of autophagy induced by the cell (271). Therefore, Hog1's regulation of Atg8 levels should influence the rate of autophagy during ER stress. To test this, an assay previously developed to measure autophagic activity (272) was used. This assay utilizes Pho8, an alkaline phosphatase that can only become activated when it is delivered to the vacuole where its C terminal peptide is cleaved. The wild type protein is delivered to the vacuole constitutively, but the mutant form pho8Δ60 cannot be delivered to the vacuole unless autophagy is induced. Therefore, in strains expressing pho8Δ60 as their only alkaline phosphatase, alkaline phosphatase activity can be used as a direct measure of autophagy. This assay was used to determine that the rate of autophagy increased 1.5 fold after 6 hours of Tm treatment (Figure 4.6G), confirming that the Atg8 induction and processing previously described by others does indeed reflect an induction of autophagy during ER stress. As a negative control, *atg8Δ* cells, which are known to be autophagy-deficient, showed no such induction. Strikingly, *hog1Δ* cells likewise showed no induction of autophagy during Tm treatment. Thus, Hog1-mediated induction of Atg8 is necessary for autophagy induction during the later stages of ER stress.

Hog1's autophagy function may be mediated by cytoplasmic activation of Rck2

Hog1 is primarily a transcriptional activator, and *ATG8* is transcriptionally activated during autophagy. Therefore, the possibility Hog1 imparts transcriptional control on *ATG8* during ER stress was examined. *ATG8* transcriptional induction occurred within one hour, much earlier than detectable Hog1 phosphorylation, and was unaffected by the loss of *HOG1* (Figure 4.7A). Therefore, Hog1 does not regulate *ATG8* transcription, but must instead regulate its translation or protein stability.

To determine whether this post-transcriptional regulation of Atg8 occurs from the nucleus or cytoplasm, Hog1 localization was analyzes at later timepoints. Surprisingly, after three hours of stress, Hog1 exited the nucleus (Figure 4.6B), despite the fact that phosphorylation levels were continuing to increase (Figure 4.2A). This behavior of Hog1 contrasted sharply with osmotic stress, where a tight correlation was observed between Hog1 nuclear exit and dephosphorylation (Figure 4.7C). In addition, 3 hours of pre-treatment with DTT or Tm prevented the nuclear accumulation of Hog1 in response to NaCl treatment (Figure 4.7D), suggesting that during the later stages of ER stress, Hog1 is actively retained in the cytoplasm.

Perhaps late-stage cytoplasmic retention of Hog1 is a key part of its regulation of autophagy. Although very little is known about potential functions for Hog1 in the cytoplasm, Hog1 does have several known cytoplasmic targets, including the kinase Rck2 (251). Cells lacking *RCK2* were severely impaired in GFP-Atg8 induction, to almost the same extent as *hog1Δ* cells (Figure 4.7E). Since Rck2 is already known to be

a direct target of Hog1, this strongly suggests that Hog1 imparts control on Atg8 through Rck2.

To gain insights into the role of autophagy during ER stress, and how it contributes to the broader late-phase ER stress response, the growth of *atg8Δ* cells and *rck2Δ* cells under conditions of ER stress was examined. Both autophagy-deficient mutants were resistant to growth on Tm plates (Figure 4.7F). This finding suggests that prolonged activation of autophagy is harmful to cells, which may be the reason that autophagy is reserved for stress that cannot be resolved by other means. Furthermore, this finding highlights the multi-faceted nature of the late-phase ER stress response. Clearly, its role in activating autophagy is not the reason that deleting *HOG1* results in sensitivity to ER stress, this must instead be the result of Hog1's transcriptional function, or another yet undiscovered function of Hog1 in the late-phase ER stress response.

4.4 DISCUSSION

We define a late-phase ER stress response pathway in yeast

Recent studies in mammalian cells suggest that persistent ER stress provokes a very different type of response than short-term stress. Specifically, in human embryonic kidney cells, activation of apoptotic pathways only occurs during the later stages of ER stress, whereas pro-survival pathways dominate the early stress response (273). This highlights the cellular need to distinguish between early and persistent stress, and tailor its response accordingly. In yeast, similarly distinct pressures are likely to exist during early and later phases of ER stress. Our data shed light on the specific nature of the late-

phase ER stress response in yeast, as we have discovered that two processes, transcriptional regulation and induction of autophagy, are regulated in a coordinated manner by a MAPK during persistent stress.

Currently, knowledge of the transcriptional component of the late-phase ER stress response is limited to one transcriptional target, *HSP12*. However, microarray experiments indicate that during ER stress, hundreds of genes are induced with kinetics similar to those of *HSP12* (2). It is likely that a large number of these genes will turn out to be bona fide stress-induced targets that depend upon *HOG1* for their induction. Future work defining the genome-wide *HOG1*-dependent transcriptional profile during ER stress will be key to defining the late-phase ER stress response pathway.

The induction of autophagy during ER stress in yeast has only recently been discovered (67, 103), and the purpose of this autophagy remains unknown. However, several interesting propositions have been put forth. In one report, although Atg8 was clearly induced, it did not appear to be degraded in the vacuole (67), leading to the proposition that autophagosomes function not to degrade stressed ER, but to sequester it and prevent toxicity while the ER recovers. However, in the current study, we do see evidence of vacuolar degradation of Atg8 during ER stress, albeit to a lesser extent than during starvation. Therefore, it seems that degradation of the ER is part of the late-phase ER stress response. However, this does not exclude the possibility that a sequestering function is also important. It has also been proposed that autophagy-induced ER degradation serves to reverse the UPR-stimulated expansion of the ER, thus helping cells

return to homeostasis (67). This model implies that extra ER is no longer necessary when autophagy is induced. However, under the conditions of persistent ER stress tested in the current study, autophagy is induced prior to alleviation of the stress. In fact, as autophagy is induced, a second wave of ER-stress responsive genes is transcriptionally activated. Therefore, rather than helping the cell wind down its stress response, it appears that autophagy actually intensifies the response.

During ER stress in mammalian cells, autophagy appears to assist the ER-Associated Degradation (ERAD) pathway in degrading misfolded ER proteins (104-106). Whereas ERAD selectively translocates misfolded proteins from the ER and targets them to the proteasome (93), autophagy may provide a backup by degrading entire portions of the ER and the unfolded proteins within. In the late-phase ER stress response in yeast, our data suggest that autophagy may perform a similar function, actually degrading misfolded ER proteins by degrading entire regions of the ER. Removing ER would reduce the toxicity of misfolded proteins, but would also reduce the ER's functional capacity at a time when it is already compromised. Thus prolonged induction of autophagy may actually harm cells, as indicated by the Tm-resistance of *atg8Δ* and *rck2Δ* strains. Therefore, the cell must strike a careful balance between the beneficial and harmful effects of degrading the ER during times of ER stress. Constraining autophagy to the later stages of ER stress may be one way that the cell handles this balance.

ER-stimulated activation of a MAPK

It appears that Ire1 potentiates a primary Hog1 activation signal by increasing the expression of components of the MAPK pathway. However, The nature of the *IRE1*-independent primary Hog1 activation signal remains unknown. MAPK pathways are generally activated either from the cytoplasm of the cell, or from the plasma membrane. We found that the ER stress-dependent Hog1 activation signal comes from the plasma membrane, at least for one of Hog1's upstream branches. Since the plasma membrane is a major target of ER-regulated protein traffic, this immediately suggests a model for MAPK activation.

A protein that normally resides in the ER might become modified during ER stress in a manner that removes or conceals an ER retention signal, and thus targets it to the plasma membrane to activate the MAPK cascades. Such a protein could be a proximal sensor of ER stress, analogous to Ire1, or it could be the target of such a sensor. Alternatively, a stress sensor from within the ER lumen might signal a lipid modification on the ER membrane. Through the secretory process, this lipid could be delivered to the plasma membrane, where it could signal activation of both Hog1 modules. Although such a mechanism has not been previously implicated for Hog1 activation, many other MAPKs are known to rely on lipid signaling for their activation (274).

Although ER stress, like osmotic stress, utilizes both *STE11* and *SSK1*-dependent Hog1 activation modules, the downstream effects of Hog1 activation are different between the two types of stress. First, the nature of the *HOG1*-dependent transcriptional response differs between osmotic stress and ER stress, with only one of the four osmotic

targets examined found to be activated during ER stress. Second, osmotic stress elicits a Hog1 nuclear localization pattern that tightly correlates with phosphorylation, whereas ER stress induces Hog1 phosphorylation that coincides with both nuclear and cytoplasmic localization. Third, ER stress causes Hog1 to stimulate Atg8 production, whereas osmotic stress does not. These differences highlight Hog1's capacity to customize its downstream response to its specific activation conditions. This type of customization is common in MAPKs, and is probably achieved through secondary condition-specific signals that interface with phosphorylated Hog1 and its targets. The identification of these signals will be of great interest for future studies.

HOG1-dependent Atg8 regulation

Little is known about how Atg8 levels are regulated during autophagy, but most models presume that transcriptional activation of *ATG8* accounts entirely for the increase in protein. Here, a post-transcriptional *HOG1*-dependent mechanism for increasing Atg8 abundance, which appears to be activated specifically during ER-induced autophagy, has been uncovered. This mechanism could involve *ATG8* mRNA transport, translation, or stability of Atg8 protein, and is likely to be mediated by Hog1's cytoplasmic target, Rck2.

Rck2 is a kinase with only one known substrate, eukaryotic elongation factor 2 (EF-2). By phosphorylating EF-2, Rck2 blocks translation (251). During various cellular stresses, it has been shown that global translational blocks can lead to preferentially stimulated translation of specific transcripts. This type of gene regulation is generally

conferred by elements in the 5'UTR of the activated transcript (37, 275, 276). During the first hour of ER stress in yeast, translation is not inhibited (86), but translation has not been examined during the later phases of ER stress. Since translation inhibition is a hallmark of the mammalian UPR (30), it is not unlikely that translational control is a part of the late-phase ER stress response in yeast. Thus, Rck2 might activate *ATG8* by blocking global translation in a manner that activates the translation of Atg8. This mechanism, as well as many other potential mechanisms for Atg8 regulation, will be the subject of future studies.

In this study, we have defined the late-phase ER stress response as the Hog1-mediated regulation of downstream events in response to long-term ER stress. Gene activation and autophagy induction are clearly a part of this response. However, Hog1 might also regulate other physiological processes during persistent ER stress. Because past studies have focused primarily on the cell's initial response to ER stress, aspects of cell physiology that are affected by persistent ER stress might have previously gone unnoticed. Therefore, our study uncovering a novel phase of the ER stress response lays the groundwork for future studies to identify new downstream events that might be functionally linked to the state of the ER.

ACKNOWLEDGEMENTS

We would like to thank Yoshinori Ohusmi for Atg8 antiserum and for the *pho8Δ60* strain and Daniel Klionsky for Atg8 antiserum and plasmids. We also thank

Randy Hampton for plasmids, yeast strains and for comments on this chapter; Lorraine Pillus and Jenny DuRose for comments on this chapter; and Peter Novick for technical advice.

Chapter 4 is modified from material that has been submitted for publication. Alicia A. Bicknell and Maho Niwa. I was the primary investigator and author of this paper under the supervision of Maho Niwa.

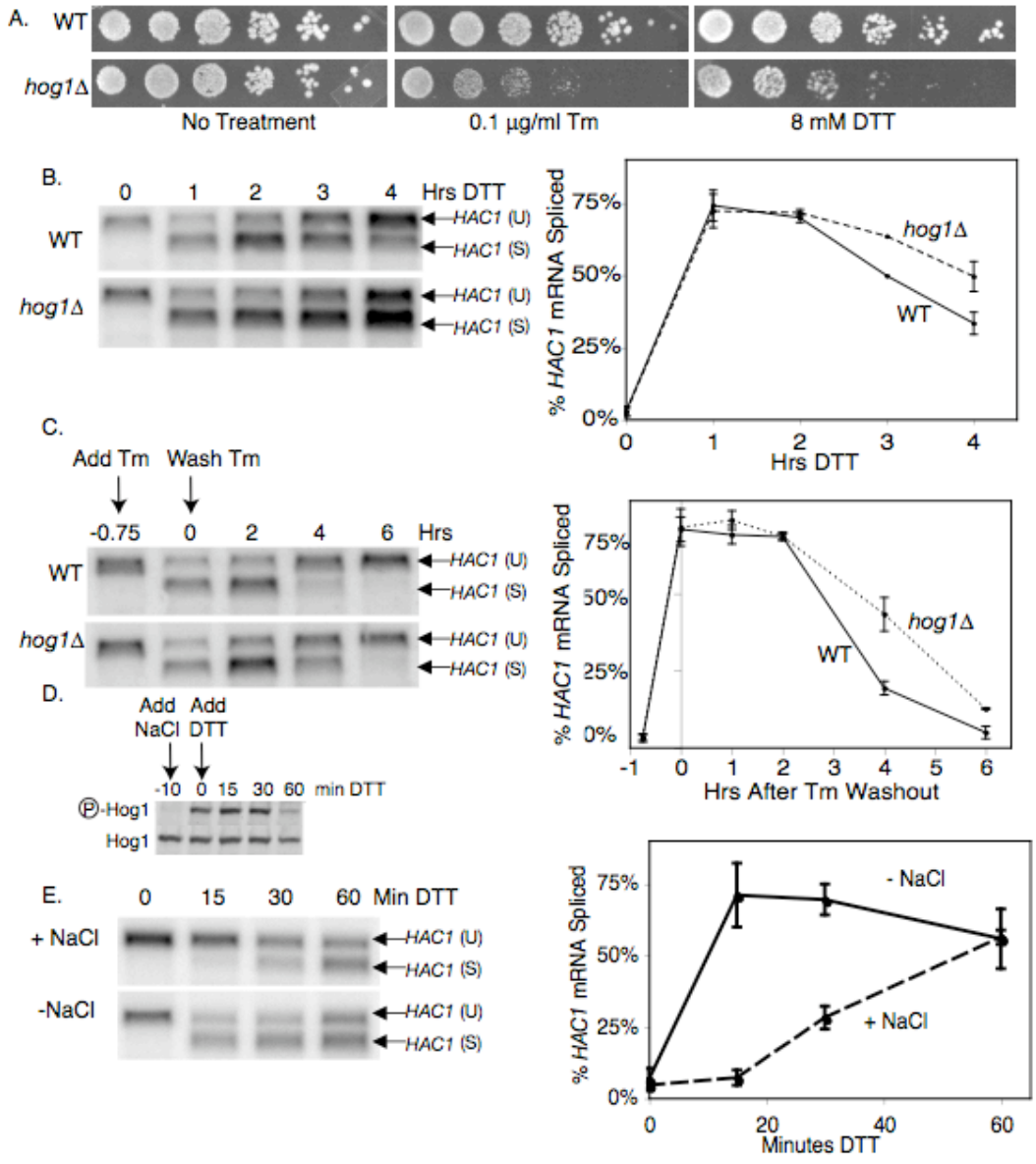

Figure 4.1 Hog1 protects cells from ER stress: (A) 5 fold serial dilutions of wild type and *hog1Δ* cells spotted onto plates with indicated additives. (B) Northern analysis with a *HAC1*-specific probe shows conversion of unspliced *HAC1* (*HAC1*(U))to spliced *HAC1* (*HAC1*(S)) during 4 mM DTT treatment in wild type and *hog1Δ* cells. Quantitation (spliced *HAC1* divided by total *HAC1*) is graphed. (C) 1 µg/ml Tm was added to wild type and *hog1Δ* cells for 45 minutes, and then washed away, followed by *HAC1* northern analysis. (D-E) Phospho Hog1 immunoblots (D) and *HAC1* northern blots (E) of cells treated with 0.8 M NaCl for 10 minutes, then 2 mM DTT for 1 hour. All error bars represent SD of three repeats.

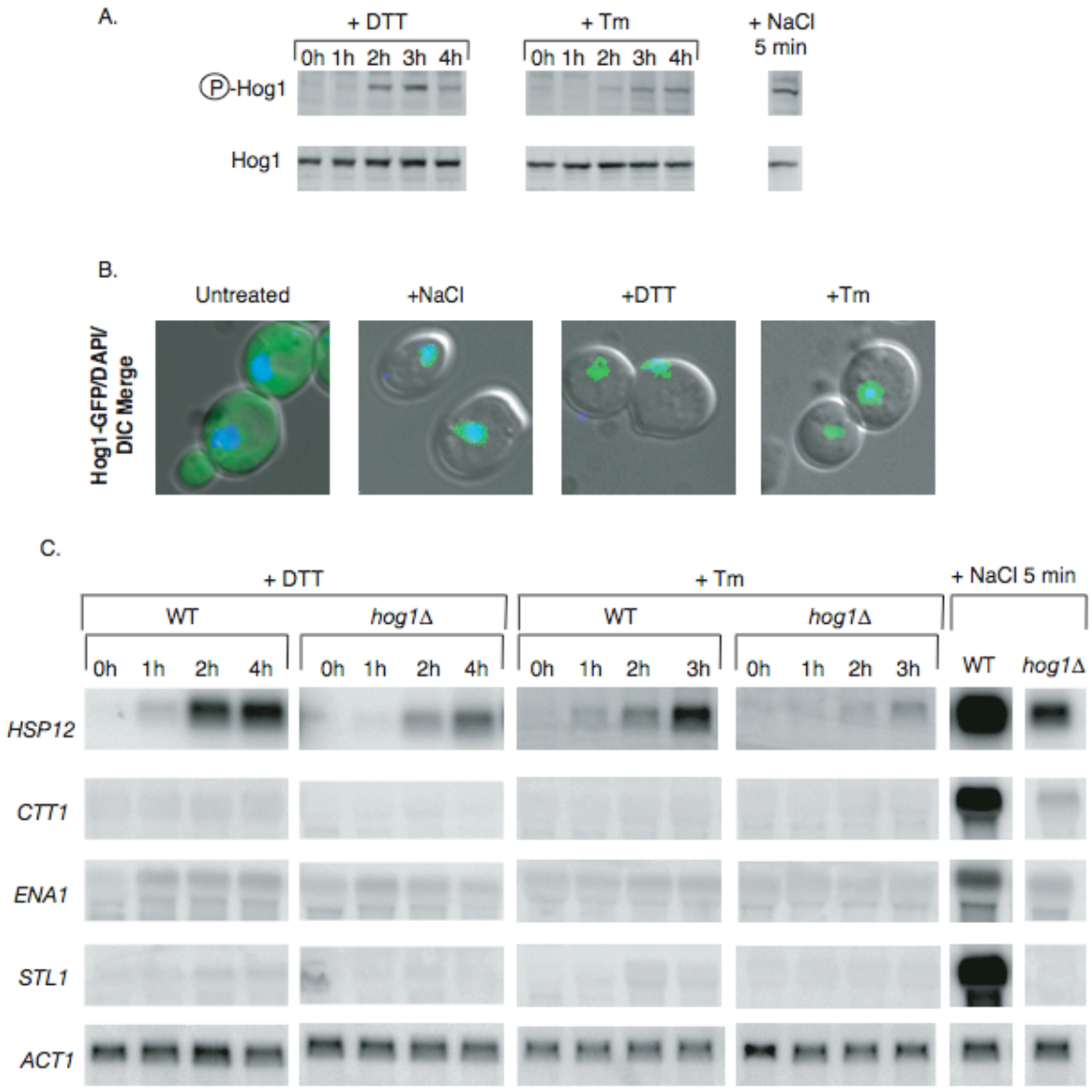

Figure 4.2 Hog1 is activated during ER stress: (A) Phospho Hog1 immunoblots of wild type cells treated with 2 mM DTT, 1 μg/ml Tm, or 0.4 M NaCl. (B) Cells expressing *HOG1*-GFP were treated with 0.4 M NaCl for 5 minutes, 2 mM DTT for 2 hours, or 1 μg/ml Tm for 2 hours. (C) Northern blots of wild type and *hog1Δ* cells treated with 4 mM DTT, 1 μg/ml Tm, or 0.4 M NaCl.

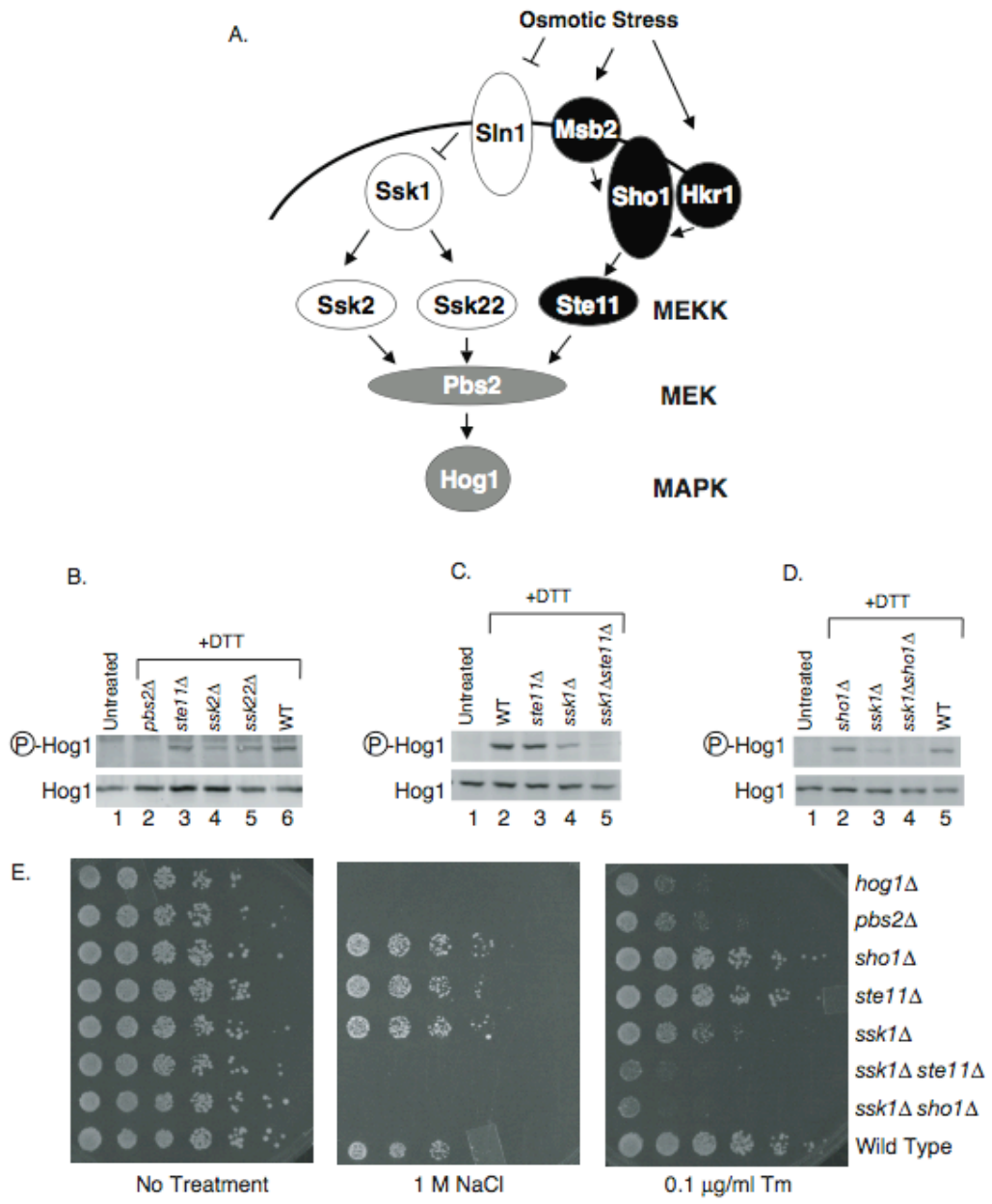

Figure 4.3 ER stress utilizes both *SSK1* and *STE11* Hog1 activation branches: (A) The two branches of the pathway previously shown to activate Hog1 during osmotic stress: *SSK1* branch depicted in white and *STE11* branch depicted in black. (B-D) Phospho Hog1 immunoblots of cells treated with 4 mM DTT for 3 h. (E) 5 fold serial dilutions of yeast cells spotted onto plates with indicated additives.

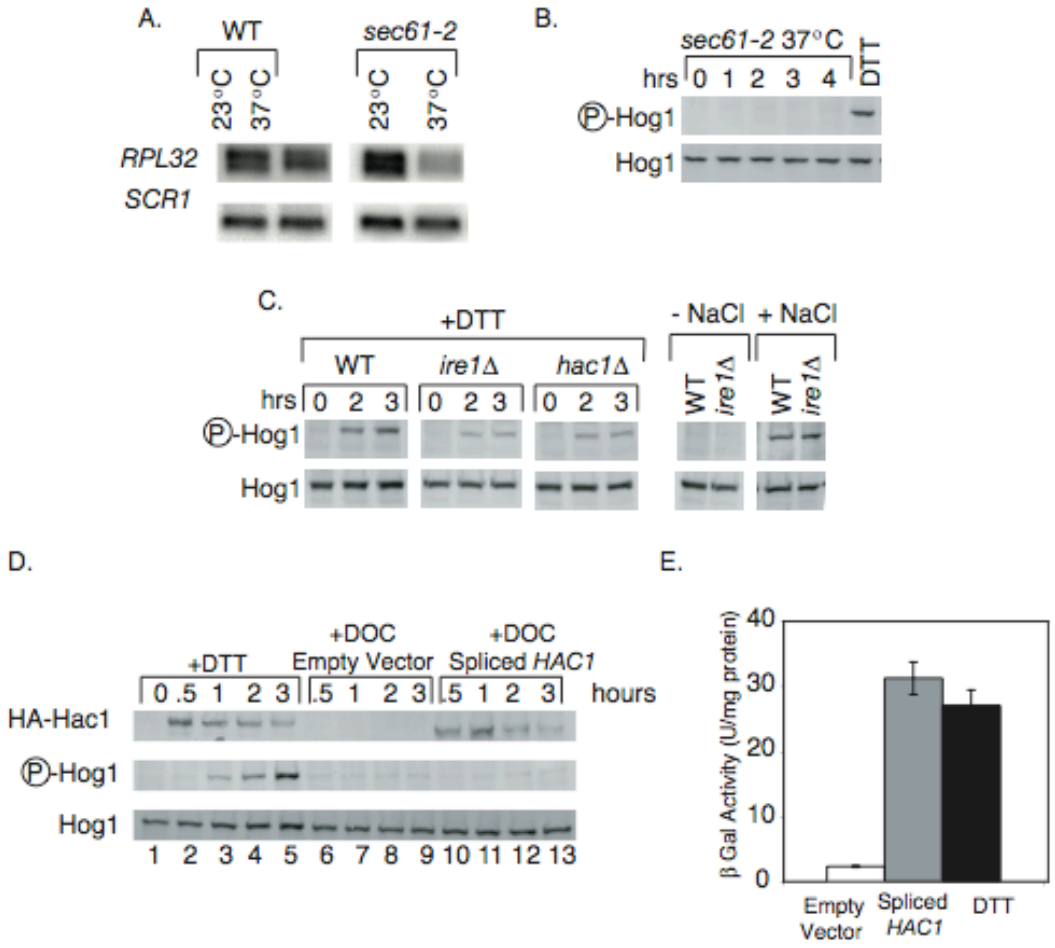

Figure 4.4 The UPR is partly necessary and not sufficient for Hog1 phosphorylation: (A-B) Following shift from 23°C to 37°C, *sec61-2* cells were subjected to *RPL32* and *SCR1* (loading control) northern analysis at the one hour timepoint (A) and phospho Hog1 immunoblot analysis at the indicated timepoints (B). (C) Phospho-Hog1 immunoblots of cells treated with 2 mM DTT or 0.4 M NaCl for 5 minutes. (D) HA-Hac1 and phospho Hog 1 immunoblots of cells expressing HA-tagged wild type *HAC1* (lanes 1-5), HA-tagged spliced *HAC1* under the control of the GRE promoter (lanes 10-13), or the GRE promoter alone (lanes 6-9), treated with 4 mM DTT (lanes 1-5) or 10 μM DOC (lanes 6-13). (E) β-Gal activity of cells from (D), which additionally expressed a UPRE-lacZ reporter, following one hour of 10 μM DOC or 2 mM DTT treatment.

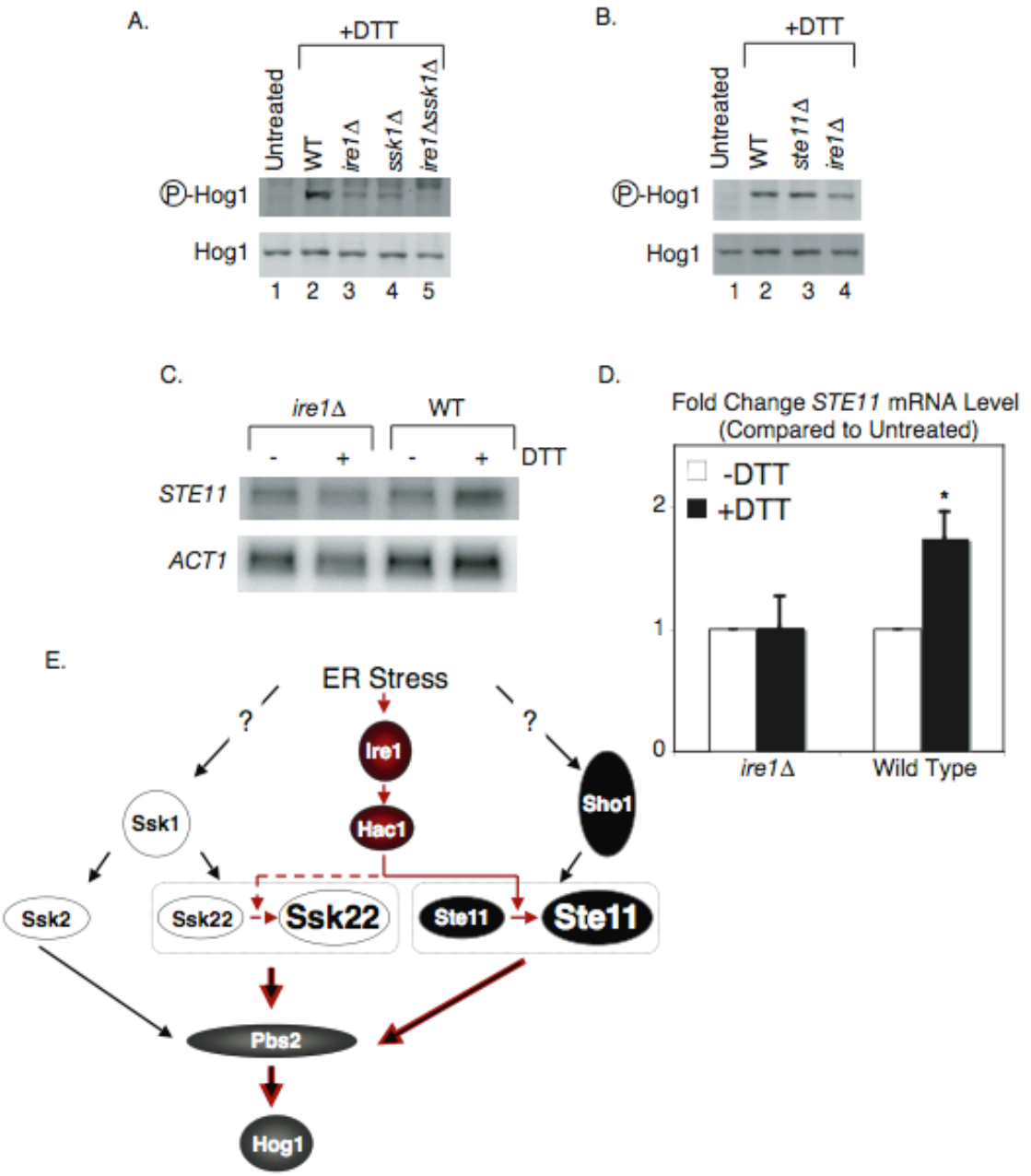

Figure 4.5 Mode of UPR involvement in Hog1 phosphorylation: (A, B) Phospho Hog1 immunoblots of cells treated 4 mM DTT for 2 h. (C) *STE11* northern blots of cells treated with 4 mM DTT for two hours. (D) Quantitation of (C), signal is normalized to *ACT1* and error bars represent SD of 3 repeats, *p < 0.01. (E) Model for ER-induced activation of Hog1. Red arrows indicate UPR's involvement, black arrows indicate UPR-independent pathways, black arrows outlined in red indicate UPR-dependent potentiation of second signal. Dotted arrow denotes a step unconfirmed in our data, but suggested by previous microarray studies.

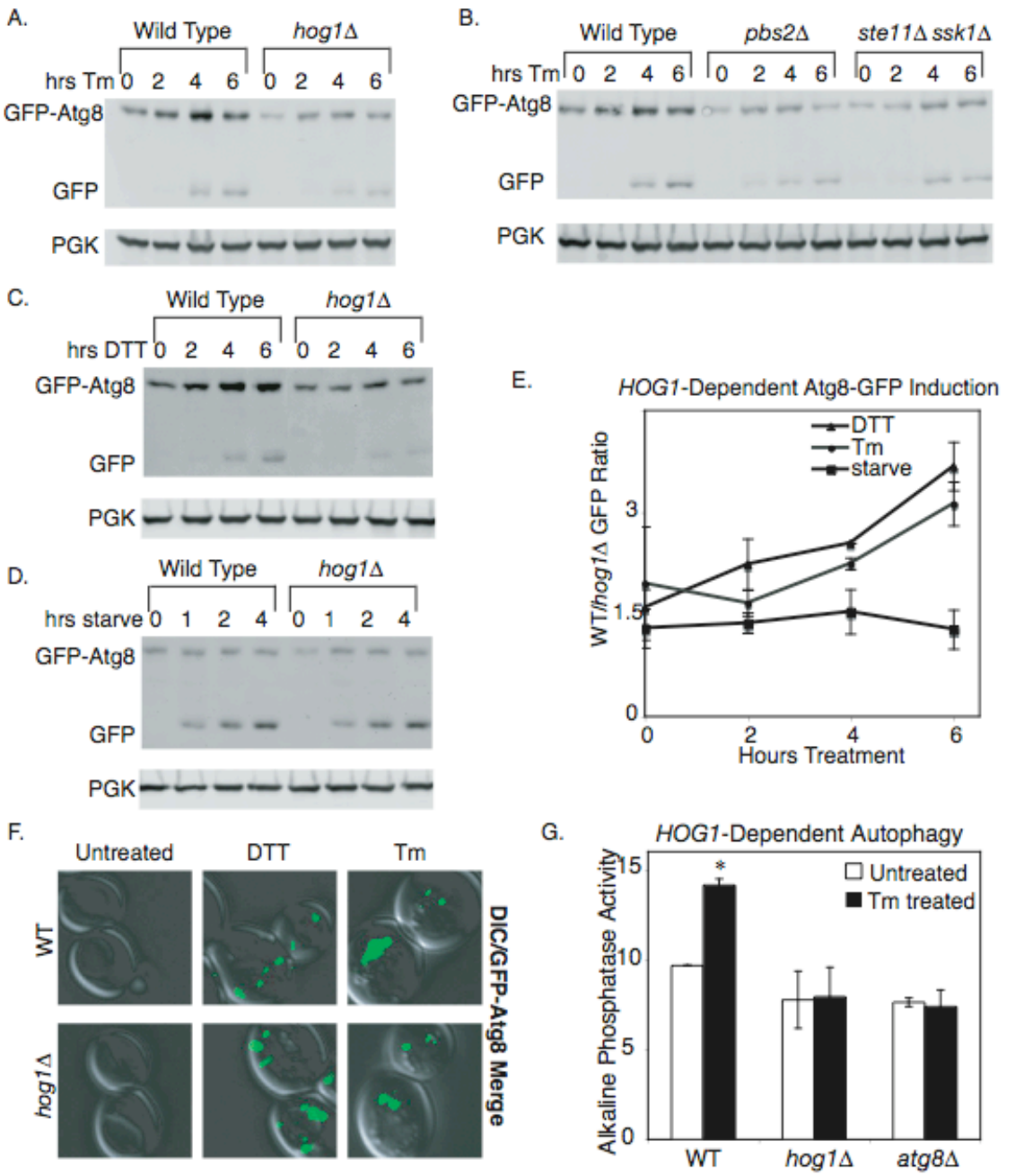

Figure 4.6 Autophagy requires Hog1 phosphorylation during ER stress: (A-D) GFP immunoblots of cells bearing the GFP-*ATG8* reporter, treated with 1 μg/ml Tm, 3 mM DTT, or nitrogen starvation. The top GFP band represents the fusion protein, and the bottom GFP band represents free GFP. (E) Quantitation of A, C, D: total wild type GFP signal divided by the total *hog1Δ* GFP signal, normalized to PGK. Error bars represent SEM of three repeats. (F) Cells expressing the GFP-ATG8 reporter were subjected to 4 h of 4 mM or 1 μg/ml Tm treatment before microscopic visualization to asses PAS formation. (G) Alkaline phosphatase activity of cells bearing the *Pho8Δ60* mutation -/+ 6 h Tm treatment. Error bars represent SD of three repeats, *p < 0.01.

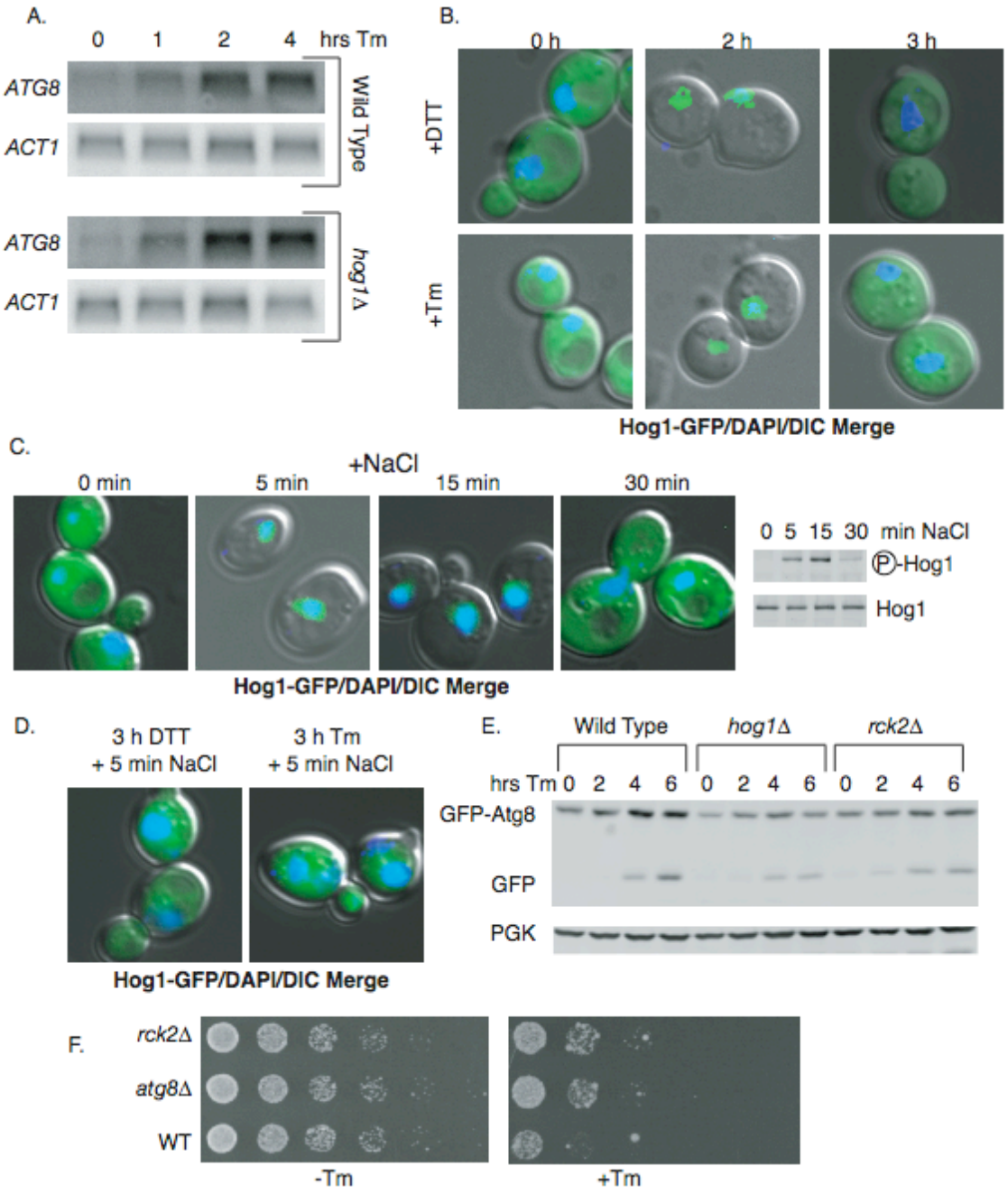

Figure 4.7 Hog1's autophagy function may be mediated by cytoplasmic activation of Rck2: (A) *ATG8* northern blots after1 μg/ml Tm treatment. (B) Cells expressing *HOG1-GFP* from the genomic *HOG1* locus were treated with 2 mM DTT or 1 μg/ml Tm. (C) *HOG1-GFP*-expressing cells were treated with 0.4 M NaCl, and cells were collected for imaging and for phospho Hog1 immunoblot analysis. (D) *HOG1-GFP*-expressing cells were treated with 2 mM DTT or 1 μg/ml Tm for 3 hours, followed by 5 minutes of 0.4 M NaCl. (E) GFP immunoblots of wild type, *hog1Δ*, and *rck2Δ* cells expressing the GFP-*ATG8* reporter, treated with 1 μg/ml Tm. (F) 5 fold serial dilutions of yeast cells spotted onto plates with indicated additives.

Chapter 5: Future Directions

In Chapters 2-4, I show that the cellular response to ER stress extends beyond the previously-characterized UPR pathway. Specifically, the ER stress response includes regulation of septin dynamics, cytokinesis, and cER inheritance, mediated by Slt2 (ERSU pathway), as well as a late-phase Hog1-mediated ER stress response pathway that activates gene transcription and induces autophagy. Strikingly, each novel ER stress response pathway requires the activation of a MAPK. Thus, although each pathway is unique, similar broad questions are raised by my work on the ERSU pathway and the late-phase ER stress response pathway. For example, how ER stress is signaled to the MAPK, how the MAPK achieves specificity of function during ER stress, what transcriptional program is induced by the MAPK, and the mechanism of MAPK regulation of downstream events, are all important outstanding questions for future work on the ERSU and late-phase ER stress response pathways. Therefore, in this chapter I will discuss potential directions for future studies on each pathway, within the framework of these broader questions.

5.1 The signal linking the MAPK to the ER

During ER stress, Slt2 and Hog1 activation are mediated by upstream proteins that reside on the plasma membrane or in the cytosol. In the case of Slt2, I have shown that the plasma membrane protein Wsc1 stimulates MAPK activation during ER stress (Figures 3.8 & 5.1). In the case of Hog1, two pathways converge to activate the MAPK.

They are mediated by Sho1 at the plasma membrane, and Ssk1 in the cytosol, although Ssk1 might be activated further upstream by components on the plasma membrane (Figures 4.3 & 5.1). One very interesting line of future research will be to define the mechanism that allows these cytosolic and plasma membrane proteins to sense ER stress (Figure 5.1). Ultimately, both pathways must be linked to one or multiple sensors that reside within the ER lumen and detect the state of the ER.

Slt2 activation is completely independent of *IRE1*, the only known direct sensor of ER stress in yeast, so the link between Wsc1 and the ER is entirely unknown. Previous studies have identified two cellular locations from which Wsc1 can be used to signal Slt2 activation. Conditions that compromise cell wall integrity activate Wsc1 from sites of polarized growth on the plasma membrane (218). However, like all plasma membrane proteins, when Wsc1 is newly synthesized, it resides in the secretory pathway. Although its localization here is transient, one study has shown that Wsc1 can actually be activated from within the secretory pathway (219). Therefore, it will be interesting to determine whether ER stress activates Wsc1 from within the secretory pathway, and specifically which compartment of the secretory pathway is involved. If Wsc1 is activated from within the ER, this opens up the possibility that Wsc1 is actually the direct sensor of ER stress.

In addition to determining Wsc1's localization during its activation by ER stress, it will be important to determine precisely how Wsc1 senses ER stress. During cell wall stress, Wsc1 is thought to directly sense the integrity of the cell wall (277). Therefore, a careful comparison of the Wsc1 residues necessary for signaling ER stress and cell wall

stress will provide key insights into the mechanism of activation for ER stress, including hints about whether Wsc1 is the direct sensor of ER stress or interacts with other proteins to receive the ER stress signal. If Wsc1 is not the direct ER stress sensor, the identification of domains within Wsc1 that are specifically necessary for ER stress signaling will provide ways of determining what the direct sensor is, and what intermediate components transmit the signal from the ER to Wsc1.

In contrast to Slt2, Hog1 activation is partly mediated by the canonical UPR signaling components, Ire1 and Hac1 (Figure 4.4). My data and previous genome-wide studies suggest that two MAPK cascade components, *STE11* (Figure 4.5C) and *SSK22* (2) are transcriptionally activated by the UPR. Therefore, one possible mechanism for UPR-induced Hog1 activation is through transcription of these genes. To test this model, future studies will need to determine whether *STE11* and *SSK22* transcription are necessary and sufficient for activation of Hog1 by the UPR.

Hog1 activation also involves a signal that is independent of the canonical UPR pathway. The details of the UPR-independent Hog1 activation pathway will be particularly interesting to work out, as this pathway must be initiated by a novel ER stress sensor. To identify this novel ER stress sensor, and other components of the UPR-independent Hog1 activation pathway, one approach would be to take advantage of the transcriptional output of Hog1 activation. By fusing a reporter gene to the *HSP12* promoter, or the promoter of another ER stress-induced Hog1 target gene, it may be possible to design a construct that can be used to rapidly verify the activation of Hog1 during ER stress. This construct could then be used in a genetic screen to identify

mutants that cannot activate Hog1 during ER stress. In addition to known pathway components, such as *PBS2*, this screen could identify the factors upstream of the known activation pathway, potentially including proteins within the ER, which would be good candidates for direct sensors of the stress.

Slt2 and Hog1 both seem to be activated by novel stress sensors within the ER lumen. One compelling possibility is that the same sensor, and possibly some of the same intermediate components, activate both pathways. Although the two pathways are usually activated independently of one another, one previous study suggests a precedent for a single stimulus activating both pathways through a shared mechanism. Specifically, zymolyase treatment, which disrupts glycosylation moieties at the cell wall, activates Slt2 in a manner that depends upon components of the Hog1 MAPK pathway (278), indicating that an overlapping mechanism might activate both MAPKs. Therefore, it will be interesting in the future to determine whether the two pathways rely on shared upstream components for their activation during ER stress.

5.2 Specificity of MAPK function during ER stress

Slt2 and Hog1 can each be activated by conditions besides ER stress. Slt2 is activated when the integrity of the cell wall is compromised (210), and Hog1 is activated by osmotic stress (238). However, the downstream effects of MAPK activation are specific to the particular type of stress (Figures 5.2A & B). When activated by ER stress, Slt2 causes morphological changes in the septin complex (Figure 3.1). However, calcofluor white activates Slt2, and does not affect septin structures (Figures 3.8A & B).

Similarly, when Hog1 is activated by ER stress, it elicits a different transcriptional response than when it is activated by osmotic stress (Figure 4.2C). In addition, Hog1 that is activated by ER stress induces autophagy, while osmotically-activated Hog1 does not (Figure 4.6). Therefore, an interesting focus of future studies will be defining the mechanism by which different downstream responses are achieved by the same phosphorylation event (Figures 5.2A & B).

SLT2-mediated changes in septin morphology correlate with the involvement of Wsc1. Tm, KOH, and CP, which induce *WSC1*-dependent Slt2 phosphorylation, all induce septin alterations, whereas CFW, which induces *WSC1*-independent Slt2 phosphorylation does not affect septins (Figures 3.8A, 3.8B, and 5.2B). This suggests that Wsc1 might be involved in conferring specificity of function to the MAPK pathway. One interesting model to explain this phenomenon is that Wsc1 either serves as a scaffold or recruits a scaffold that binds both Slt2 and its septin-specific downstream target. Since Wsc1 has not previously been shown to provide a scaffolding function, this possibility will be an interesting area of future research.

During Hog1 activation, there is also stress-specific regulation of downstream events. I examined the transcription of four genes that are activated by Hog1 during osmotic stress. Of these four, only *HSP12* was activated during ER stress (Figure 4.2C), even though Hog1 is actually phosphorylated more during ER stress than during osmotic stress (Figure 4.2A). During osmotic stress, Hog1 is known to regulate six different transcription factors (242, 244, 246), but *HSP12* is specifically controlled by Hot1, Msn2, and Msn4 (246). Therefore, it is possible that Hog1 confers transcriptional specificity by

only activating Hot1, Msn2, or Msn4 during ER stress, and allowing the other Hog1-dependent transcription factors to remain dormant.

Atg8 is activated by Hog1 during ER stress, but not during osmotic stress. During osmotic stress, when Atg8 levels do not increase, high levels of Hog1 phosphorylation correlate closely with nuclear localization (Figures 4.7B & 5.2C). By contrast, during ER stress, high levels of Hog1 phosphorylation are associated with nuclear and cytoplasmically localized Hog1 (Figures 4.7B & 5.2C). Furthermore, ER stress-induced activation of Atg8 seems to depend upon Hog1's cytoplasmic target, *RCK2* (Figure 4.7E). Therefore, it would be interesting to test a model in which the presence of phosphorylated Hog1 in the cytoplasm is sufficient to increase Atg8 levels (Figure 5.2C). In this case, specificity might be conferred by differential regulation of localization, and an examination of Hog1's import and export factors would be essential to understanding the MAPK specificity.

During ER stress, specificity of the *HOG1*-dependent cellular response may also be achieved by cross-talk between the Hog1 pathway and the UPR (Figure 5.2A). For example, the UPR may repress the activation of certain Hog1-responsive transcription factors, thus causing only a subset to become activated during ER stress. The UPR might also modulate the localization pattern of Hog1, causing it to be exported from the nucleus in a phosphorylated state, thus contributing to the ER stress-specific autophagy role of Hog1. Therefore, it will be interesting in the future to examine the activation of Hog1 transcription factors, the localization of Hog1, and the *HOG1*-dependent downstream response in the absence of the UPR signaling components during ER stress.

5.3 The MAPK-dependent transcriptional response during ER stress

Although transcriptional regulation is a key feature of most MAPK activation, my studies have only begun to address the role of MAPK-mediated transcription in the ER stress response. Thus far, I have shown that during the late-phase ER stress response, *HSP12* is activated by Hog1 (Figure 4.2C). Future studies will need to determine the mechanism for *HSP12* activation, as well as the identity of other genes that are targeted by Hog1 during ER stress. ER stress-specific Hog1 targets may comprise a subset of the targets known to be activated by Hog1 during osmotic stress, or they may include novel targets, previously unknown to be regulated by Hog1. Identification of Hog1's target transcripts will lay the groundwork for further studies to investigate the function of these genes and how they contribute to long-term ER stress resistance.

Slt2 is also known to activate transcription, at least in response to cell wall damage (279). Although I have not specifically investigated the possibility of *SLT2*-mediated transcription during ER stress, there are hints that it might occur. During ER stress, the transcription of *SLT2* itself is stimulated by the transcription factor, Rlm1 (Figure 3.5B). Previously, it has been shown that Rlm1 is activated by Slt2 (280). Therefore, during ER stress, *SLT2* transcription is very likely activated by a positive feedback mechanism in which the initial activation of Slt2 stimulates Rlm1 activation, which in turn further activates *SLT2* by increasing its transcription (Figure 5.3). This model implies that during ER stress, Rlm1 is activated by Slt2, and opens up the possibility that the Slt2 pathway regulates multiple transcriptional targets during ER stress.

Previously, only two transcription factors, Hac1 and Gcn4, have been shown to mediate the yeast transcriptional response to ER stress (11, 22). It now appears that at least two other factors are activated during ER stress: Rlm1 and the factor that controls *HSP12* expression (probably either Msn2, Msn4, or Hot1). It will be interesting in the future to determine how these transcription factors interact. They might have distinct transcriptional targets and therefore regulate unique features of the transcriptional response, or they may regulate some of the same genes. If they regulate the same genes, they might occupy the same promoters at different times, or they might actually enhance one another's function by occupying the same promoters at the same time.

5.4 Mechanisms and functions of MAPK-dependent downstream events

I have shown that during ER stress, Slt2 MAPK regulate changes in septin morphology, a cytokinesis delay, and a delay in cER inheritance; and Hog1 MAPK enhances expression of Atg8. Since each of these events was previously unknown to be regulated by a MAPK, their precise regulatory mechanisms and their functions during ER stress will be an interesting area of future research (Figure 5.4).

Septins and cytokinesis

During ER stress, septin alterations and cytokinesis delay are both dependent on *SLT2* (Figures 3.5). Previously, it has been shown that increasing the stability of the septin ring is sufficient to cause a cytokinesis delay (196). Therefore, I hypothesize that during ER stress, septin stabilization is upstream of the cytokinesis delay (Figure 5.4). Future work may focus on testing this hypothesis, as well as determining precisely how

Slt2 regulates septins. First, it will be useful to more specifically define the morphological changes in septin structures that are induced by ER stress. For example, time lapse experiments might help determine at what point in the cell cycle septin structures begin to change, and whether aberrant septin structures are the result of abnormal assembly or disassembly of the septin ring.

In addition, because ER stress rescues mutants with a destabilized septin ring (Figures 3.1C & 3.1D), I hypothesize that ER stress causes a stabilization of the septin complex, and that this accounts for the *SLT2*-mediated morphological changes to the septins. Future studies could examine this possibility by comparing the stability of the septin ring in the presence and absence of ER stress. This could be done using fluorescence recovery after photobleaching (FRAP) experiments to directly measure the rate at which fluorescently labeled septin subunits within the ring exchange with unlabeled subunits.

After further characterization of the ER stress-induced septin alterations, it will be important to examine the signaling events that cause these alterations. During the normal cell cycle, changes in the dynamic properties of the septin ring are regulated by post-translational modifications of the septin subunits (203, 281-285). Therefore, it will be important to determine whether ER stress induces modifications of any of the five septin subunits in an *SLT2*-dependent manner. After identifying these modifications, further studies can be conducted to identify the proteins that directly catalyze these modifications, and determine how these proteins are regulated by Slt2 during ER stress.

cER inheritance

Slt2 activation signals a delay in cER inheritance during ER stress (Figure 3.5E). Although other studies have shown that Slt2 activation can delay cER inheritance (285), the mechanism for this remains entirely unknown. One possibility is that Slt2 delays cER inheritance through its regulation of the septin ring (Figure 5.4). Although septins have not previously been shown to affect cER inheritance, genetic interactions have been reported between septin subunits and cER inheritance components (226). Furthermore, throughout most of the cell cycle, septins are positioned at the bud neck where they have the potential to regulate passage of the cER into the daughter cell. In addition, septins are known to influence protein diffusion within the ER membrane (286), suggesting that they have some way of communicating with the ER. Therefore, it will be interesting to determine whether the ER stress-induced delay in cER inheritance is the direct result of Slt2-mediated changes in septin dynamics.

It is also possible that Slt2 regulates cER inheritance independent of its effect on the septin ring (Figure 5.4). Instead, Slt2 might signal directly to the proteins that deliver cER to the bud, anchor the cER to the bud tip, or distribute cER within the bud. In this case, it will be interesting to determine which components of the cER inheritance machinery are regulated by Slt2, and how Slt2 confers this regulation. Initial clues may come from a detailed analysis of the specific step(s) of cER inheritance that are delayed during ER stress, and a targeted examination of the proteins that are known to regulate those particular steps.

Broader questions about the Slt2-induced cER inheritance delay will also be interesting to investigate in the future. Delaying cER inheritance seems to preserve mother cell survival, while allowing the daughter cell to die (Figures 3.6 & 3.9). It is not yet clear why that is the case. One interesting possibility is that the perinuclear ER, whose inheritance is not delayed during ER stress does not provide sufficient ER functionality to the daughter cell. This would imply that either perinuclear ER function falls below the threshold needed to sustain life, or that there are functional distinctions between the two subdomains, and certain vital functions can only be achieved by the cER.

Autophagy

In Chapter 4, I have shown that Hog1 promotes an increase in Atg8 levels during ER stress, and that this increase is necessary for the induction of autophagy. Based on my data and data from the literature, I have proposed a model for *HOG1*-dependent regulation of Atg8. According to this model, during the later stages of ER stress, Hog1 is exported from the nucleus into the cytoplasm, where it phosphorylates the kinase, Rck2. Rck2 then phosphorylates EF-2, thus signaling an inhibition of translation. If the *ATG8* transcript contains elements that cause its translation to be preferentially stimulated under conditions of broad translational repression, this could account for the *HOG1*-dependent increase in Atg8 protein during ER stress (Figure 5.4). Although this translation-dependent mechanism is an attractive model to explain my findings, it includes many features that have not yet been tested, and will need to be the subject of future studies.

First, it will be important to confirm that cytoplasmically-localized Hog1 is responsible for regulating Atg8. I have found a correlation between cytoplasmic localization and Atg8 regulation, and I have found that the regulation is post-transcriptional (Figures 4.7A & 4.7B). However, to prove that Hog1 regulates Atg8 from the cytoplasm, it will be necessary to show that preventing export of Hog1 to the cytoplasm inhibits its function in activating Atg8, whereas preventing it from entering the nucleus does not inhibit its function. These predictions should be easy to test, as Hog1's nuclear import factor is known to be the importin β homolog, Nmd5, and Hog1's nuclear export factor is known to be Crm1 (287).

Additionally, it will be necessary to test the idea that *RCK2*-dependent translational inhibition activates Atg8 during ER stress. I have shown that *rck2Δ* cells are defective in their ability to induce Atg8 (Figure 4.7E), and it is known that Rck2 is a direct target of Hog1 that functions to inhibit translation by phosphorylating EF-2 (251). Future studies will need to confirm that during ER stress specifically, Hog1 phosphorylates Rck2, Rck2 phosphorylates EF-2, and as a result, translation is blocked. Furthermore, although I have shown that *ATG8* transcript levels are not regulated by Hog1 (Figure 4.7A), more studies will need to be done to determine whether Hog1 actually regulates *ATG8* translation, or whether it regulates transcript localization or protein stability. Finally, if it turns out that *ATG8* translation is stimulated by Hog1, and that this correlates with a cell-wide translational repression, future studies will need to identify the elements within the *ATG8* transcript that allow it preferential translation under conditions of broad translational repression.

If it true that translation is blocked during the later stages of ER stress in yeast, this would have many interesting implications aside from a potential role in stimulating Atg8 production. In mammalian cells, the UPR pathway induces a very rapid translational repression during ER stress (30), which prevents the influx of nascent proteins into the ER until homeostasis can be re-established. In yeast, translational inhibition does not occur immediately (86), as it does in mammalian cells. If it occurs at all, it is reserved for the late-phase ER stress response. In light of this difference, it will be interesting to investigate the unique effects of translational repression in both yeast and mammalian cells, and ask what different purposes this repression might serve in each particular system.

In addition to these mechanistic questions, questions about the function of autophagy will be interesting to explore in the future. As discussed in Chapter 4, ER stress in mammalian cells also induces autophagy, and this appears to provide a secondary mechanism for degrading misfolded proteins within the ER (104-106). In yeast, autophagy may perform a similar function. To examine this possibility, future studies might measure the rate of misfolded substrate degradation in the presence or absence of a functional autophagy pathway. In addition, the fact that autophagy-deficient cells are actually resistant to ER stress (Figure 4.7F) will need to be explored further. This implies that under some circumstances, the induction of autophagy during ER stress actually results in more cell death, and raises the question of why cells have evolved to induce autophagy during ER stress. One possible explanation is that under conditions of ER stress that are found in natural environments, autophagy protects cells be removing

the ER and the unfolded proteins within it. However, treatment with Tm or DTT might cause a stronger or more prolonged induction of autophagy, which might harm the cell by degrading too much ER. Another possible explanation is that within clusters of genetically identical cells, there is evolutionary pressure to remove cells that are under significantly high amounts of stress, and that autophagy is a mechanism for cell removal.

5.5 Conclusion

In this dissertation, I have uncovered two novel pathways that complement the UPR pathway in the yeast ER stress response. Slt2 activation links cell cycle progression with the ER's functional capacity and Hog1 activation provides a response to ER stress that is persistent. The discovery of these two pathways broadens our conception of how cells respond to ER stress, and opens up many fundamental questions about how ER stress affects cells. It will be very interesting to see how this story continue to unfold as the details of these pathways are uncovered by future studies.

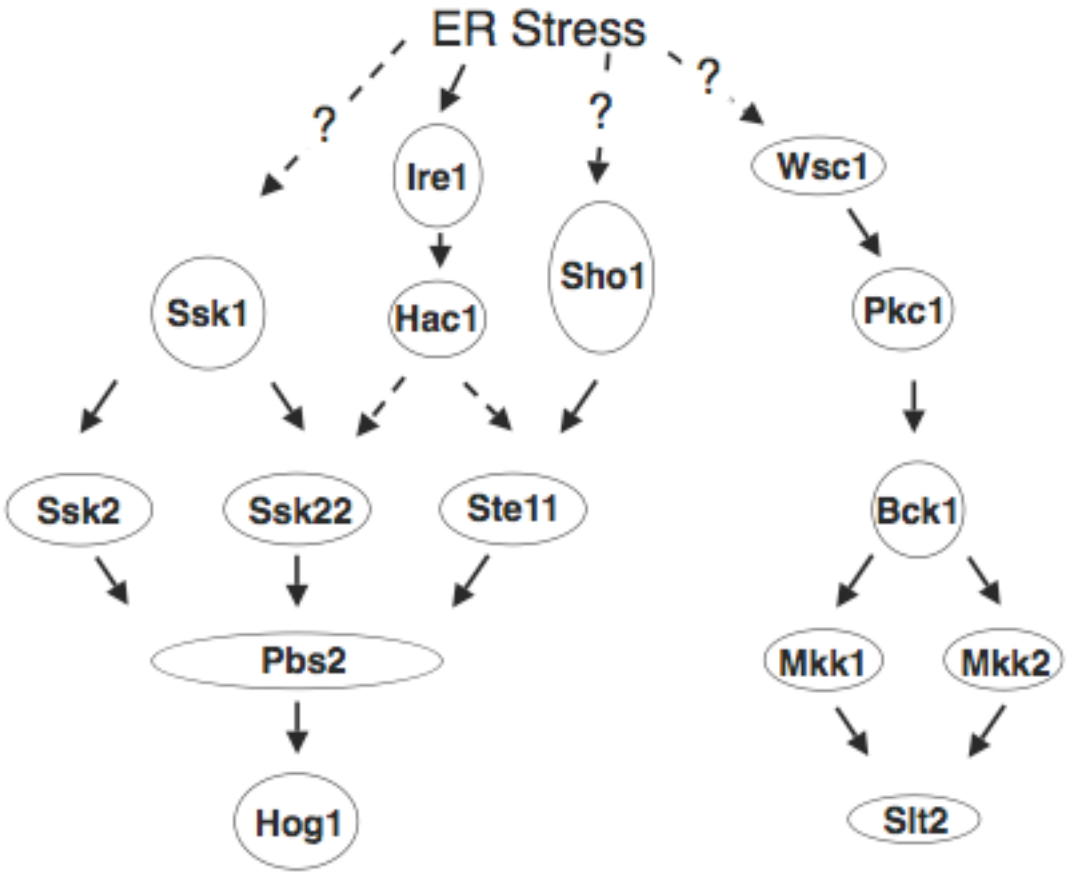

Figure 5.1 Mechanism of MAPK activation during ER stress: Proteins shown to be involved in activation of Hog1 and Slt2 are depicted. Solid arrows depict steps with known mechanisms, based on previous work. Dotted arrows depict unknown mechanisms. Of particular interest are the unknown steps that link these MAPK activation modules to the ER (depicted with a question mark).

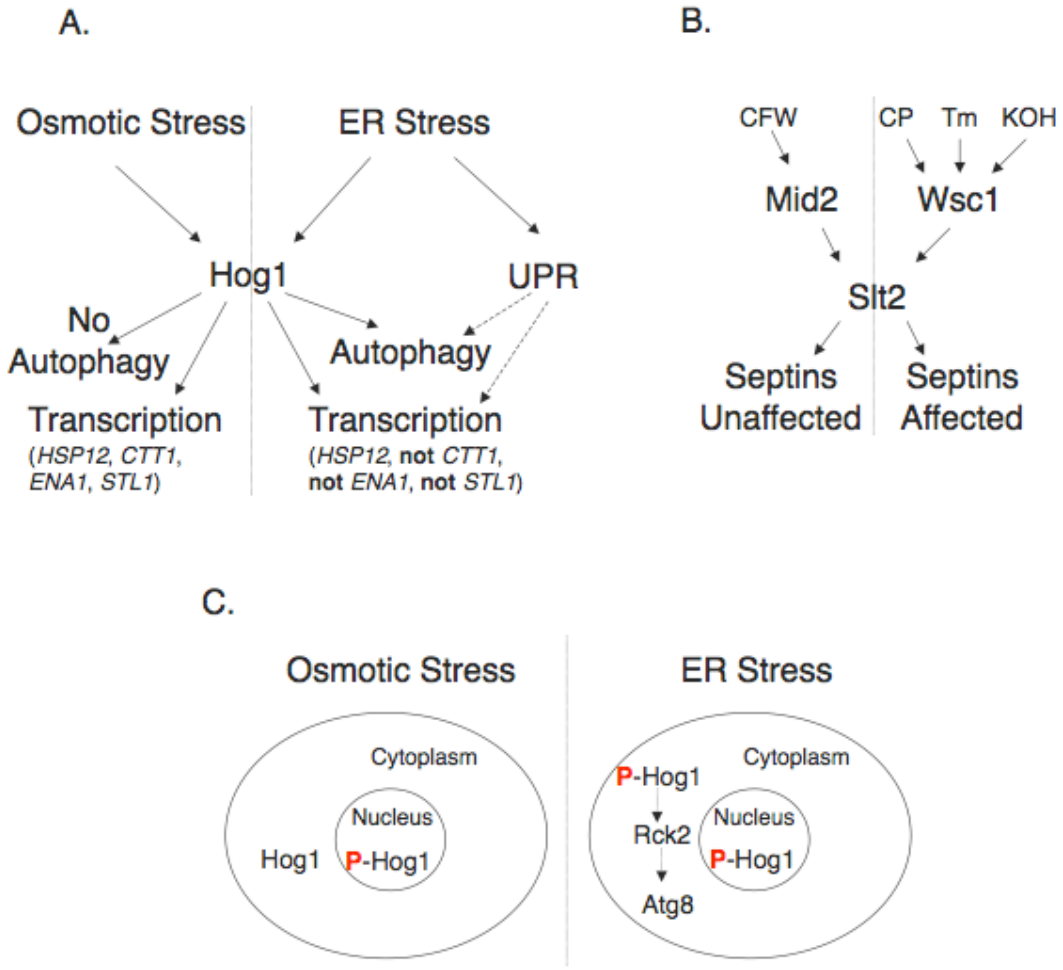

Figure 5.2 Specificity of MAPK function during ER stress: (A) Hog1 activates a different transcriptional response and autophagy response when activated by osmotic stress versus ER stress. Dotted arrows depict the potential for cross-talk with the UPR pathway to achieve this specificity. (B) Slt2 activation does not always lead to septin effects. A correlation between the involvement of Wsc1 and effects on septins has been observed, suggesting that Wsc1 might provide this specificity. (C) Hog1 localization is regulated differently during ER stress than during osmotic stress. Because cytoplasmic localization of Hog1 correlates with its phosphorylation only during ER stress, this localization might be the key to providing ER stress-specific functions, such as Atg8 regulation.

Figure 5.3 *RLM1*-dependent transcription of *SLT2*: During ER stress, *SLT2* transcription is mediated by Rlm1, a known target of Slt2, suggesting a positive feedback mechanism. This hints that Slt2 regulates gene transcription during ER stress, and opens up the possibility that other transcriptional targets of Slt2 are activated.

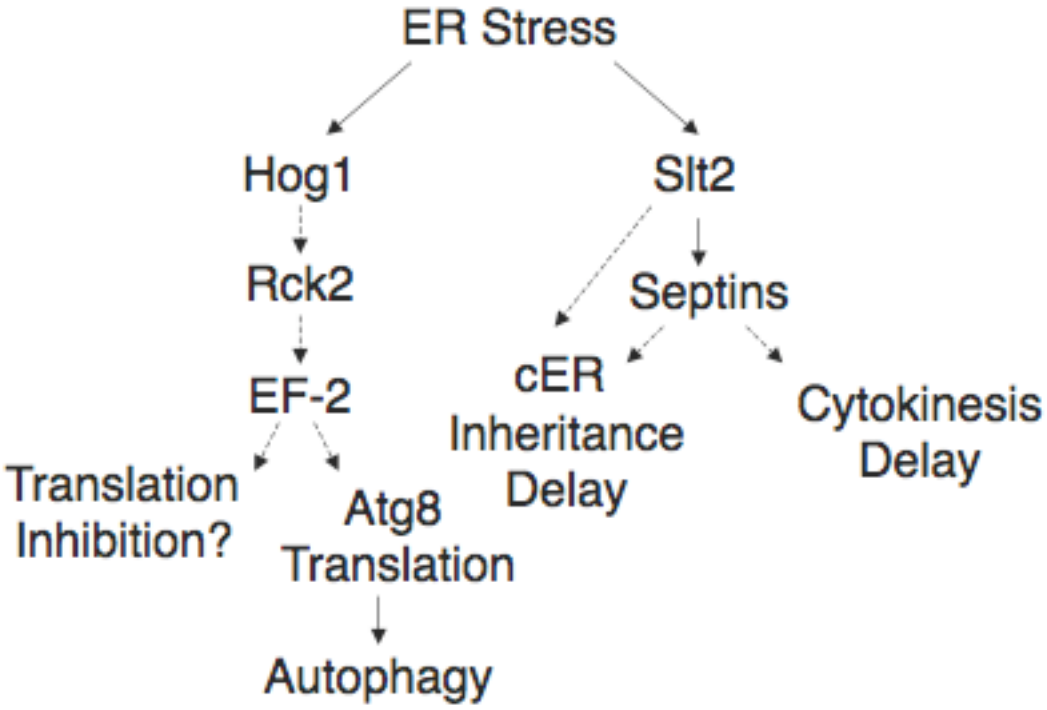

Figure 5.4 Downstream effects of MAPK activation during ER stress: During ER stress, Hog1 and Slt2 are both activated. Hog1 regulates Atg8 levels, which activates autophagy. Dotted arrows depict proposed translation-mediated mechanism for this regulation. Slt2 regulates septins, cER inheritance, and a cytokinesis delay. Dotted arrows depict my hypothesis that the cytokinesis delay is the direct result of septin stabilization, as well as my proposal that the cER inheritance delay might be mediated by septins, or might be directly signaled by Slt2.

Appendix 1: Materials and Methods

Strains, media, growth conditions, and synchronization

All yeast strains were generated using standard genetic methods and are listed in Table A1.1. MNY1008 and MNY1009 were constructed by integrating StuI-linearized pAFS125 (160) at the *URA3* locus. MNY1037, MNY1040, MNY1043, and MNY1045 were generated by integrating StuI-linearized pRH475 (288) at the *URA3* locus. MNY1068 was constructed by integrating HpaI-linearized pRH1827 (a gift from Randy Hampton) at the *ADE2* locus. All strains carrying the UPRE-GFP reporter were constructed by integrating StuI-linearized pJCI86-GFP (77) at the *URA3* locus. Each integrated strain was confirmed by flow cytometry to be a single integrant. All other plasmids used in this study were independent replicons, and are listed in Table A1.2. Deletion and epitope tagged strains were constructed using a one-step recombination-mediated technique (289).

Cells were grown in YPD medium (1% yeast extract, 2% bactopeptone, 2% glucose) at 30°C unless otherwise noted. During DTT treatments, YPD was pH 5.4. Strains carrying plasmids pJCI86, p2188, p2190, p2193, pG-N795, pCP274, pRS425GRE, pJC316, or pRS316 GFP-AUT7 were grown in synthetic complete medium. For synchronization, α factor (stored as 1 mg/ml stock in PBS at –20°C) was added to early log phase cultures to a final concentration of 50 ng/ml for 2.5 h (30°C growth conditions) or 3 h (25°C growth conditions). To release cells from α factor arrest, cells were collected by centrifugation, washed twice with equal volume medium,

resuspended in fresh medium to an OD of 0.25, and allowed to recover for the indicated amount of time before induction of ER stress. For Slt2 immunoblot experiments, cells were grown to an OD of 1, then diluted to an OD of 0.25 before treatment. To induce nitrogen starvation, cells were collected by centrifugation, washed twice and resuspended in starvation medium (1x YNB without amino acids and ammonium sulfate (Difco), 2% dextrose, 0.5 mg/ml inositol). To induce osmotic stress, NaCl was added at a final concentration of 0.4 M. To induce ER stress, Tm (Calbiochem) was added at a final concentration of 1 μg/ml, or DTT (Fisher) was added at a final concentration of 2 mM, 3 mM, or 4 mM as indicated. Tm was stored as a 10 mg/ml stock in DMSO, and DTT was stored as 1 M stock in H_2O. To induce expression of spliced *HAC1* from the *GRE* promoter, DOC was added to the medium at a final concentration of 10 μM (Sigma, 25 mM stock in ethanol). For actin depolymerization, LatB (CalBiochem, 10mM stock in DMSO) was added a final concentration of 400 μM. Activation of Slt2 was achieved with 35 mM KOH (5 M stock), 10 μg/ml CFW (Sigma, 50 mg/ml stock), or 10 ng/ml Caspofungin acetate (a gift from Merck, 20 mg/ml stock)

Immunoblotting

For immunoblot analysis, approximately 3 x 10^7 cells were harvested by centrifugation at 4°C, washed with 1 ml H_2O, frozen with liquid N_2 and stored at –80°C. Pellets were resuspended in 100 μl lysis buffer (50 mM Tris-HCl pH 7.5, 150 mM NaCl, 5 mM EDTA, 1% NP-40, 1 mM sodium pyrophosphate, 1 mM PMSF, 1 mM sodium orthovanadate, 2 μg/ml pepstatin A, 2 μg/ml leupeptin, 20 mM NaF, 5 μg/ml aprotinin,

1.75 mM ß glycerophosphate). 100 µl of acid washed glass beads were added and cells were vortexed at 4°C for 5 min. Lysates were centrifuged at 13K for 8 min at 4°C and the supernatant was collected. Protein concentration was determined using BCA protein assay kit (ThermoScientific). 20 µg of protein (phospho Slt2, phospho/total Hog1, GFP), 30 µg of protein (Clb2), or 40 µg of protein (total Slt2) were denatured at 95°C in 2X loading buffer (125 mM Tris-HCl pH 6.8, 2% SDS, 50% glycerol, 12% BME, .02% bromophenol blue) and then separated on an 8% (Slt2) or 10% (Clb2, Hog1, GFP) SDS-polyacrylamide gel, and transferred to nitrocellulose. Primary antibodies and antisera were Clb2 (Santa Cruz Biotechnology, Inc.) at a 1:1000 dilution for 36 hours, phospho p44/p42 MAP Kinase (NEB) at a 1:1000 dilution overnight, total Slt2 (Santa Cruz Biotechnology, Inc) at a 1:100 dilution overnight, PGK (Molecular Probes) at a 1:10,000 dilution for one hour, phospho-p38 (Cell Signaling) at a 1:1000 dilution overnight, total Hog1 (Santa Cruz Biotech) at a 1:2000 dilution for one hour, GFP (ClonTech) at a 1:10000 dilution for one hour, or HA (Covance Research Prod) at a 1:2500 dilution for one hour. Secondary antisera were HRP-conjugated donkey anti-rabbit (GE Healthcare) at a 1:10000 dilution for phospho p44/p42 and phospho p38, rabbit anti-goat (Zymax) at a 1:5000 dilution for total Slt2, and goat anti-mouse (Biorad) at a 1:10000 dilution for PGK, HA, and GFP. Membranes were developed with ECL Plus Western blotting detection reagent (GE Healthcare), imaged using a typhoon phosphorimager (GE Healthcare), and analyzed using ImageQuant software (GE Healthcare).

Northern blotting

RNA isolation and northern blotting were carried out as previously described (11). Briefly, RNA was isolated using a modified hot phenol method, and 5 μg (*RPL32* northerns), 10 μg (*HAC1* and *SLT2* northerns) or 25 μg (*HSP12*, *ENA1*, *CTT1*, *STL1*, *ATG8*, and *STE11* northerns) of RNA were loaded on a 1.5% agarose gel with 6.7% formaldehyde, and transferred to zeta probe membrane (BioRad) in 10x SSC by capillary action overnight. Following UV-crosslinking, membranes were probed overnight with a DNA probe generated by random primed DNA labeling. Blots were scanned on a typhoon phosphorimager (GE Healthcare) and analyzed using ImageQuant software (GE Healthcare).

DNA staining and flow cytometry

Approximately 10^7 cells were collected by centrifugation at 4°C, washed with 1 ml ice cold H_2O and resuspended in 400 μl cold H_2O. 1 ml of ice cold EtOH was added slowly and cells were fixed at 4°C overnight or longer. Following fixation, cells were collected by centrifugation, washed with 1 ml PBS, and treated with 1 mg/ml RNase A in 100 μl PBS at 37°C for 2-12 hours. Cells were then treated with 5 mg/ml pepsin in 200 μl H_2O pH 2 at 37°C for 20 min, followed by washing and resuspension in 1 ml PBS. Cells were sonicated for 15 sec at 15%. 100 μl of cells (10^6 cells) were stained with 1 μM Sytox Green (Molecular Probes) in PBS. Data was collected using a FACSCalibur Flow Cytometer and analyzed using FlowJo Software.

Strains carrying the 4xUPRE-GFP reporter construct were analyzed for UPR induction by measuring GFP fluorescence in live log phase cells with a FACSCalibur Flow Cytometer. The mean fluorescence for each strain was divided by the mean fluorescence of an isogenic wild type strain to calculate fold induction.

Microscopy

Cells were either imaged live or fixed in 4% paraformaldehyde overnight. Budding index was calculated as the number of cells with an obvious bud divided by the total number of cells counted. For visualization of nuclei, DAPI was added to a concentration of 0.04 μg/ml. Nuclear division was scored as positive when two separate DAPI bodies were present in as single cell. To visualize sister chromatid segregation, MNY1005 cells expressed a LacI12-GFP fusion protein and contained a lac operon at the *trp1* locus. This caused both copies of chromosome IV to be GFP-marked (156). To visualize ER, plasmids expressing *HMG1-GFP* or *HDEL-DsRed* were integrated at the *URA3* and *ADE2* loci respectively. To visualize Hog1, a C-terminal GFP tag was integrated at the *HOG1* genomic locus. For visualization of actin, cells were fixed in 4% paraformaldehyde/PBS, washed with PBS, and then incubated with 6.6 μM AlexaFluor546 Phalloidin (Molecular Probes). To quantitate ER inheritance, 300 budded cells were counted, divided into 3 classes, and scored for presence or absence of cortical ER in the bud. Viability staining was performed using FUN1 dye (Molecular Probes) at a final concentration of 10 μM for 1 ml of 3.10^6 cells/ml for 30 minutes at 30°C in the dark. All cells were visualized using a Zeiss Axiovert 200M microscope 100X 1.3 NA

objective. Images were captured using an Axiocam monochrome digital camera (Carl Zeiss) and analyzed using Axiovision software (Carl Zeiss).

Lyticase treatment

Cells were fixed in YPD/4% formaldehyde for 10 min followed by 1 h in 400 mM $KHPO_4$ pH 6.5, 500 μM $MgCl_2$, 4% formaldedyhe. Cells were then washed in 400 mM $KHPO_4$ pH6.5, 500 μM $MgCl_2$, and resuspended in 400 mM $KHPO_4$ pH6.5, 500 μM $MgCl_2$, 1 M sorbitol. Fixed cells were sonicated (15%, 15 sec) and treated with 80 U/ml lyticase at 37°C for 1 h.

Enzymatic assays

To measure alkaline phosphatase (ALP) activity, strains bearing the *pho8Δ60* mutation and deleted for *PHO13*, the other known alkaline phosphatase in yeast, were obtained from Y. Ohsumi. Alkaline phosphatase activity was determined by providing para-nitrophenyl phosphate (Sigma) as a substrate to extracts, and measuring its conversion to para-nitrophenol by reading the absorbance at 400 nm, as described previously (272, 290).

To measure β-Galactosidase (β-Gal) activity, extracts from strains bearing the *UPRE-lacZ* reporter construct were provided *o*-nitrophenyl-galactoside (ONPG, Sigma) as a substrate. Conversion of ONPG to *o*-nitrophenol was measured by reading the absorbance at 420 nm, as described previously (291). For both ALP and β-Gal assays, a BCA protein assay kit (Thermo Scientific) was used to normalize readings to total protein concentrations.

Table A1.1: Yeast strains used in this study

Strain	Relevant Genotype	Source
MNY1000	*MATa*, *leu2-3,112, trp1-1, can1-100, ura3-1, ade2-1, his3-11,15*	(9)
MNY1001	*MATa*, *leu2-3,112, trp1-1, can1-100, ura3-1, ade2-1, his3-11,15, ero1-1::HIS3*	(152)
MNY1002	*MATa*, *leu2-3,112, trp1-1, can1-100, ura3-1, ade2-1*, *his3-11,15::HIS3, bar1Δ::LEU2*	This study
MNY1003	*MATa*, *leu2-3,112, trp1-1, can1-100, ura3-1, ade2-1, his3-11,15, ero1-1::HIS3*, *bar1Δ::LEU2*	This study
MNY1004	*MATa*, *leu2-3,112, trp1-1, can1-100, ura3-1, ade2-1, his3-11,15::UPRE-lacZ:HIS3*	(9)
MNY1005	*MATa*, *leu2-3,112, , trp1-1::lacO:TRP1*, *can1-100, ura3-1, ade2-1, his3-11,15::pCUP1-GFP12-LacI12:HIS3*, *bar1Δ*	(156)
MNY1006	*MATa*, *leu2-3,112, trp1-1, can1-100, ura3-1, ade2-1, his3-11,15::HIS3, bar1Δ::LEU2*, *CDC14-GFP::KanMX*	This study
MNY1007	*MATa*, *leu2-3,112, trp1-1, can1-100, ura3-1, ade2-1, his3-11,15, bar1Δ::LEU2*, *ero1-1::HIS3*, *CDC14-GFP::KanMX*	This study
MNY1008	*MATa*, *leu2-3,112, trp1-1, can1-100, ura3-1::TUB1-GFP:URA3*, *ade2-1, his3-11,15::HIS3, bar1Δ::LEU2*	This study
MNY1009	*MATa*, *leu2-3,112, trp1-1, can1-100, ura3-1::TUB1-GFP:URA3*, *ade2-1, his3-11,15, bar1Δ::LEU2*, *ero1-1::HIS3*	This study
MNY1010	*MATa*, *leu2-3,112, trp1-1, can1-100, ura3-1, ade2-1, , his3-11,15::HIS3, bar1Δ::LEU2*, *hac1Δ::KanMX*	This study
MNY1011	*MATa*, *leu2-3,112, trp1-1, can1-100, ura3-1, ade2-1*, *his3-11,15::HIS3, bar1Δ::LEU2*, *ire1Δ::KanMX*	This study
MNY1012	*MATa*, *leu2-3,112, trp1-1, can1-100, ura3-1, ade2-1*, *his3-11,15::HIS3, bar1Δ::LEU2*, *cts1Δ::KanMX*	This study
RHY2724	*MATα*, *met2*, *lys2-801*, *ura3-52::4xUPRE-GFP:URA3*, *ade2-101*, *his3Δ200*	This study
RHY5088	*MATα*, *met2*, *lys2-801*, *ura3-52::4xUPRE-GFP:URA3*, *ade2-101*, *his3Δ200*, *hrd1Δ::KanMX*	This study
RHY5954	*MATα*, *met2*, *lys2-801*, *ura3-52::4xUPRE-GFP:URA3*, *ade2-101*, *his3Δ200*, *hof1Δ::KanMX*	This study
RHY5955	*MATα*, *met2*, *lys2-801*, *ura3-52::4xUPRE-GFP:URA3*, *ade2-101*, *his3Δ200*, *chs2Δ::KanMX*	This study
RHY5956	*MATα*, *met2*, *lys2-801*, *ura3-52::4xUPRE-GFP:URA3*, *ade2-101*, *his3Δ200*, *cyk3Δ::KanMX*	This study
RHY5957	*MATα*, *met2*, *lys2-801*, *ura3-52::4xUPRE-GFP:URA3*, *ade2-101*, *his3Δ200*, *mlc2Δ::KanMX*	This study

Table A1.1: Yeast trains used in this study, continued

Strain	Relevant Genotype	Source
RHY5958	*MATα, met2, lys2-801, ura3-52::4xUPRE-GFP:URA3, ade2-101, his3Δ200, doa10Δ::NatMX*	This study
RHY5959	*MATα, met2, lys2-801, ura3-52::4xUPRE-GFP:URA3, ade2-101, his3Δ200, bni1Δ::NatMX*	This study
MNY1031	*MATa, leu2-3,112, trp1-1, can1-100, ura3-1, his3-11,15, bar1Δ::LEU2, CDC10-GFP::KanMX*	This study
MNY1032	*MATa, leu2-3,112, trp1-1, can1-100, ura3-1, his3-11,15, bar1Δ::LEU2, SHS1-GFP::KanMX*	This study
MNY1033	*MATa, leu2-3,112, trp1-1, can1-100, ura3-1, his3-11,15, bar1Δ::LEU2, CDC11-GFP::KanMX*	This study
MNY1034	*MATa, leu2-3,112, trp1-1, can1-100, ura3-1, ade2-1, his3-11,15, ero1-1::HIS3, barΔ::LEU2*	This study
MNY1035	*MATa, cdc12-6, his3, leu2, lys2, trp1, ura3, ade2*	(286)
MNY1036	*MATa, cdc12-6, his3, leu2, lys2, trp1, ura3, ade2, CDC10-mCherry::KanMX*	This study
MNY1037	*MATa, leu2-3,112, trp1-1, can1-100, ura3-1::HMG1-GFP:URA3, ade2-1, his3-11,15::UPRE-lacZ:HIS3*	This study
MNY1038	*MATa, leu2-3,112, trp1-1, can1-100, ura3-1, ade2-1, his3-11, bar1Δ::LEU2*	This study
MNY1039	*MATa, leu2-3,112, trp1-1, can1-100, ura3-1, ade2-1, his3-11, bar1Δ::LEU2, ire1Δ::KanMX*	This study
MNY1040	*MATa, leu2-3,112, trp1-1::CDC10-mCherry:TRP1, can1-100, ura3-1::HMG1-GFP:URA3, ade2-1, his3-11,15::UPRE-lacZ:HIS3*	This study
MNY1041	*MATa, leu2-3,112, trp1-1::CDC10-mCherry:TRP1, can1-100, ura3-1::HMG1-GFP:URA3, ade2-1, his3-11,15::UPRE-lacZ:HIS3, ire1 Δ::KanMX*	This study
MNY1042	*MATa, leu2-3,112, trp1-1, can1-100, ura3-1, his3-11,bar1Δ::LEU2, slt2Δ::KanMX*	This study
MNY1043	*MATa, leu2-3,112, trp1-1, can1-100, ura3-1::HMG1-GFP:URA3, ade2-1, his3-11,15::UPRE-lacZ:HIS3, slt2 Δ::KanMX*	This study
MNY1044	*MATa, leu2-3,112, trp1-1, can1-100, ura3-1, his3-11,bar1Δ::LEU2, CDC10-GFP::KanMX, slt2 Δ::NatMX*	This study

Table A1.1: Yeast trains used in this study, continued

Strain	Relevant Genotype	Source
MNY1045	*MATa, leu2-3,112, trp1-1::CDC10-mCherry:TRP1, can1-100, ura3-1::HMG1-GFP:URA3, ade2-1, his3-11,15::UPRE-lacZ:HIS3, slt2Δ::KanMX*	This study
MNY1046	*MATa, leu2-3,112, trp1-1::CDC10-mCherry:TRP1, can1-100, ura3-1::HMG1-GFP:URA3, ade2-1, his3-11,15::UPRE-lacZ:HIS3, wsc1Δ::KanMX*	This study
MNY1047	*MATa, his3Δ1, leu2Δ0, met15Δ0, ura3Δ0::wsc1Δ:URA3, wsc2Δ::KanMX*	This study
MNY1048	*MATa, his3Δ1, leu2Δ0, met15Δ0, ura3Δ0::wsc1Δ:URA3, wsc3Δ::KanMX*	This study
MNY1049	*MATa, his3Δ1, leu2Δ0, met15Δ0, ura3Δ0::wsc1Δ:URA3, wsc4Δ::KanMX*	This study
MNY1050	*MATa, his3Δ1, leu2Δ0, met15Δ0, ura3Δ0, rlm1Δ::KanMX*	Yeast KO collection
MNY1051	*MATa, his3Δ1, leu2Δ0, met15Δ0, ura3Δ0, ire1Δ::KanMX*	Yeast KO collection
MNY1052	*MATa, his3Δ1, leu2Δ0, met15Δ0, ura3Δ0, slt2Δ::KanMX*	Yeast KO collection
MNY1053	*MATa, his3Δ1, leu2Δ0, met15Δ0, ura3Δ0, wsc1Δ::KanMX*	Yeast KO collection
MNY1054	*MATa, his3Δ1, leu2Δ0, met15Δ0, ura3Δ0, wsc2Δ::KanMX*	Yeast KO collection
MNY1055	*MATa, his3Δ1, leu2Δ0, met15Δ0, ura3Δ0, wsc3Δ::KanMX*	Yeast KO collection
MNY1056	*MATa, his3Δ1, leu2Δ0, met15Δ0, ura3Δ0, wsc4Δ::KanMX*	Yeast KO collection
MNY1057	*MATa, his3Δ1, leu2Δ0, met15Δ0, ura3Δ0, mid2Δ::KanMX*	Yeast KO collection
MNY1058	*MATa, his3Δ1, leu2Δ0, met15Δ0, ura3Δ0, mtl1Δ::KanMX*	Yeast KO collection
MNY1059	*MATa /MATα, his3Δ1/his2Δ1, leu2Δ0/leu2Δ0, LYS2/lys2Δ0, met15Δ0/MET15, ura3Δ0/ura3Δ0*	(209)
MNY1060	*MATa /MATα, trp1-1/trp1-1, leu2-3,112/leu2-3,112, ura3-52/ura3-52, his4/his4, bck1Δ::G418/bck1Δ::G418*	(209)
MNY1061	*MATa /MATα, his3Δ1/his2Δ1, leu2Δ0/leu2Δ0,LYS2/lys2Δ0, met15Δ0/MET15,ura3Δ0/ura3Δ, mkk1Δ::G418/mkk1Δ::G418 mkk2Δ::G418/mkk2Δ::G418*	(209)
MNY1062	*MATa, leu2-3,112, ura3-52, trp1-1, his4, can1r*	(292)

Table A1.1: Yeast trains used in this study, continued

Strain	Relevant Genotype	Source
MNY1063	*MATa, leu2-3,112, ura3-52, trp1-1, his4, can1r, pkclΔ::LEU2*	(292)
MNY1064	*MATa*, *ura3-52*	(293)
MNY1065	*MATa, ura3-52, sec1-1*	(293)
MNY1066	*MATα, ura3-52, leu2-3,112, his3Δ200, trp1Δ901, lys2-801, suc2Δ9, WSC1-GFP::HIS3*	(218)
MNY1067	*MATα, ura3-52, leu2-3,112, his3Δ200, trp1Δ901, lys2-801, suc2Δ9, WSC1^{AAA}-GFP::HIS3*	(218)
MNY1068	*MATa*, *leu2-3,112, trp1-1, can1-100, ura3-1, his3-11,15, ade2-1, bar1Δ::LEU2, HDEL-DsRed::ADE2*	This study
MNY1069	*MATa, leu2-3,112, trp1-1::CDC10-mCherry:TRP1, can1-100, ura3-1::HMG1-GFP:URA3, ade2-1, his3-11,15::UPRE-lacZ:HIS3, slt2Δ::KanMX*, p2188	This study
MNY1070	*MATa, leu2-3,112, trp1-1::CDC10-mCherry:TRP1, can1-100, ura3-1::HMG1-GFP:URA3, ade2-1, his3-11,15::UPRE-lacZ:HIS3, slt2Δ::KanMX*, p2190	This study
MNY1071	*MATa, leu2-3,112, trp1-1::CDC10-mCherry:TRP1, can1-100, ura3-1::HMG1-GFP:URA3, ade2-1, his3-11,15::UPRE-lacZ:HIS3, slt2Δ::KanMX*, p2193	This study
MNY1100	*MAT**a***, *leu2-3,112, trp1-1, can1-100, ura3-1, ade2-1, his3-11,15::UPRE-lacZ:HIS3, hog1Δ::KanMX*	This study
MNY1101	*MAT**a***, *leu2-3,112, trp1-1, can1-100, ura3-1, his3-11,15::UPRE-lacZ:HIS3*, *HOG1-GFP::KanMX*	This study
MNY1102	*MAT**a***, *leu2-3,112, trp1-1, can1-100, ura3-1, ade2-1, his3-11,15::UPRE-lacZ:HIS3, pbs2Δ::KanMX*	This study
MNY1103	*MAT**a***, *leu2-3,112, trp1-1, can1-100, ura3-1, ade2-1, his3-11,15::UPRE-lacZ:HIS3, ste11Δ::KanMX*	This study
MNY1104	*MAT**a***, *leu2-3,112, trp1-1, can1-100, ura3-1, ade2-1, his3-11,15::UPRE-lacZ:HIS3, ssk2Δ::KanMX*	This study
MNY1105	*MAT**a***, *leu2-3,112, trp1-1, can1-100, ura3-1, ade2-1, his3-11,15::UPRE-lacZ:HIS3, ssk22Δ::KanMX*	This study
MNY1106	*MAT**a***, *leu2-3,112, trp1-1, can1-100, ura3-1, ade2-1, his3-11,15::UPRE-lacZ:HIS3, ssk1Δ::KanMX*	This study
MNY1107	*MAT**a***, *leu2-3,112, trp1-1, can1-100, ura3-1, ade2-1, his3-11,15::UPRE-lacZ:HIS3, ste11Δ::KanMX*, *ssk1Δ::NatMX*	This study
MNY1108	*MAT**a***, *leu2-3,112, trp1-1, can1-100, ura3-1, ade2-1, his3-11,15::UPRE-lacZ:HIS3, sho1Δ::KanMX*	This study

Table A1.1: Yeast trains used in this study, continued

Strain	Relevant Genotype	Source
MNY1109	*MAT**a**, leu2-3,112, trp1-1, can1-100, ura3-1, ade2-1, his3-11,15::UPRE-lacZ:HIS3, sho1Δ::KanMX , ssk1Δ::NatMX*	This study
MNY1110	*MAT**a**, leu2-3,112, ura3-52, ade2-1, pep4-3, sec61-2*	(294)
MNY1111	*MAT**a**, leu2-3,112, trp1-1, can1-100, ura3-1, ade2-1, his3-11,15::UPRE-lacZ:HIS3, ire1Δ::KanMX*	This study
MNY1112	*MAT**a**, leu2-3,112, trp1-1, can1-100, ura3-1, ade2-1, his3-11,15::UPRE-lacZ:HIS3, hac1Δ::KanMX*	This study
MNY1113	*MAT**a**, leu2-3,112, trp1-1, can1-100, ura3-1, ade2-1, his3-11,15::UPRE-lacZ:HIS3, hac1Δ::KanMX*, pGN795, pRS425GRE	This study
MNY1114	*MAT**a**, leu2-3,112, trp1-1, can1-100, ura3-1, ade2-1, his3-11,15::UPRE-lacZ:HIS3, hac1Δ::KanMX*, pGN795, pCP274	This study
MNY1115	*MAT**a**, leu2-3,112, trp1-1, can1-100, ura3-1, ade2-1, his3-11,15::UPRE-lacZ:HIS3, hac1Δ::KanMX*, pJC316	This study
MNY1116	*MAT**a**, leu2-3,112, trp1-1, can1-100, ura3-1, ade2-1, his3-11,15::UPRE-lacZ:HIS3, ire1Δ::KanMX , ssk1Δ::NatMX*	This study
MNY1117	*MAT**a**, leu2-3,112, trp1-1, can1-100, ura3-1, ade2-1, his3-11,15::UPRE-lacZ:HIS3*, pRS316 GFP-AUT7	This study
MNY1118	*MAT**a**, leu2-3,112, trp1-1, can1-100, ura3-1, ade2-1, his3-11,15::UPRE-lacZ:HIS3, hog1Δ::KanMX* , pRS316 GFP-AUT7	This study
MNY1119	*MAT**a**, leu2-3,112, trp1-1, can1-100, ura3-1, ade2-1, his3-11,15::UPRE-lacZ:HIS3, pbs2Δ::KanMX*, pRS316 GFP-AUT7	This study
MNY1120	*MAT**a**, leu2-3,112, trp1-1, can1-100, ura3-1, ade2-1, his3-11,15::UPRE-lacZ:HIS3, ste11Δ::KanMX*, *ssk1Δ::NatMX*, pRS316 GFP-AUT7	This study
MNY1121	*MAT**a**, leu2-3,112, trp1, ura3-52, pho8::pho8Δ60, pho13::URA3*	(272)
MNY1122	*MAT**a**, leu2-3,112, trp1, ura3-52, pho8::pho8Δ60, pho13::URA3, hog1Δ::KanMX*	This study
MNY1123	*MAT**a**, leu2-3,112, trp1, ura3-52, pho8::pho8Δ60, pho13::URA3, atg8Δ::KanMX*	This study
MNY1124	*MAT**a**, leu2-3,112, trp1-1, can1-100, ura3-1, ade2-1, his3-11,15::UPRE-lacZ:HIS3, rck2Δ::KanMX*, pRS316 GFP-AUT7	This study

Table A1.2: Plasmids used in this study

Plasmid name	Description	Source
pG-N795	Encodes glucocorticoid receptor	(262)
pCP274	HA-tagged Spliced *HAC1* downstream of 3 tandem GREs	(2)
pRS425GRE	3 tandem GREs upstream of multiple cloning site	(2)
pJC316	HA-tagged *HAC1* from native promoter	(11)
pRS316 GFP-AUT7	GFP-tagged *ATG8* (*AUT7*) from native promoter	(267)
p2188	Wild type *SLT2*	(209)
p2190	*slt2(T190A Y192F)*	(209)
p2193	*slt2(K54R)*	(209)

References

1. Brown JD, Ng DTW, Ogg SC, Walter P. (1995) Targeting pathways to the endoplasmic reticulum membrane. *Cold Spring Harbor Symposia on Quantitative Biology* **60:** 23-30.

2. Travers KJ, Patil CK, Wodicka L, Lockhart DJ, Weissman JS, Walter P. (2000) Functional and genomic analyses reveal an essential coordination between the unfolded protein response and ER-associated degradation. *Cell* **101:** 249-258.

3. Ng DT, Spear ED, Walter P. (2000) The unfolded protein response regulates multiple aspects of secretory and membrane protein biogenesis and endoplasmic reticulum quality control. *J Cell Biol* **150:** 77-88.

4. Plemper RK, Wolf DH. (1999) Retrograde protein translocation: ERADication of secretory proteins in health and disease. *Trends in Biochemical Sciences* **24:** 266-270.

5. Gardner RG, Shearer AG, Hampton RY. (2001) In vivo action of the HRD ubiquitin ligase complex: Mechanisms of endoplasmic reticulum quality control and sterol regulation. *Molecular and Cellular Biology* **21:** 4276-4291.

6. Patil C, Walter P. (2001) Intracellular signaling from the endoplasmic reticulum to the nucleus: the unfolded protein response in yeast and mammals. *Curr Opin Cell Biol* **13:** 349-355.

7. Shaffer AL, Shapiro-Shelef M, Iwakoshi NN, et al. (2004) XBP1, downstream of Blimp-1, expands the secretory apparatus and other organelles, and increases protein synthesis in plasma cell differentiation. *Immunity* **21:** 81-93.

8. Larsson O, Carlberg M, Zetterberg A. (1993) Selective killing induced by an inhibitor of N-linked glycosylation. *J Cell Sci* **106 (Pt 1):** 299-307.

9. Cox JS, Shamu CE, Walter P. (1993) Transcriptional induction of genes encoding endoplasmic reticulum resident proteins requires a transmembrane protein kinase. *Cell* **73:** 1197-1206.

10. Shamu CE, Walter P. (1996) Oligomerization and phosphorylation of the Ire1p kinase during intracellular signaling from the endoplasmic reticulum to the nucleus. *Embo J* **15:** 3028-3039.

11. Cox JS, Walter P. (1996) A novel mechanism for regulating activity of a transcription factor that controls the unfolded protein response. *Cell* **87:** 391-404.

12. Sidrauski C, Walter P. (1997) The transmembrane kinase Ire1p is a site-specific endonuclease that initiates mRNA splicing in the unfolded protein response. *Cell* **90:** 1031-1039.

13. Mori K, Kawahara T, Yanagi H, Yura T. (1997) ER stress-induced mRNA splicing permits synthesis of transcription factor Hac1p/Ern4p that activates the unfolded protein response. *Molecular Biology of the Cell* **8:** 2056-2056.

14. Mori K, Kawahara T, Yoshida H, Yanagi H, Yura T. (1996) Signalling from endoplasmic reticulum to nucleus: transcription factor with a basic-leucine zipper motif is required for the unfolded protein-response pathway. *Genes Cells* **1:** 803-817.

15. Sidrauski C, Cox JS, Walter P. (1996) tRNA ligase is required for regulated mRNA splicing in the unfolded protein response. *Cell* **87:** 405-413.

16. Abelson J, Trotta CR, Li H. (1998) tRNA splicing. *J Biol Chem* **273:** 12685-12688.

17. Culver GM, McCraith SM, Consaul SA, Stanford DR, Phizicky EM. (1997) A 2'-phosphotransferase implicated in tRNA splicing is essential in Saccharomyces cerevisiae. *J Biol Chem* **272:** 13203-13210.

18. Harding HP, Lackey JG, Hsu HC, et al. (2008) An intact unfolded protein response in Trpt1 knockout mice reveals phylogenic divergence in pathways for RNA ligation. *Rna* **14:** 225-232.

19. Ruegsegger U, Leber JH, Walter P. (2001) Block of HAC1 mRNA translation by long-range base pairing is released by cytoplasmic splicing upon induction of the unfolded protein response. *Cell* **107:** 103-114.

20. Yamamoto K, Yoshida H, Kokame K, Kaufman RJ, Mori K. (2004) Differential contributions of ATF6 and XBP1 to the activation of endoplasmic reticulum stress-responsive cis-acting elements ERSE, UPRE and ERSE-II. *J Biochem* **136:** 343-350.

21. Mori K, Sant A, Kohno K, Normington K, Gething MJ, Sambrook JF. (1992) A 22 bp cis-acting element is necessary and sufficient for the induction of the yeast KAR2 (BiP) gene by unfolded proteins. *Embo J* **11:** 2583-2593.

22. Patil CK, Li H, Walter P. (2004) Gcn4p and novel upstream activating sequences regulate targets of the unfolded protein response. *PLoS Biol* **2:** E246.

23. Chapman RE, Walter P. (1997) Translational attenuation mediated by an mRNA intron. *Curr Biol* **7:** 850-859.

24. Yoshida H, Matsui T, Yamamoto A, Okada T, Mori K. (2001) XBP1 mRNA is induced by ATF6 and spliced by IRE1 in response to ER stress to produce a highly active transcription factor. *Cell* **107:** 881-891.

25. Ogawa N, Mori K. (2004) Autoregulation of the HAC1 gene is required for sustained activation of the yeast unfolded protein response. *Genes Cells* **9:** 95-104.

26. Urano F, Wang X, Bertolotti A, et al. (2000) Coupling of stress in the ER to activation of JNK protein kinases by transmembrane protein kinase IRE1. *Science* **287:** 664-666.

27. Nishitoh H, Matsuzawa A, Tobiume K, et al. (2002) ASK1 is essential for endoplasmic reticulum stress-induced neuronal cell death triggered by expanded polyglutamine repeats. *Genes Dev*. **16:** 1345-1355.

28. Nishitoh H, Saitoh M, Mochida Y, et al. (1998) ASK1 is essential for JNK/SAPK activation by TRAF2. *Mol Cell* **2:** 389-395.

29. Bogoyevitch MA, Kobe B. (2006) Uses for JNK: the many and varied substrates of the c-Jun N-terminal kinases. *Microbiol Mol Biol Rev* **70:** 1061-1095.

30. Harding HP, Zhang Y, Ron D. (1999) Protein translation and folding are coupled by an endoplasmic-reticulum-resident kinase. *Nature* **397:** 271-274.

31. Shi YG, Vattem KM, Sood R, et al. (1998) Identification and characterization of pancreatic eukaryotic initiation factor 2 alpha-subunit kinase, PEK, involved in translational control. *Molecular and Cellular Biology* **18:** 7499-7509.

32. Hinnebusch AG. (1997) Translational regulation of yeast GCN4. A window on factors that control initiator-trna binding to the ribosome. *J Biol Chem* **272:** 21661-21664.

33. Srivastava SP, Kumar KU, Kaufman RJ. (1998) Phosphorylation of eukaryotic translation initiation factor 2 mediates apoptosis in response to activation of the double-stranded RNA-dependent protein kinase. *J Biol Chem* **273:** 2416-2423.

34. Scheuner D, Song B, McEwen E, et al. (2001) Translational control is required for the unfolded protein response and in vivo glucose homeostasis. *Mol Cell* **7:** 1165-1176.

35. Brewer JW, Diehl JA. (2000) PERK mediates cell-cycle exit during the mammalian unfolded protein response. *Proc Natl Acad Sci U S A* **97:** 12625-12630.

36. Niwa M, Walter P. (2000) Pausing to decide. *Proc Natl Acad Sci U S A* **97:** 12396-12397.

37. Harding HP, Novoa I, Zhang YH, et al. (2000) Regulated translation initiation controls stress-induced gene expression in mammalian cells. *Mol. Cell* **6:** 1099-1108.

38. Harding HP, Zhang YH, Zeng HQ, et al. (2003) An integrated stress response regulates amino acid metabolism and resistance to oxidative stress. *Mol. Cell* **11:** 619-633.

39. Cullinan SB, Zhang D, Hannink M, Arvisais E, Kaufman RJ, Diehl JA. (2003) Nrf2 is a direct PERK substrate and effector of PERK-dependent cell survival. *Mol Cell Biol* **23:** 7198-7209.

40. DuRose JB, Tam AB, Niwa M. (2006) Intrinsic capacities of molecular sensors of the unfolded protein response to sense alternate forms of endoplasmic reticulum stress. *Mol Biol Cell* **17:** 3095-3107.

41. Wang Y, Shen JS, Arenzana N, Tirasophon W, Kaufman RJ, Prywes R. (2000) Activation of ATF6 and an ATF6 DNA binding site by the endoplasmic reticulum stress response. *Journal of Biological Chemistry* **275:** 27013-27020.

42. Haze K, Yoshida H, Yanagi H, Yura T, Mori K. (1999) Mammalian transcription factor ATF6 is synthesized as a transmembrane protein and activated by proteolysis in response to endoplasmic reticulum stress. *Mol Biol Cell* **10:** 3787-3799.

43. Ye J, Rawson RB, Dave UP, Prywes R, Goldstein JL, Brown MS. (2000) Site-1 protease (S1P) and site-2 protease (S2P), the two proteases that cleave membrane-bound SREBPs, also cleave ATF6 upon ER stress. *Mol Biol Cell* **11:** 1511.

44. Kokame K, Kato H, Miyata T. (2001) Identification of ERSE-II, a new cis-actin element responsible for the ATF6-dependent mammalian unfolded protein response. *J. Biol. Chem.* **276:** 9199-9205.

45. Yoshida H, Haze K, Yanagi H, Yura T, Mori K. (1998) Identification of the cis-acting endoplasmic reticulum stress response element responsible for transcriptional induction of mammalian glucose-regulated proteins - Involvement of basic leucine zipper transcription factors. *J. Biol. Chem.* **273:** 33741-33749.

46. Shamu CE, Cox JS, Walter P. (1994) The unfolded-protein-response pathway in yeast. *Trends Cell Biol* **4:** 56-60.

47. Bertolotti A, Zhang Y, Hendershot LM, Harding HP, Ron D. (2000) Dynamic interaction of BiP and ER stress transducers in the unfolded-protein response. *Nat Cell Biol* **2:** 326-332.

48. Kimata Y, Oikawa D, Shimizu Y, Ishiwata-Kimata Y, Kohno K. (2004) A role for BiP as an adjustor for the endoplasmic reticulum stress-sensing protein Ire1. *J Cell Biol* **167:** 445-456.

49. Credle JJ, Finer-Moore JS, Papa FR, Stroud RM, Walter P. (2005) Inaugural Article: On the mechanism of sensing unfolded protein in the endoplasmic reticulum. *Proc Natl Acad Sci U S A* **102:** 18773-18784.

50. Shen JS, Chen X, Hendershot L, Prywes R. (2002) ER stress regulation of ATF6 localization by dissociation of BiP/GRP78 binding and unmasking of golgi localization signals. *Dev. Cell* **3:** 99-111.

51. Ma K, Vattem KM, Wek RC. (2002) Dimerization and release of molecular chaperone inhibition facilitate activation of eukaryotic initiation factor-2 kinase in response to endoplasmic reticulum stress. *J. Biol. Chem.* **277:** 18728-18735.

52. Nadanaka S, Okada T, Yoshida H, Mori K. (2007) Role of disulfide bridges formed in the luminal domain of ATF6 in sensing endoplasmic reticulum stress. *Mol Cell Biol* **27:** 1027-1043.

53. Hong M, Luo S, Baumeister P, et al. (2004) Underglycosylation of ATF6 as a Novel Sensing Mechanism for Activation of the Unfolded Protein Response. *J Biol Chem* **279:** 11354-11363.

54. Ma K, Vattem KM, Wek RC. (2002) Dimerization and release of molecular chaperone inhibition facilitate activation of eukaryotic initiation factor-2 kinase in response to endoplasmic reticulum stress. *J Biol Chem* **277:** 18728-18735.

55. Liu CY, Schroder M, Kaufman RJ. (2000) Ligand-independent dimerization activates the stress response kinases IRE1 and PERK in the lumen of the endoplasmic reticulum. *J. Biol. Chem.* **275:** 24881-24885.

56. Welihinda AA, Tirasophon W, Green SR, Kaufman RJ. (1998) Protein serine/threonine phosphatase Ptc2p negatively regulates the unfolded-protein response by dephosphorylating Ire1p kinase. *Mol Cell Biol* **18:** 1967-1977.

57. Guo J, Polymenis M. (2006) Dcr2 targets Ire1 and downregulates the unfolded protein response in Saccharomyces cerevisiae. *EMBO Rep* **7:** 1124-1127.

58. Yoshida H, Oku M, Suzuki M, Mori K. (2006) pXBP1(U) encoded in XBP1 pre-mRNA negatively regulates unfolded protein response activator pXBP1(S) in mammalian ER stress response. *J Cell Biol* **172:** 565-575.

59. Thuerauf DJ, Morrison LE, Hoover H, Glembotski CC. (2002) Coordination of ATF6-mediated transcription and ATF6 degradation by a domain that is shared with the viral transcription factor, VP16. *J Biol Chem* **277:** 20734-20739.

60. Thuerauf DJ, Marcinko M, Belmont PJ, Glembotski CC. (2007) Effects of the Isoform-specific Characteristics of ATF6{alpha} and ATF6beta on Endoplasmic Reticulum Stress Response Gene Expression and Cell Viability. *J Biol Chem* **282:** 22865-22878.

61. Tsukumo Y, Tomida A, Kitahara O, et al. (2007) Nucleobindin 1 Controls the Unfolded Protein Response by Inhibiting ATF6 Activation. *J Biol Chem* **282:** 29264-29272.

62. Yan W, Frank CL, Korth MJ, et al. (2002) Control of PERK eIF2alpha kinase activity by the endoplasmic reticulum stress-induced molecular chaperone P58IPK. *Proc Natl Acad Sci U S A* **99:** 15920-15925.

63. van Huizen R, Martindale JL, Gorospe M, Holbrook NJ. (2003) P58IPK, a novel endoplasmic reticulum stress-inducible protein and potential negative regulator of eIF2alpha signaling. *J Biol Chem* **278:** 15558-15564.

64. Novoa I, Zeng HQ, Harding HP, Ron D. (2001) Feedback inhibition of the unfolded protein response by GADD34- mediated dephosphorylation of eIF2 alpha. *J Cell Biol* **153:** 1011-1021.

65. Novoa I, Zhang YH, Zeng HQ, Jungreis R, Harding HP, Ron D. (2003) Stress-induced gene expression requires programmed recovery from translational repression. *Embo J*. **22:** 1180-1187.

66. Ma Y, Hendershot LM. (2003) Delineation of a negative feedback regulatory loop that controls protein translation during endoplasmic reticulum stress. *J Biol Chem* **278:** 34864-34873.

67. Bernales S, McDonald KL, Walter P. (2006) Autophagy Counterbalances Endoplasmic Reticulum Expansion during the Unfolded Protein Response. *PLoS Biol* **4:** e423.

68. Sriburi R, Jackowski S, Mori K, Brewer JW. (2004) XBP1: a link between the unfolded protein response, lipid biosynthesis, and biogenesis of the endoplasmic reticulum. *J Cell Biol* **167:** 35-41.

69. Tirosh B, Iwakoshi NN, Glimcher LH, Ploegh HL. (2005) XBP-1 specifically promotes IgM synthesis and secretion, but is dispensable for degradation of glycoproteins in primary B cells. *J Exp Med* **202:** 505-516.

70. Sriburi R, Bommiasamy H, Buldak GL, et al. (2007) Coordinate regulation of phospholipid biosynthesis and secretory pathway gene expression in XBP-1(S)-induced endoplasmic reticulum biogenesis. *J Biol Chem* **282:** 7024-7034.

71. Lee AH, Iwakoshi NN, Glimcher LH. (2003) XBP-1 regulates a subset of endoplasmic reticulum resident chaperone genes in the unfolded protein response. *Mol Cell Biol* **23:** 7448-7459.

72. Kleizen B, Braakman I. (2004) Protein folding and quality control in the endoplasmic reticulum. *Curr Opin Cell Biol* **16:** 343-349.

73. Ni M, Lee AS. (2007) ER chaperones in mammalian development and human diseases. *FEBS Lett* **581:** 3641-3651.

74. Helenius A, Aebi M. (2004) Roles of N-linked glycans in the endoplasmic reticulum. *Annu Rev Biochem* **73:** 1019-1049.

75. Tu BP, Weissman JS. (2004) Oxidative protein folding in eukaryotes: mechanisms and consequences. *J Cell Biol* **164:** 341-346.

76. Frand AR, Kaiser CA. (1998) The ERO1 gene of yeast is required for oxidation of protein dithiols in the endoplasmic reticulum. *Mol. Cell* **1:** 161-170.

77. Pollard MG, Travers KJ, Weissman JS. (1998) Ero1p: a novel and ubiquitous protein with an essential role in oxidative protein folding in the endoplasmic reticulum. *Mol. Cell* **1:** 171-182.

78. Cabibbo A, Pagani M, Fabbri M, et al. (2000) ERO1-L, a human protein that favors disulfide bond formation in the endoplasmic reticulum. *J Biol Chem* **275:** 4827-4833.

79. Acosta-Alvear D, Zhou Y, Blais A, et al. (2007) XBP1 controls diverse cell type- and condition-specific transcriptional regulatory networks. *Mol Cell* **27:** 53-66.

80. Kawai T, Fan J, Mazan-Mamczarz K, Gorospe M. (2004) Global mRNA stabilization preferentially linked to translational repression during the endoplasmic reticulum stress response. *Mol Cell Biol* **24:** 6773-6787.

81. Hollien J, Weissman JS. (2006) Decay of endoplasmic reticulum-localized mRNAs during the unfolded protein response. *Science* **313:** 104-107.

82. Iwawaki T, Hosoda A, Okuda T, et al. (2001) Translational control by the ER transmembrane kinase/ribonuclease IRE1 under ER stress. *Nat. Cell Biol.* **3:** 158-164.

83. Clemens MJ. (1994) Regulation of eukaryotic protein synthesis by protein kinases that phosphorylate initiation factor eIF-2. *Mol Biol Rep* **19:** 201-210.

84. Ron D. (2002) Translational control in the endoplasmic reticulum stress response. *J Clin Invest* **110:** 1383-1388.

85. Harding HP, Zhang Y, Bertolotti A, Zeng H, Ron D. (2000) Perk is essential for translational regulation and cell survival during the unfolded protein response. *Mol Cell* **5:** 897-904.

86. Spear ED, Ng DT. (2003) Stress tolerance of misfolded carboxypeptidase Y requires maintenance of protein trafficking and degradative pathways. *Mol Biol Cell* **14:** 2756-2767.

87. Stephens SB, Dodd RD, Brewer JW, Lager PJ, Keene JD, Nicchitta CV. (2005) Stable Ribosome Binding to the Endoplasmic Reticulum Enables Compartment-specific Regulation of mRNA Translation. *Mol Biol Cell*.

88. Osborne AR, Rapoport TA, van den Berg B. (2005) Protein translocation by the Sec61/SecY channel. *Annu Rev Cell Dev Biol* **21:** 529-550.

89. Kim SJ, Mitra D, Salerno JR, Hegde RS. (2002) Signal sequences control gating of the protein translocation channel in a substrate-specific manner. *Dev Cell* **2:** 207-217.

90. Kang SW, Rane NS, Kim SJ, Garrison JL, Taunton J, Hegde RS. (2006) Substrate-Specific Translocational Attenuation during ER Stress Defines a Pre-Emptive Quality Control Pathway. *Cell* **127:** 999-1013.

91. Oyadomari S, Yun C, Fisher EA, et al. (2006) Cotranslocational degradation protects the stressed endoplasmic reticulum from protein overload. *Cell* **126:** 727-739.

92. Marquardt T, Hebert DN, Helenius A. (1993) Post-translational folding of influenza hemagglutinin in isolated endoplasmic reticulum-derived microsomes. *J Biol Chem* **268:** 19618-19625.

93. Hampton RY. (2002) ER-associated degradation in protein quality control and cellular regulation. *Curr Opin Cell Biol* **14:** 476-482.

94. Okuda-Shimizu Y, Hendershot LM. (2007) Characterization of an ERAD Pathway for Nonglycosylated BiP Substrates, which Require Herp. *Mol Cell* **28:** 544-554.

95. Carvalho P, Goder V, Rapoport TA. (2006) Distinct ubiquitin-ligase complexes define convergent pathways for the degradation of ER proteins. *Cell* **126:** 361-373.

96. Denic V, Quan EM, Weissman JS. (2006) A luminal surveillance complex that selects misfolded glycoproteins for ER-associated degradation. *Cell* **126:** 349-359.

97. Jakob CA, Bodmer D, Spirig U, et al. (2001) Htm1p, a mannosidase-like protein, is involved in glycoprotein degradation in yeast. *EMBO Rep* **2:** 423-430.

98. Bays NW, Gardner RG, Seelig LP, Joazeiro CA, Hampton RY. (2001) Hrd1p/Der3p is a membrane-anchored ubiquitin ligase required for ER-associated degradation. *Nat Cell Biol* **3:** 24-29.

99. Gardner RG, Swarbrick GM, Bays NW, et al. (2000) Endoplasmic reticulum degradation requires lumen to cytosol signaling. Transmembrane control of Hrd1p by Hrd3p. *J Cell Biol* **151:** 69-82.

100. Ye Y, Meyer HH, Rapoport TA. (2001) The AAA ATPase Cdc48/p97 and its partners transport proteins from the ER into the cytosol. *Nature* **414:** 652-656.

101. Suzuki K, Ohsumi Y. (2007) Molecular machinery of autophagosome formation in yeast, Saccharomyces cerevisiae. *FEBS Lett* **581:** 2156-2161.

102. Ogata M, Hino S, Saito A, et al. (2006) Autophagy is activated for cell survival after endoplasmic reticulum stress. *Mol Cell Biol* **26:** 9220-9231.

103. Yorimitsu T, Nair U, Yang Z, Klionsky DJ. (2006) Endoplasmic reticulum stress triggers autophagy. *J Biol Chem* **281:** 30299-30304.

104. Ding WX, Ni HM, Gao W, et al. (2007) Linking of autophagy to ubiquitin-proteasome system is important for the regulation of endoplasmic reticulum stress and cell viability. *Am J Pathol* **171:** 513-524.

105. Kruse KB, Brodsky JL, McCracken AA. (2006) Characterization of an ERAD gene as VPS30/ATG6 reveals two alternative and functionally distinct protein quality control pathways: one for soluble Z variant of human alpha-1 proteinase inhibitor (A1PiZ) and another for aggregates of A1PiZ. *Mol Biol Cell* **17:** 203-212.

106. Kamimoto T, Shoji S, Hidvegi T, et al. (2006) Intracellular inclusions containing mutant alpha1-antitrypsin Z are propagated in the absence of autophagic activity. *J Biol Chem* **281:** 4467-4476.

107. Kouroku Y, Fujita E, Tanida I, et al. (2007) ER stress (PERK/eIF2alpha phosphorylation) mediates the polyglutamine-induced LC3 conversion, an essential step for autophagy formation. *Cell Death Differ* **14:** 230-239.

108. Wei MC, Zong WX, Cheng EH, et al. (2001) Proapoptotic BAX and BAK: a requisite gateway to mitochondrial dysfunction and death. *Science* **292:** 727-730.

109. Hetz C, Bernasconi P, Fisher J, et al. (2006) Proapoptotic BAX and BAK modulate the unfolded protein response by a direct interaction with IRE1alpha. *Science* **312:** 572-576.

110. Boya P, Cohen I, Zamzami N, Vieira HL, Kroemer G. (2002) Endoplasmic reticulum stress-induced cell death requires mitochondrial membrane permeabilization. *Cell Death Differ* **9:** 465-467.

111. Zong WX, Li C, Hatzivassiliou G, et al. (2003) Bax and Bak can localize to the endoplasmic reticulum to initiate apoptosis. *J Cell Biol* **162:** 59-69.

112. Nakagawa T, Zhu H, Morishima N, et al. (2000) Caspase-12 mediates endoplasmic-reticulum-specific apoptosis and cytotoxicity by amyloid-beta. *Nature* **403:** 98-103.

113. Zinszner H, Kuroda M, Wang X, et al. (1998) CHOP is implicated in programmed cell death in response to impaired function of the endoplasmic reticulum. *Genes Dev* **12:** 982-995.

114. McCullough KD, Martindale JL, Klotz LO, Aw TY, Holbrook NJ. (2001) Gadd153 sensitizes cells to endoplasmic reticulum stress by down-regulating Bcl2 and perturbing the cellular redox state. *Mol Cell Biol* **21:** 1249-1259.

115. Yamaguchi H, Wang HG. (2004) CHOP is involved in endoplasmic reticulum stress-induced apoptosis by enhancing DR5 expression in human carcinoma cells. *J Biol Chem* **279:** 45495-45502.

116. Reimold AM, Etkin A, Clauss I, et al. (2000) An essential role in liver development for transcription factor XBP-1. *Genes Dev* **14:** 152-157.

117. Zhang K, Wong HN, Song B, Miller CN, Scheuner D, Kaufman RJ. (2005) The unfolded protein response sensor IRE1alpha is required at 2 distinct steps in B cell lymphopoiesis. *J Clin Invest* **115:** 268-281.

118. Lee AH, Chu GC, Iwakoshi NN, Glimcher LH. (2005) XBP-1 is required for biogenesis of cellular secretory machinery of exocrine glands. *Embo J* **24:** 4368-4380.

119. Tirasophon W, Welihinda AA, Kaufman RJ. (1998) A stress response pathway from the endoplasmic reticulum to the nucleus requires a novel bifunctional protein kinase/endoribonuclease (Ire1p) in mammalian cells. *Genes and Development* **12:** 1812-1824.

120. Clauss IM, Gravallese EM, Darling JM, Shapiro F, Glimcher MJ, Glimcher LH. (1993) In situ hybridization studies suggest a role for the basic region-leucine zipper protein hXBP-1 in exocrine gland and skeletal development during mouse embryogenesis. *Dev Dyn* **197:** 146-156.

121. Iwawaki T, Akai R, Kohno K, Miura M. (2004) A transgenic mouse model for monitoring endoplasmic reticulum stress. *Nat Med* **10:** 98-102.

122. Souid S, Lepesant JA, Yanicostas C. (2007) The xbp-1 gene is essential for development in Drosophila. *Dev Genes Evol* **217:** 159-167.

123. Zhang P, McGrath B, Li S, et al. (2002) The PERK eukaryotic initiation factor 2 alpha kinase is required for the development of the skeletal system, postnatal growth, and the function and viability of the pancreas. *Mol Cell Biol* **22:** 3864-3874.

124. Harding HP, Zeng H, Zhang Y, et al. (2001) Diabetes mellitus and exocrine pancreatic dysfunction in perk-/- mice reveals a role for translational control in secretory cell survival. *Mol Cell* **7:** 1153-1163.

125. Delepine M, Nicolino M, Barrett T, Golamaully M, Lathrop GM, Julier C. (2000) EIF2AK3, encoding translation initiation factor 2-alpha kinase 3, is mutated in patients with Wolcott-Rallison syndrome. *Nat Genet* **25:** 406-409.

126. Ozcan U, Cao Q, Yilmaz E, et al. (2004) Endoplasmic reticulum stress links obesity, insulin action, and type 2 diabetes. *Science* **306:** 457-461.

127. Calfon M, Zeng H, Urano F, et al. (2002) IRE1 couples endoplasmic reticulum load to secretory capacity by processing the XBP-1 mRNA. *Nature* **415:** 92-96.

128. Reimold AM, Iwakoshi NN, Manis J, et al. (2001) Plasma cell differentiation requires the transcription factor XBP-1. *Nature* **412:** 300-307.

129. Iwakoshi NN, Lee AH, Vallabhajosyula P, Otipoby KL, Rajewsky K, Glimcher LH. (2003) Plasma cell differentiation and the unfolded protein response intersect at the transcription factor XBP-1. *Nat. Immunol.* **4:** 321-329.

130. Gass JN, Gifford NM, Brewer JW. (2002) Activation of an unfolded protein response during differentiation of antibody-secreting B cells. *J Biol Chem* **277:** 49047-49054.

131. Yamamoto K, Sato T, Matsui T, et al. (2007) Transcriptional Induction of Mammalian ER Quality Control Proteins Is Mediated by Single or Combined Action of ATF6alpha and XBP1. *Dev Cell* **13:** 365-376.

132. Wu J, Rutkowski DT, Dubois M, et al. (2007) ATF6alpha Optimizes Long-Term Endoplasmic Reticulum Function to Protect Cells from Chronic Stress. *Dev Cell* **13:** 351-364.

133. Gass JN, Jiang HY, Wek RC, Brewer JW. (2008) The unfolded protein response of B-lymphocytes: PERK-independent development of antibody-secreting cells. *Mol Immunol* **45:** 1035-1043.

134. Skalet AH, Isler JA, King LB, Harding HP, Ron D, Monroe JG. (2005) Rapid B cell receptor-induced unfolded protein response in nonsecretory B cells correlates with pro- versus antiapoptotic cell fate. *J Biol Chem* **280:** 39762-39771.

135. van Anken E, Romijn EP, Maggioni C, et al. (2003) Sequential waves of functionally related proteins are expressed when B cells prepare for antibody secretion. *Immunity* **18:** 243-253.

136. Hayashi A, Kasahara T, Iwamoto K, et al. (2007) The role of brain-derived neurotrophic factor (BDNF)-induced XBP1 splicing during brain development. *J Biol Chem* **282:** 34525-34534.

137. Shen Y, Hendershot LM. (2007) Identification of ERdj3 and OBF-1/BOB-1/OCA-B as Direct Targets of XBP-1 during Plasma Cell Differentiation. *J Immunol* **179:** 2969-2978.

138. Sequeira SJ, Ranganathan AC, Adam AP, Iglesias BV, Farias EF, Aguirre-Ghiso JA. (2007) Inhibition of proliferation by PERK regulates mammary acinar morphogenesis and tumor formation. *PLoS ONE* **2:** e615.

139. Nakanishi K, Sudo T, Morishima N. (2005) Endoplasmic reticulum stress signaling transmitted by ATF6 mediates apoptosis during muscle development. *J Cell Biol* **169:** 555-560.

140. Schroder M, Chang JS, Kaufman RJ. (2000) The unfolded protein response represses nitrogen-starvation induced developmental differentiation in yeast. *Genes Dev* **14:** 2962-2975.

141. Bicknell AA, Babour A, Federovitch CM, Niwa M. (2007) A novel role in cytokinesis reveals a housekeeping function for the unfolded protein response. *J Cell Biol* **177:** 1017-1027.

142. Ellgaard L, Molinari M, Helenius A. (1999) Setting the standards: Quality control in the secretory pathway. *Science* **286:** 1882-1888.

143. Daum G, Lees ND, Bard M, Dickson R. (1998) Biochemistry, cell biology and molecular biology of lipids of Saccharomyces cerevisiae. *Yeast* **14:** 1471-1510.

144. Mori K. (2000) Tripartite management of unfolded proteins in the endoplasmic reticulum. *Cell* **101:** 451-454.

145. Harding HP, Zeng HQ, Zhang YH, et al. (2001) Diabetes mellitus and exocrine pancreatic dysfunction in Perk- - mice reveals a role for translational control in secretory cell survival. *Mol. Cell* **7:** 1153-1163.

146. Kaufman RJ. (2002) Orchestrating the unfolded protein response in health and disease. *J Clin Invest* **110:** 1389-1398.

147. Mori K, Ma W, Gething MJ, Sambrook J. (1993) A transmembrane protein with a cdc2+/CDC28-related kinase activity is required for signaling from the ER to the nucleus. *Cell* **74:** 743-756.

148. Chapman R, Sidrauski C, Walter P. (1998) Intracellular signaling from the endoplasmic reticulum to the nucleus. *Annu Rev Cell Dev Biol* **14:** 459-485.

149. Kawahara T, Yanagi H, Yura T, Mori K. (1997) Endoplasmic reticulum stress-induced mRNA splicing permits synthesis of transcription factor Hac1p/Ern4p that activates the unfolded protein response. *Mol Biol Cell* **8:** 1845-1862.

150. Tu BP, Ho-Schleyer SC, Travers KJ, Weissman JS. (2000) Biochemical basis of oxidative protein folding in the endoplasmic reticulum. *Science* **290:** 1571-1574.

151. Frand AR, Kaiser CA. (1999) Ero1p oxidizes protein disulfide isomerase in a pathway for disulfide bond formation in the endoplasmic reticulum. *Mol Cell* **4:** 469-477.

152. Frand AR, Kaiser CA. (1998) The ERO1 gene of yeast is required for oxidation of protein dithiols in the endoplasmic reticulum. *Mol Cell* **1:** 161-170.

153. Vai M, Popolo L, Alberghina L. (1987) Effect of tunicamycin on cell cycle progression in budding yeast. *Exp Cell Res* **171:** 448-459.

154. Arnold E, Tanner W. (1982) An obligatory role of protein glycosylation in the life cycle of yeast cells. *FEBS Lett* **148:** 49-53.

155. McMillan JN, Sia RA, Lew DJ. (1998) A morphogenesis checkpoint monitors the actin cytoskeleton in yeast. *J Cell Biol* **142:** 1487-1499.

156. Biggins S, Severin FF, Bhalla N, Sassoon I, Hyman AA, Murray AW. (1999) The conserved protein kinase Ipl1 regulates microtubule binding to kinetochores in budding yeast. *Genes Dev* **13:** 532-544.

157. Mendenhall MD, Hodge AE. (1998) Regulation of Cdc28 cyclin-dependent protein kinase activity during the cell cycle of the yeast Saccharomyces cerevisiae. *Microbiol Mol Biol Rev* **62:** 1191-1243.

158. Stegmeier F, Amon A. (2004) Closing Mitosis: The Functions of the Cdc14 Phosphatase and Its Regulation. *Annu Rev Genet*.

159. Shou W, Seol JH, Shevchenko A, et al. (1999) Exit from mitosis is triggered by Tem1-dependent release of the protein phosphatase Cdc14 from nucleolar RENT complex. *Cell* **97:** 233-244.

160. Straight AF, Marshall WF, Sedat JW, Murray AW. (1997) Mitosis in living budding yeast: anaphase A but no metaphase plate. *Science* **277:** 574-578.

161. Yeong FM. (2005) Severing all ties between mother and daughter: cell separation in budding yeast. *Mol Microbiol* **55:** 1325-1331.

162. Kuranda MJ, Robbins PW. (1991) Chitinase is required for cell separation during growth of Saccharomyces cerevisiae. *J Biol Chem* **266:** 19758-19767.

163. Novick P, Botstein D. (1985) Phenotypic analysis of temperature-sensitive yeast actin mutants. *Cell* **40:** 405-416.

164. Waddle JA, Karpova TS, Waterston RH, Cooper JA. (1996) Movement of cortical actin patches in yeast. *J Cell Biol* **132:** 861-870.

165. Doyle T, Botstein D. (1996) Movement of yeast cortical actin cytoskeleton visualized in vivo. *Proc Natl Acad Sci U S A* **93:** 3886-3891.

166. Mulholland J, Preuss D, Moon A, Wong A, Drubin D, Botstein D. (1994) Ultrastructure of the yeast actin cytoskeleton and its association with the plasma membrane. *J Cell Biol* **125:** 381-391.

167. Kilmartin JV, Adams AE. (1984) Structural rearrangements of tubulin and actin during the cell cycle of the yeast Saccharomyces. *J Cell Biol* **98:** 922-933.

168. Swanson R, Locher M, Hochstrasser M. (2001) A conserved ubiquitin ligase of the nuclear envelope/endoplasmic reticulum that functions in both ER-associated and Matalpha2 repressor degradation. *Genes Dev* **15:** 2660-2674.

169. Nikawa J, Yamashita S. (1992) IRE1 encodes a putative protein kinase containing a membrane-spanning domain and is required for inositol phototrophy in Saccharomyces cerevisiae. *Mol Microbiol* **6:** 1441-1446.

170. Friedlander R, Jarosch E, Urban J, Volkwein C, Sommer T. (2000) A regulatory link between ER-associated protein degradation and the unfolded-protein response. *Nat Cell Biol* **2:** 379-384.

171. Friedlander. (2000) A regulatory link between ER-associated protein degradation and the unfolded-protein response (vol 2, pg 379, 2000). *Nat. Cell Biol.* **2:** 676-676.

172. Casagrande R, Stern P, Diehn M, et al. (2000) Degradation of proteins from the ER of S. cerevisiae requires an intact unfolded protein response pathway. *Mol Cell* **5:** 729-735.

173. Shuster CB, Burgess DR. (2002) Targeted new membrane addition in the cleavage furrow is a late, separate event in cytokinesis. *Proc Natl Acad Sci U S A* **99:** 3633-3638.

174. Skop AR, Bergmann D, Mohler WA, White JG. (2001) Completion of cytokinesis in C. elegans requires a brefeldin A-sensitive membrane accumulation at the cleavage furrow apex. *Curr Biol* **11:** 735-746.

175. VerPlank L, Li R. (2005) Cell cycle-regulated trafficking of Chs2 controls actomyosin ring stability during cytokinesis. *Mol Biol Cell* **16:** 2529-2543.

176. Shaw JA, Mol PC, Bowers B, et al. (1991) The function of chitin synthases 2 and 3 in the Saccharomyces cerevisiae cell cycle. *J Cell Biol* **114:** 111-123.

177. Valdivia RH, Schekman R. (2003) The yeasts Rho1p and Pkc1p regulate the transport of chitin synthase III (Chs3p) from internal stores to the plasma membrane. *Proc Natl Acad Sci U S A* **100:** 10287-10292.

178. Janetopoulos C, Devreotes P. (2006) Phosphoinositide signaling plays a key role in cytokinesis. *J Cell Biol* **174:** 485-490.

179. Emoto K, Umeda M. (2001) Membrane lipid control of cytokinesis. *Cell Struct Funct* **26:** 659-665.

180. Emoto K, Inadome H, Kanaho Y, Narumiya S, Umeda M. (2005) Local change in phospholipid composition at the cleavage furrow is essential for completion of cytokinesis. *J Biol Chem* **280:** 37901-37907.

181. Brill JA, Hime GR, Scharer-Schuksz M, Fuller MT. (2000) A phospholipid kinase regulates actin organization and intercellular bridge formation during germline cytokinesis. *Development* **127:** 3855-3864.

182. Luo J, Vallen EA, Dravis C, Tcheperegine SE, Drees B, Bi E. (2004) Identification and functional analysis of the essential and regulatory light chains of the only type II myosin Myo1p in Saccharomyces cerevisiae. *J Cell Biol* **165:** 843-855.

183. Tolliday N, VerPlank L, Li R. (2002) Rho1 directs formin-mediated actin ring assembly during budding yeast cytokinesis. *Curr Biol* **12:** 1864-1870.

184. Lippincott J, Li R. (1998) Dual function of Cyk2, a cdc15/PSTPIP family protein, in regulating actomyosin ring dynamics and septin distribution. *J Cell Biol* **143:** 1947-1960.

185. Korinek WS, Bi E, Epp JA, Wang L, Ho J, Chant J. (2000) Cyk3, a novel SH3-domain protein, affects cytokinesis in yeast. *Curr Biol* **10:** 947-950.

186. Shin DY, Matsumoto K, Iida H, Uno I, Ishikawa T. (1987) Heat shock response of Saccharomyces cerevisiae mutants altered in cyclic AMP-dependent protein phosphorylation. *Mol Cell Biol* **7:** 244-250.

187. Hartwell LH. (1974) Saccharomyces cerevisiae cell cycle. *Bacteriol Rev* **38:** 164-198.

188. Haase SB, Reed SI. (2002) Improved flow cytometric analysis of the budding yeast cell cycle. *Cell Cycle* **1:** 132-136.

189. Ron D, Walter P. (2007) Signal integration in the endoplasmic reticulum unfolded protein response. *Nat Rev Mol Cell Biol* **8:** 519-529.

190. Voeltz GK, Rolls MM, Rapoport TA. (2002) Structural organization of the endoplasmic reticulum. *EMBO Rep* **3:** 944-950.

191. Du Y, Ferro-Novick S, Novick P. (2004) Dynamics and inheritance of the endoplasmic reticulum. *J Cell Sci* **117:** 2871-2878.

192. Estrada de Martin P, Novick P, Ferro-Novick S. (2005) The organization, structure, and inheritance of the ER in higher and lower eukaryotes. *Biochem Cell Biol* **83:** 752-761.

193. Brewer JW, Hendershot LM, Sherr CJ, Diehl JA. (1999) Mammalian unfolded protein response inhibits cyclin D1 translation and cell-cycle progression. *Proc Natl Acad Sci U S A* **96:** 8505-8510.

194. Caviston JP, Longtine M, Pringle JR, Bi E. (2003) The role of Cdc42p GTPase-activating proteins in assembly of the septin ring in yeast. *Mol Biol Cell* **14:** 4051-4066.

195. McMurray MA, Thorner J. (2009) Reuse, replace, recycle. Specificity in subunit inheritance and assembly of higher-order septin structures during mitotic and meiotic division in budding yeast. *Cell Cycle* **8:** 195-203.

196. Dobbelaere J, Gentry MS, Hallberg RL, Barral Y. (2003) Phosphorylation-dependent regulation of septin dynamics during the cell cycle. *Dev Cell* **4:** 345-357.

197. Hartwell LH, Culotti J, Reid B. (1970) Genetic control of the cell-division cycle in yeast. I. Detection of mutants. *Proc Natl Acad Sci U S A* **66:** 352-359.

198. Kim HB, Haarer BK, Pringle JR. (1991) Cellular morphogenesis in the Saccharomyces cerevisiae cell cycle: localization of the CDC3 gene product and the timing of events at the budding site. *J Cell Biol* **112:** 535-544.

199. Hampton RY, Koning A, Wright R, Rine J. (1996) In vivo examination of membrane protein localization and degradation with green fluorescent protein. *Proc Natl Acad Sci U S A* **93:** 828-833.

200. Du Y, Pypaert M, Novick P, Ferro-Novick S. (2001) Aux1p/Swa2p is required for cortical endoplasmic reticulum inheritance in Saccharomyces cerevisiae. *Mol Biol Cell* **12:** 2614-2628.

201. Chen Y, Feldman DE, Deng C, et al. (2005) Identification of mitogen-activated protein kinase signaling pathways that confer resistance to endoplasmic reticulum stress in Saccharomyces cerevisiae. *Mol Cancer Res* **3:** 669-677.

202. Bonilla M, Cunningham KW. (2003) Mitogen-activated protein kinase stimulation of Ca(2+) signaling is required for survival of endoplasmic reticulum stress in yeast. *Mol Biol Cell* **14:** 4296-4305.

203. Longtine MS, Fares H, Pringle JR. (1998) Role of the yeast Gin4p protein kinase in septin assembly and the relationship between septin assembly and septin function. *J Cell Biol* **143:** 719-736.

204. Du Y, Walker L, Novick P, Ferro-Novick S. (2006) Ptc1p regulates cortical ER inheritance via Slt2p. *Embo J* **25:** 4413-4422.

205. Reinoso-Martin C, Schuller C, Schuetzer-Muehlbauer M, Kuchler K. (2003) The yeast protein kinase C cell integrity pathway mediates tolerance to the antifungal drug caspofungin through activation of Slt2p mitogen-activated protein kinase signaling. *Eukaryot Cell* **2:** 1200-1210.

206. Spector I, Shochet NR, Kashman Y, Groweiss A. (1983) Latrunculins: novel marine toxins that disrupt microfilament organization in cultured cells. *Science* **219:** 493-495.

207. Estrada P, Kim J, Coleman J, et al. (2003) Myo4p and She3p are required for cortical ER inheritance in Saccharomyces cerevisiae. *J Cell Biol* **163:** 1255-1266.

208. Kozubowski L, Larson JR, Tatchell K. (2005) Role of the septin ring in the asymmetric localization of proteins at the mother-bud neck in Saccharomyces cerevisiae. *Mol Biol Cell* **16:** 3455-3466.

209. Kim KY, Truman AW, Levin DE. (2008) Yeast Mpk1 mitogen-activated protein kinase activates transcription through Swi4/Swi6 by a noncatalytic mechanism that requires upstream signal. *Mol Cell Biol* **28:** 2579-2589.

210. Levin DE. (2005) Cell wall integrity signaling in Saccharomyces cerevisiae. *Microbiol Mol Biol Rev* **69:** 262-291.

211. de Nobel H, Ruiz C, Martin H, et al. (2000) Cell wall perturbation in yeast results in dual phosphorylation of the Slt2/Mpk1 MAP kinase and in an Slt2-mediated increase in FKS2-lacZ expression, glucanase resistance and thermotolerance. *Microbiology* **146 (Pt 9):** 2121-2132.

212. Philip B, Levin DE. (2001) Wsc1 and Mid2 are cell surface sensors for cell wall integrity signaling that act through Rom2, a guanine nucleotide exchange factor for Rho1. *Mol Cell Biol* **21:** 271-280.

213. Serrano R, Martin H, Casamayor A, Arino J. (2006) Signaling alkaline pH stress in the yeast Saccharomyces cerevisiae through the Wsc1 cell surface sensor and the Slt2 MAPK pathway. *J Biol Chem* **281:** 39785-39795.

214. Gray JV, Ogas JP, Kamada Y, Stone M, Levin DE, Herskowitz I. (1997) A role for the Pkc1 MAP kinase pathway of Saccharomyces cerevisiae in bud emergence and identification of a putative upstream regulator. *Embo J* **16:** 4924-4937.

215. Ketela T, Green R, Bussey H. (1999) Saccharomyces cerevisiae mid2p is a potential cell wall stress sensor and upstream activator of the PKC1-MPK1 cell integrity pathway. *J Bacteriol* **181:** 3330-3340.

216. Verna J, Lodder A, Lee K, Vagts A, Ballester R. (1997) A family of genes required for maintenance of cell wall integrity and for the stress response in Saccharomyces cerevisiae. *Proc Natl Acad Sci U S A* **94:** 13804-13809.

217. Zu T, Verna J, Ballester R. (2001) Mutations in WSC genes for putative stress receptors result in sensitivity to multiple stress conditions and impairment of Rlm1-dependent gene expression in Saccharomyces cerevisiae. *Mol Genet Genomics* **266:** 142-155.

218. Piao HL, Machado IM, Payne GS. (2007) NPFXD-mediated endocytosis is required for polarity and function of a yeast cell wall stress sensor. *Mol Biol Cell* **18:** 57-65.

219. Nanduri J, Tartakoff AM. (2001) The arrest of secretion response in yeast: signaling from the secretory path to the nucleus via Wsc proteins and Pkc1p. *Mol Cell* **8:** 281-289.

220. Sinclair DA, Guarente L. (1997) Extrachromosomal rDNA circles--a cause of aging in yeast. *Cell* **91:** 1033-1042.

221. Erjavec N, Larsson L, Grantham J, Nystrom T. (2007) Accelerated aging and failure to segregate damaged proteins in Sir2 mutants can be suppressed by overproducing the protein aggregation-remodeling factor Hsp104p. *Genes Dev* **21:** 2410-2421.

222. Murray AW, Szostak JW. (1983) Pedigree analysis of plasmid segregation in yeast. *Cell* **34:** 961-970.

223. Shcheprova Z, Baldi S, Frei SB, Gonnet G, Barral Y. (2008) A mechanism for asymmetric segregation of age during yeast budding. *Nature* **454:** 728-734.

224. Tessarz P, Schwarz M, Mogk A, Bukau B. (2009) The yeast AAA+ chaperone Hsp104 is part of a network that links the actin cytoskeleton with the inheritance of damaged proteins. *Mol Cell Biol* **29:** 3738-3745.

225. van Drogen F, Peter M. (2002) Spa2p functions as a scaffold-like protein to recruit the Mpk1p MAP kinase module to sites of polarized growth. *Curr Biol* **12:** 1698-1703.

226. Loewen CJ, Young BP, Tavassoli S, Levine TP. (2007) Inheritance of cortical ER in yeast is required for normal septin organization. *J Cell Biol* **179:** 467-483.

227. Merksamer PI, Trusina A, Papa FR. (2008) Real-time redox measurements during endoplasmic reticulum stress reveal interlinked protein folding functions. *Cell* **135:** 933-947.

228. Lindholm D, Wootz H, Korhonen L. (2006) ER stress and neurodegenerative diseases. *Cell Death Differ* **13:** 385-392.

229. Posas F, Chambers JR, Heyman JA, Hoeffler JP, de Nadal E, Arino J. (2000) The transcriptional response of yeast to saline stress. *J Biol Chem* **275:** 17249-17255.

230. Gasch AP, Spellman PT, Kao CM, et al. (2000) Genomic expression programs in the response of yeast cells to environmental changes. *Mol Biol Cell* **11:** 4241-4257.

231. O'Rourke SM, Herskowitz I. (2004) Unique and redundant roles for HOG MAPK pathway components as revealed by whole-genome expression analysis. *Mol Biol Cell* **15:** 532-542.

232. Prick T, Thumm M, Kohrer K, Haussinger D, Vom Dahl S. (2006) In yeast, loss of Hog1 leads to osmosensitivity of autophagy. *Biochem J* **394:** 153-161.

233. Xu Y, Jagannath C, Liu XD, Sharafkhaneh A, Kolodziejska KE, Eissa NT. (2007) Toll-like receptor 4 is a sensor for autophagy associated with innate immunity. *Immunity* **27:** 135-144.

234. Cheng Y, Qiu F, Ye YC, et al. (2009) Autophagy inhibits reactive oxygen species-mediated apoptosis via activating p38-nuclear factor-kappa B survival pathways in oridonin-treated murine fibrosarcoma L929 cells. *Febs J* **276:** 1291-1306.

235. Cui Q, Tashiro S, Onodera S, Minami M, Ikejima T. (2007) Oridonin induced autophagy in human cervical carcinoma HeLa cells through Ras, JNK, and P38 regulation. *J Pharmacol Sci* **105:** 317-325.

236. Liu B, Cheng Y, Zhang B, Bian HJ, Bao JK. (2009) Polygonatum cyrtonema lectin induces apoptosis and autophagy in human melanoma A375 cells through a mitochondria-mediated ROS-p38-p53 pathway. *Cancer Lett* **275:** 54-60.

237. Chen Z, Gibson TB, Robinson F, et al. (2001) MAP kinases. *Chem Rev* **101:** 2449-2476.

238. Brewster JL, de Valoir T, Dwyer ND, Winter E, Gustin MC. (1993) An osmosensing signal transduction pathway in yeast. *Science* **259:** 1760-1763.

239. Maeda T, Takekawa M, Saito H. (1995) Activation of yeast PBS2 MAPKK by MAPKKKs or by binding of an SH3-containing osmosensor. *Science* **269:** 554-558.

240. Reiser V, Ruis H, Ammerer G. (1999) Kinase activity-dependent nuclear export opposes stress-induced nuclear accumulation and retention of Hog1 mitogen-activated protein kinase in the budding yeast Saccharomyces cerevisiae. *Mol Biol Cell* **10:** 1147-1161.

241. Marquez JA, Pascual-Ahuir A, Proft M, Serrano R. (1998) The Ssn6-Tup1 repressor complex of Saccharomyces cerevisiae is involved in the osmotic induction of HOG-dependent and -independent genes. *Embo J* **17:** 2543-2553.

242. Proft M, Pascual-Ahuir A, de Nadal E, Arino J, Serrano R, Posas F. (2001) Regulation of the Sko1 transcriptional repressor by the Hog1 MAP kinase in response to osmotic stress. *Embo J* **20:** 1123-1133.

243. Proft M, Mas G, de Nadal E, et al. (2006) The stress-activated Hog1 kinase is a selective transcriptional elongation factor for genes responding to osmotic stress. *Mol Cell* **23:** 241-250.

244. de Nadal E, Casadome L, Posas F. (2003) Targeting the MEF2-like transcription factor Smp1 by the stress-activated Hog1 mitogen-activated protein kinase. *Mol Cell Biol* **23:** 229-237.

245. De Nadal E, Zapater M, Alepuz PM, Sumoy L, Mas G, Posas F. (2004) The MAPK Hog1 recruits Rpd3 histone deacetylase to activate osmoresponsive genes. *Nature* **427:** 370-374.

246. Rep M, Reiser V, Gartner U, et al. (1999) Osmotic stress-induced gene expression in Saccharomyces cerevisiae requires Msn1p and the novel nuclear factor Hot1p. *Mol Cell Biol* **19:** 5474-5485.

247. Warmka J, Hanneman J, Lee J, Amin D, Ota I. (2001) Ptc1, a type 2C Ser/Thr phosphatase, inactivates the HOG pathway by dephosphorylating the mitogen-activated protein kinase Hog1. *Mol Cell Biol* **21:** 51-60.

248. Jacoby T, Flanagan H, Faykin A, Seto AG, Mattison C, Ota I. (1997) Two protein-tyrosine phosphatases inactivate the osmotic stress response pathway in yeast by targeting the mitogen-activated protein kinase, Hog1. *J Biol Chem* **272:** 17749-17755.

249. Wurgler-Murphy SM, Maeda T, Witten EA, Saito H. (1997) Regulation of the Saccharomyces cerevisiae HOG1 mitogen-activated protein kinase by the PTP2 and PTP3 protein tyrosine phosphatases. *Mol Cell Biol* **17:** 1289-1297.

250. Mattison CP, Ota IM. (2000) Two protein tyrosine phosphatases, Ptp2 and Ptp3, modulate the subcellular localization of the Hog1 MAP kinase in yeast. *Genes Dev* **14:** 1229-1235.

251. Teige M, Scheikl E, Reiser V, Ruis H, Ammerer G. (2001) Rck2, a member of the calmodulin-protein kinase family, links protein synthesis to high osmolarity MAP kinase signaling in budding yeast. *Proc Natl Acad Sci U S A* **98:** 5625-5630.

252. Clotet J, Escote X, Adrover MA, et al. (2006) Phosphorylation of Hsl1 by Hog1 leads to a G2 arrest essential for cell survival at high osmolarity. *Embo J* **25:** 2338-2346.

253. Marquez JA, Serrano R. (1996) Multiple transduction pathways regulate the sodium-extrusion gene PMR2/ENA1 during salt stress in yeast. *FEBS Lett* **382:** 89-92.

254. Raman M, Cobb MH. (2003) MAP kinase modules: many roads home. *Curr Biol* **13:** R886-888.

255. Maeda T, Wurgler-Murphy SM, Saito H. (1994) A two-component system that regulates an osmosensing MAP kinase cascade in yeast. *Nature* **369:** 242-245.

256. Posas F, Saito H. (1997) Osmotic activation of the HOG MAPK pathway via Ste11p MAPKKK: scaffold role of Pbs2p MAPKK. *Science* **276:** 1702-1705.

257. Posas F, Saito H. (1998) Activation of the yeast SSK2 MAP kinase kinase kinase by the SSK1 two-component response regulator. *Embo J* **17:** 1385-1394.

258. Posas F, Wurgler-Murphy SM, Maeda T, Witten EA, Thai TC, Saito H. (1996) Yeast HOG1 MAP kinase cascade is regulated by a multistep phosphorelay mechanism in the SLN1-YPD1-SSK1 "two-component" osmosensor. *Cell* **86:** 865-875.

259. Tatebayashi K, Tanaka K, Yang HY, et al. (2007) Transmembrane mucins Hkr1 and Msb2 are putative osmosensors in the SHO1 branch of yeast HOG pathway. *Embo J* **26:** 3521-3533.

260. Deshaies RJ, Schekman R. (1987) A yeast mutant defective at an early stage in import of secretory protein precursors into the endoplasmic reticulum. *J Cell Biol* **105:** 633-645.

261. Mizuta K, Warner JR. (1994) Continued functioning of the secretory pathway is essential for ribosome synthesis. *Mol Cell Biol* **14:** 2493-2502.

262. Schena M, Picard D, Yamamoto KR. (1991) Vectors for constitutive and inducible gene expression in yeast. *Methods Enzymol* **194:** 389-398.

263. Kirisako T, Baba M, Ishihara N, et al. (1999) Formation process of autophagosome is traced with Apg8/Aut7p in yeast. *J Cell Biol* **147:** 435-446.

264. Huang WP, Scott SV, Kim J, Klionsky DJ. (2000) The itinerary of a vesicle component, Aut7p/Cvt5p, terminates in the yeast vacuole via the autophagy/Cvt pathways. *J Biol Chem* **275:** 5845-5851.

265. Klionsky DJ, Ohsumi Y. (1999) Vacuolar import of proteins and organelles from the cytoplasm. *Annu Rev Cell Dev Biol* **15:** 1-32.

266. Kim J, Huang WP, Klionsky DJ. (2001) Membrane recruitment of Aut7p in the autophagy and cytoplasm to vacuole targeting pathways requires Aut1p, Aut2p, and the autophagy conjugation complex. *J Cell Biol* **152:** 51-64.

267. Suzuki K, Kirisako T, Kamada Y, Mizushima N, Noda T, Ohsumi Y. (2001) The pre-autophagosomal structure organized by concerted functions of APG genes is essential for autophagosome formation. *Embo J* **20:** 5971-5981.

268. Shintani T, Klionsky DJ. (2004) Cargo proteins facilitate the formation of transport vesicles in the cytoplasm to vacuole targeting pathway. *J Biol Chem* **279:** 29889-29894.

269. Takeshige K, Baba M, Tsuboi S, Noda T, Ohsumi Y. (1992) Autophagy in yeast demonstrated with proteinase-deficient mutants and conditions for its induction. *J Cell Biol* **119:** 301-311.

270. Thumm M, Egner R, Koch B, et al. (1994) Isolation of autophagocytosis mutants of Saccharomyces cerevisiae. *FEBS Lett* **349:** 275-280.

271. Xie Z, Nair U, Klionsky DJ. (2008) Atg8 controls phagophore expansion during autophagosome formation. *Mol Biol Cell* **19:** 3290-3298.

272. Noda T, Matsuura A, Wada Y, Ohsumi Y. (1995) Novel system for monitoring autophagy in the yeast Saccharomyces cerevisiae. *Biochem Biophys Res Commun* **210:** 126-132.

273. Lin JH, Li H, Yasumura D, et al. (2007) IRE1 signaling affects cell fate during the unfolded protein response. *Science* **318:** 944-949.

274. Anderson DH. (2006) Role of lipids in the MAPK signaling pathway. *Prog Lipid Res* **45:** 102-119.

275. Hinnebusch AG. (1993) Gene-specific translational control of the yeast GCN4 gene by phosphorylation of eukaryotic initiation factor 2. *Mol Microbiol* **10:** 215-223.

276. Lu PD, Harding HP, Ron D. (2004) Translation reinitiation at alternative open reading frames regulates gene expression in an integrated stress response. *J Cell Biol* **167:** 27-33.

277. Lodder AL, Lee TK, Ballester R. (1999) Characterization of the Wsc1 protein, a putative receptor in the stress response of Saccharomyces cerevisiae. *Genetics* **152:** 1487-1499.

278. Bermejo C, Rodriguez E, Garcia R, et al. (2008) The sequential activation of the yeast HOG and SLT2 pathways is required for cell survival to cell wall stress. *Mol Biol Cell* **19:** 1113-1124.

279. Jung US, Levin DE. (1999) Genome-wide analysis of gene expression regulated by the yeast cell wall integrity signalling pathway. *Mol Microbiol* **34:** 1049-1057.

280. Jung US, Sobering AK, Romeo MJ, Levin DE. (2002) Regulation of the yeast Rlm1 transcription factor by the Mpk1 cell wall integrity MAP kinase. *Mol Microbiol* **46:** 781-789.

281. Mortensen EM, McDonald H, Yates J, 3rd, Kellogg DR. (2002) Cell cycle-dependent assembly of a Gin4-septin complex. *Mol Biol Cell* **13:** 2091-2105.

282. Versele M, Thorner J. (2004) Septin collar formation in budding yeast requires GTP binding and direct phosphorylation by the PAK, Cla4. *J Cell Biol* **164:** 701-715.

283. Kadota J, Yamamoto T, Yoshiuchi S, Bi E, Tanaka K. (2004) Septin ring assembly requires concerted action of polarisome components, a PAK kinase Cla4p, and the actin cytoskeleton in Saccharomyces cerevisiae. *Mol Biol Cell* **15:** 5329-5345.

284. Tang CS, Reed SI. (2002) Phosphorylation of the septin cdc3 in g1 by the cdc28 kinase is essential for efficient septin ring disassembly. *Cell Cycle* **1:** 42-49.

285. Johnson ES, Blobel G. (1999) Cell cycle-regulated attachment of the ubiquitin-related protein SUMO to the yeast septins. *J Cell Biol* **147:** 981-994.

286. Luedeke C, Frei SB, Sbalzarini I, Schwarz H, Spang A, Barral Y. (2005) Septin-dependent compartmentalization of the endoplasmic reticulum during yeast polarized growth. *J Cell Biol* **169:** 897-908.

287. Ferrigno P, Posas F, Koepp D, Saito H, Silver PA. (1998) Regulated nucleo/cytoplasmic exchange of HOG1 MAPK requires the importin beta homologs NMD5 and XPO1. *Embo J* **17:** 5606-5614.

288. Wilhovsky S, Gardner R, Hampton R. (2000) HRD gene dependence of endoplasmic reticulum-associated degradation. *Mol Biol Cell* **11:** 1697-1708.

289. Longtine MS, McKenzie A, 3rd, Demarini DJ, et al. (1998) Additional modules for versatile and economical PCR-based gene deletion and modification in Saccharomyces cerevisiae. *Yeast* **14:** 953-961.

290. Klionsky DJ. (2007) Monitoring autophagy in yeast: the Pho8Delta60 assay. *Methods Mol Biol* **390:** 363-371.

291. Rose M, Botstein D. (1983) Construction and use of gene fusions to lacZ (beta-galactosidase) that are expressed in yeast. *Methods Enzymol* **101:** 167-180.

292. Watanabe M, Chen CY, Levin DE. (1994) Saccharomyces cerevisiae PKC1 encodes a protein kinase C (PKC) homolog with a substrate specificity similar to that of mammalian PKC. *J Biol Chem* **269:** 16829-16836.

293. Carr CM, Grote E, Munson M, Hughson FM, Novick PJ. (1999) Sec1p binds to SNARE complexes and concentrates at sites of secretion. *J Cell Biol* **146:** 333-344.

294. Pilon M, Romisch K, Quach D, Schekman R. (1998) Sec61p serves multiple roles in secretory precursor binding and translocation into the endoplasmic reticulum membrane. *Mol Biol Cell* **9:** 3455-3473.